THE
PHYSICAL REVIEW
A Journal of Experimental and Theoretical Physics Established by E. L. Nichols in 1893
VOL. 58, No. 3 AUGUST 1, 1940 SECOND SERIES

X-Ray Emission Spectra and Electronic Energy Bands of Compounds

JOSEPH VALASEK
University of Minnesota, Minneapolis, Minnesota
(Received May 25, 1940)

Measurements of emission wave-lengths in the $K\beta$ group of Ca and S in CaS and $CaSO_4$, of Mg and S in MgS, of S in SrS and BaS, of Ca and Cl in $CaCl_2$ have been made from the secondary radiation from pressed blocks of the salts. An attempt is made to determine the origin of as many x-ray lines as possible by means of electronic energy band systems in the cases of CaS, MgS, and ZnS. The $K\beta_5$ line of Zn in ZnS and the $K\beta_1$ line of Mg in MgS are found to be due to cross transitions from the outermost filled band of the negative ion.

IT has been pointed out that information in regard to electronic energy bands in solids may be obtained by a study of x-ray emission[1] and absorption[2] spectra. In the second paper of reference 1, it is shown that the principal lines in the x-ray emission spectra of alkali halides fit the energy level diagrams for the solid state with fair accuracy, leaving no doubt as to the levels and transitions which account for some of these lines. However, there are still several prominent lines which cannot be accounted for with certainty. The present paper summarizes recent measurements of wave-lengths in the $K\beta$-radiation from alkaline earth sulphides and a few other compounds. The discussion reveals anomalies which were absent in the spectra of the alkali halides.

The radiation was excited by placing pressed blocks of the compound near the focal spot on a tungsten-surfaced anticathode as described in a previous article.[3] An attempt was made at this time to record as many of the satellites of $K\beta_1$ as possible with this indirect method of excitation. A Siegbahn vacuum spectrograph equipped with a quartz crystal was employed. The power input to the tube was kept low enough so that the material did not show any appreciable alteration. However, the material was changed every 24 hours during the exposures, which ranged from 100 to 500 hours. The power input was 1 to 3 ma at 12 kv depending on the stability of the substance.

For the Mg $K\beta_1$ line a focusing spectrograph with a curved mica crystal was employed. The radiation was from a pressed block of MgS which received radiation from an adjacent tungsten plate which was bombarded by electrons. The wave-length was measured relative to that of copper $K\alpha_1$ in the eighth and tenth orders as well as Al $K\alpha$ in the second order.

In the other cases, the wave-lengths were measured relative to those previously given for the principal $K\beta_1$ lines[1] from the same compounds. The line intervals were measured with a Gaertner comparator. Each spectrogram contained a number of lines which were too weak

[1] J. Valasek, Phys. Rev. **51**, 832 (1937); Phys. Rev. **53**, 274 (1938).
[2] R. Landshoff, Rev. Sci. Inst. **9**, 143 (1938); Phys. Rev. **55**, 631 (1939).
[3] J. Valasek, Phys. Rev. **47**, 896 (1935).

to measure directly since they disappeared into the granular background even under low magnification. When microphotometer traces were made of these lines, it was found difficult to locate accurately the exact maximum because of the line breadth and the accidental irregularities in the trace. It was found just as accurate to mark carefully the location of the line on the plate with a sharp pencil and to measure the mark. Repetition of this procedure on the same and on different plates gave results which were usually consistent to about 1 X.U. and the average should be good to about 0.5 X.U. as a rule. These lines are designated by *b* in Table I. The lines designated by *a* were always measured directly and are probably correct to 0.1 X.U. in general.

The auxiliary data needed to assist in the interpretation of the lines are most complete in the case of CaS. In Fig. 1, the emission lines of Ca and S are plotted on a scale of electron volts below the *K*-absorption edge for the corresponding element. The wave-length of the *K* edge of S in CaS, 5006.6 X.U., was obtained from the measurements of Lindh.[4] That for the *K* edge of Ca in CaS, 3059.5 X.U., was obtained by applying a correction to the measurements of Aoyama, Kimura, and Nishina.[5] These authors as well as Lindsay and Van Dyke[6] have measured the *K*-absorption wave-lengths of Ca in various compounds. There is an average difference of 3.1 X.U. between the two sets of measurements on the same compound, although Lindsay and Van Dyke give no values for CaS. The difference between the two groups of observers is largely due to the fact that the former measured the middle of the first white line in the absorption spectrum, while Lindsay and Van Dyke measured the beginning of absorption. In view of both sets of data, it is considered that the most probable value of the *K*-absorption edge of Ca in CaS is determined by the most rapid rise in absorption which is estimated to be 1.6 X.U. above the value given by Aoyama, Kimura, and Nishina, namely at 3059.5 X.U.

TABLE I. *Wave-lengths in X.U.*

LINE	TYPE	WAVE-LENGTHS					
		Negative ion, S^{--} (and Cl^{-})					
		MgS	CaS	SrS	BaS	$CaSO_4$	$CaCl_2$
	b	5124.3	5083.5	5084.4	5093.4	5087.1	
β_4	*b*	5067.3	5065.3	5065.3	5067.1	5067.3	
β_2	*b*	5046.2	5046.2	5046.4	5044.3	5046.2	4419.6
β_1	*sid*	5018.40	5019.00	5019.39	5019.74	5017.81	4394.61
β_x	*a*	5011.9	5012.6	5012.3	5012.4	5011.1	4380.9
β_5	*b*	4993.5	4993.6	4994.0	4994.2	4990.1	4368.9
β'''	*b*	4950.0	4950.6	4951.2	4954.6	4951.6	
β''''	*b*	4933.3	4934.0	4934.3	4931.1	4933.1	
	b	4889.0	4891.3	4885.5	4891.6	4896.7	
	b	4862.5	4871.6	4871.5	4866.0	4865.1	
	b					4970.8	
		Positive ion, Ca^{++} (and Mg^{++})					
		CaS	$CaSO_4$	$CaCl_2$		MgS	
η	*b*	3122.	3122.	3125.			
β'	*b*	3111.	3110.	3114.			
β_3	*sid*	3083.43	3083.43	3083.43	β_1 *a*	9545.	
β''	*a*	3079.2	3079.3	3079.3			
β_2	*a*	3067.3	3068.1	3068.1			
β'''	*b*	3048.3	3048.1	3048.1			
β''''	*b*	3041.3	3042.7	3041.2			

Finally, in order to fit the energy levels of both ions to the same energy scale, it will be assumed at first that the *K* electron, at the beginning of the continuous *K* absorption, is raised to the lower edge of the same band of empty states of the crystal lattice regardless of whether it comes from the *K* shell of the positive or the negative ion. Accordingly, when they are both known, the absorption edges of both ions are placed at the same point in the energy level diagram. The locations of the emission lines should then show the locations of the initial occupied level from which the emitting electron falls into the *K* shell. This assumes a single excitation and a single electron transition, and hence does not apply to the spark lines.

In the cases of NaCl and KCl reported in a previous article, the origin of four of the emission lines was plainly indicated when a diagram prepared as above was compared with an energy level diagram prepared from the atomic levels by the method of Slater and Shockley.[7] Two of these lines were, as expected, due to transitions of a $3p$ electron into a *K* shell vacancy in the same ion, while two were due to transitions of a $3p$ electron into a *K* shell vacancy in a neighboring ion of opposite sign. The latter are usually much weaker than the former except when the $3p$, or sometimes the $2p$, shell is not occupied in one of the ions because of its low atomic number. Then the cross transitions give rise to principal lines. Further evidence on this point is presented below.

[4] A. Lindh, Handb. d. Exp. Physik, Vol. 24, No. 2, p. 296.
[5] S. Aoyama, K. Kimura, and Y. Nishina, Zeits. f. Physik **44**, 810 (1927).
[6] G. Lindsay, and G. Van Dyke, Phys. Rev. **28**, 613 (1926).
[7] J. Slater and W. Shockley, Phys. Rev. **50**, 705 (1936).

Because the alkaline earth sulphides also have a rocksalt type of structure, one can readily apply the same calculations to find the locations of their energy bands for the purpose of comparison with similar results obtained from the x-ray data. Because of the double charge on each ion, the electrostatic potential energy term must be multiplied by two. Accordingly

$$e\phi = \frac{3.495\ e^2\ 300}{r} \text{ electron volts,}$$

where r is the distance between closest neighbors of opposite sign. The ionization potential, or electron affinity, of the S^{--} ion is calculated by extrapolating the ionization potentials of the isoelectronic sequence Ca^{++}, K^{+}, A, Cl^{-} by means of a quadratic formula.[8] The potentials used are taken from Bacher and Goudsmit's *Atomic Energy States*. The work required to remove one electron from S^{--} is thus found to be -4.18 electron volts. Seitz[9] has recently used a value of -5 volts which he obtained by subtracting an estimated binding energy for the first electron from the electron affinity found by the use of a Born cycle. The cycle gives the work done to remove both electrons. The negative sign applied to the electron affinity indicates that the free doubly charged ion is unstable. In a crystal lattice, however, more than enough binding energy is supplied through the external screening by surrounding ions to result in a positive binding energy of some 10 to 15 electron volts, depending on the compound.

The ionization potentials for the doubly charged positive ions of Mg and Ca are also from Bacher and Goudsmit's tables. However those for Sr^{++} and Ba^{++} are not listed, and since the K-absorption edges of these ions in the corresponding sulphides are also unknown, they are omitted from the following discussion.

Calculated positions of the energy bands for CaS are shown in Fig. 1. It is difficult to determine the extent of the continuum of empty states, but the experimental data can be used to supply this information. In order to do this, it is assumed that the intervals between the occupied energy bands of the positive ion are

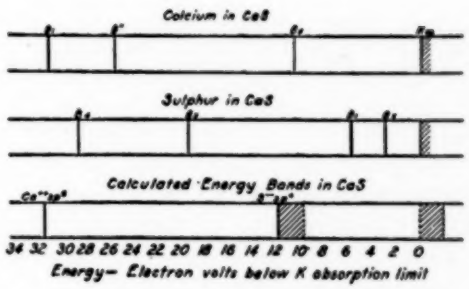
Calcium in CaS
Sulphur in CaS
Calculated Energy Bands in CaS
34 32 30 28 26 24 22 20 18 16 14 12 10 8 6 4 2 0
Energy– Electron volts below K absorption limit

FIG. 1. Top: K-series emission lines of calcium in CaS on energy scale relative to the K-absorption edge. Center: ditto, sulphur in CaS. Bottom: electron energy bands of CaS.

not altered by chemical combination. This is indicated by the exceedingly small effects of such combination on the emission wave-lengths of the positive ion. Hence, if the $3p$ level of Ca is placed at the same point on the energy scale as the $K\beta_1$ line, the location of the K-absorption edge will give the location of the lower edge of the empty states in the compound. The other K lines should then indicate the upper filled states from which they originate. The Ca $K\beta_5$ line is thus seen to be due to a cross transition of an S $3p$ electron into the vacancy in the K shell of Ca.

However, it is evident on Fig. 1 that the placing of the K-absorption edge of the negative ion in coincidence with that of the positive ion, results in a large discrepancy in the location of the S $K\beta_1$ line with respect to the S $3p$ band. It should be noted that this displacement did not occur as a result of the application of the same considerations to the spectra of NaCl and KCl in an earlier article.[1] Obviously, one can remove the discrepancy in this case by an appropriate shift in the position of the empty states belonging to the sulphur ion. This would require a displacement of 5 to 7 electron volts with selection rules to reserve the shifted states for the negative ion. The existence of two such empty bands "belonging" to the respective ions does not seem improbable, for an examination of the wave-mechanical problem leads to a result of this general nature. When K excitation of the positive ion takes place, the K electron goes into a band derived from the lowest vacant p state of the positive ion. On the other hand when the K excitation of S^{--} takes place, the electron probably goes over into the vicinity of one of

[8] G. Glockler, Phys. Rev. **46**, 111 (1934).
[9] F. Seitz, J. Chem. Phys. **6**, 454 (1938).

the neighboring Ca^{++} ions. This is essentially the same state of Ca, but modified by the fact that the net charge on the ion core is one unit less. An application of Moseley's law as a first approximation gives much too small a displacement of the upper level to account for that observed. Thus it seems necessary to assume a great distortion of the outer levels of the negative ion either as a result of the nature of the chemical bond, or as a result of some secondary process which occurs between excitation and emission.

The first interpretation is ruled out because the cross-transition line $K\beta_5$ of Ca shows that the initial level S^{--} $3p$ is in its normal state when it is the positive ion which is excited. This conclusion is supported by similar lines in the spectra of MgS and ZnS as will be shown in the following. Thus the displacement of the S^{--} $3p$ level accompanies only the K excitation of the S ion itself and, by the Franck-Condon principle, should follow the excitation. Accordingly, the K-absorption frequency of S^{--} will be at its expected place in the compound but its $K\beta$-emission line will be displaced.

Following Gurney, one may assume two principal sources of such secondary effects on the energy levels, namely the displacement of surrounding ions and polarization. The net effect is to elevate the energy levels of the electrons in the K-excited ion whether it is positive or negative, that is to say, to decrease the binding energy. Aoyama, Kimura, and Nishina[5] have calculated the energy u_2 of rearrangement of surrounding ions when the central ion loses an electron. They used this as one of the terms in their explanation of the effect of chemical combination on absorption frequencies. Pauling[10] points out that this is incorrect because the rearrangement cannot take place during absorption, but must follow after it, and he substitutes an electron affinity of the crystal which he obtains from the diamagnetic susceptibility of the compound.

Aoyama, Kimura, and Nishina find that the energy u_2 is only 1 electron volt in the case of chlorine in sodium and potassium chloride, but becomes 10 electron volts in the case of sulphur in CaS, and 11 electron volts for sulphur in MgS and ZnS. Furthermore, it is very small in the cases of the positive ions in all these substances. From the manner in which u_2 is calculated, this energy includes energy of polarization as well as displacement, though the former is not mentioned in the original article. It is questionable whether the lifetime of the K-excited states is large enough to permit ion displacements, but polarization should be considered and it is estimated that this will lead to a displacement of the valence levels of the central ion by some 5 to 6 electron volts. The discussion by Aoyama, Kimura, and Nishina shows that a similar effect escapes notice in the alkali halides and in the spectra of positive ions in general, because u_2 is relatively small in these cases.

A further indication that the energy levels of the negative ion can be shifted by several electron volts as a result of changes in the internal and external screening, is shown by the spectra of sulphur in the sulphates as compared with the corresponding sulphides.[1] The K-absorption edge of sulphur is found to be displaced toward higher energy values by 9.5 electron volts on the average. The $K\alpha$ lines are displaced to higher frequencies by 1.7 volts, showing that the L levels are also displaced considerably, the shift being 7.8 electron volts. On the other hand, the $K\beta$ lines are displaced by only 0.5 volt on the average. This shows an unusually large amount of distortion or relative displacement of the energy levels.

The above considerations show that energy level displacements of the indicated value can occur when the region around a sulphur ion is made more negative. The principal displacement applies to all levels equally, like the crystal potential effect previously considered. However a secondary effect of opposite sign applies principally to the outermost levels and makes for a decrease in binding. This differential shift takes place between excitation of the negative ion and emission by the same ion and is negligible in the case of the positive ion. Any influence which acts equally on the M and K levels cannot explain the effects of chemical combination on the observed emission wave-lengths. It is just this point which makes it difficult to calculate the exact magnitude of the effect beyond the rough approximation discussed above. One might ex-

[10] L. Pauling, Phys. Rev. **34**, 954 (1929).

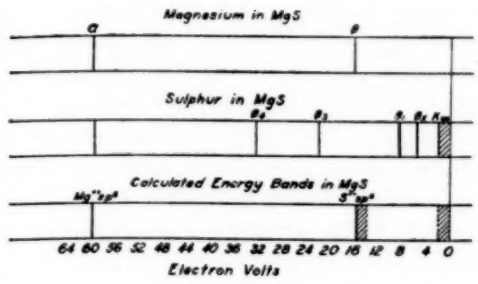

FIG. 2. Top: K-series emission lines of Mg in MgS on energy scale. Center: ditto, sulphur in MgS showing relative location of K-absorption edge. Bottom: electron energy bands of MgS.

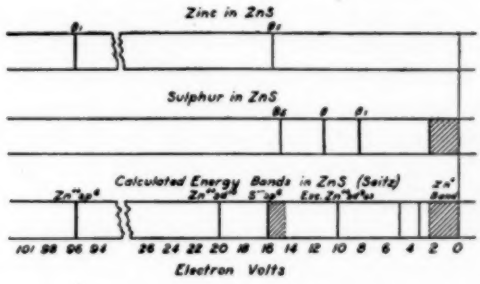

FIG. 3. Top: K-series emission lines of zinc in ZnS on energy scale. Center: ditto, sulphur in ZnS showing relative location of K-absorption edge. Bottom: electron energy bands of ZnS according to Seitz.

pect that it would increase with the polarizability of the ion concerned and the valence of the surrounding ions and their proximity. This is in accord with the observations, for the effects are greatest in the doubly charged negative ion in a divalent lattice with small lattice constant.

In the case of the spectrum of MgS, the wave-length of the K-absorption edge of Mg in the compound is not known, making it impossible to link together the spectra of S^{--} and Mg^{++} by making the vacant bands coincide as was done in the case of CaS. However, the locations of the energy levels in the crystal can be estimated as before by applying the crystal potential term to the levels for the free ion. The lower limit of the continuum of vacant states can be estimated to lie at about 2 electron volts by analogy with CaS, or by calculating the average energy of a free electron in the crystal from a formula given by Pauling.[10] Figure 2 shows the resulting diagram. The K edge of sulphur is made to coincide with the lower limit of the continuum and the magnesium $K\alpha$ line is placed opposite the Mg^{++} $2p$ level. There is no $3p$ level in a free magnesium ion from which a $K\beta$ line might originate. Nevertheless such a line is observed. Its location in the energy level diagram shows that it must be interpreted as a cross transition from the S^{--} $3p$ band. The same interpretation applies to the $K\beta_1$ line of Na in NaCl. The displacement of the S $K\beta_1$ line with respect to the parent S^{--} $3p$ energy band is about 6 electron volts which is in concordance with the result noted for CaS.

Recently F. Seitz[9] has published an energy level diagram for ZnS which is reproduced in Fig. 3 with x-ray emission data for Zn[11] and S[12] in the same compound. The K-absorption edge of S in ZnS is taken from the tabulation by Lindh, but the wave-length of the K edge of Zn in this compound could not be found in the literature. When the K-absorption edge of S is lined up with the lower edge of the continuum given by Seitz it is seen that the S $K\beta_1$ line falls nearly seven electron volts above the S $3p$ band. This is the same as the effect observed in CaS and MgS and is explained in the same way. It should be noted that in the S $K\beta$ group, the strongest line is taken to be the S $K\beta_1$ line and that it is accompanied by weaker satellites on the long wave-length side instead of the short wave-length side as in the alkaline earth sulphides. This line structure and intensity relation was observed in zinc blende and wurtzite as well as in pellets pressed from the chemically pure reagent.

To locate the Zn $K\beta_5$ line correctly, the Zn $3p$ band was taken as the origin of the Zn $K\beta_1$ line. The Zn $3p$ level was located relative to the Zn $3d$ band by a combination of x-ray data,[13] without the use of Zn $K\beta_5$, the origin of which is doubtful. The equation used was:

$$M_{\text{IV,V}} - M_{\text{II,III}} = K\alpha_1 + L\alpha_{1,2} - K\beta_1,$$

the $L\alpha$ wave-length being obtained from the measurements of Tyren.[14] The interval between Zn $3d$ and Zn $3p$ was found to be 76.0 electron volts. When the Zn $K\beta_1$ line is placed in coincidence with the Zn $3p$ band, the $K\beta_5$ line falls at

[11] J. C. McDonald, Phys. Rev. **50**, 694 (1936).
[12] J. Valasek, Phys. Rev. **43**, 612 (1933).
[13] M. Siegbahn, *Spektroskopie der Roentgenstrahlen* (1931).
[14] F. Tyren, Archiv f. Mat., Astr. och Fysik **25A**, 1 (1936).

S^{--} $3p$ as shown in Fig. 3. This indicates that the Zn $K\beta_5$ line which is usually regarded as due to a "forbidden" or quadrupole transition ($\Delta l = 2$) is due instead to a cross transition of a S^{--} $3p$ electron into a K-shell vacancy in the zinc ion. One can thus understand the relatively low intensity of this line and its anomalous variation with atomic number. The above applies to zinc sulphide and probably to all salts of elements in the iron group. The $K\beta_5$ line has also been observed in the x-ray emission spectrum of metallic zinc, in fact, accompanied by a weak and scarcely resolvable $K\beta_2$ line.[15] These lines show a breadth and lack of symmetry which is characteristic of the conduction band in metals. Their origin is discussed by Beeman and Friedman[16] in connection with their study of the structure of the K-absorption edges of compounds in the neighborhood of the iron group. They also give excellent reasons against the usual interpretation of $K\beta_5$ as a forbidden or quadrupole transition in those cases where there is conduction band formation in the solid. The present observations give support to a similar interpretation in regard to compounds.

The writer takes this opportunity to thank the Graduate School of the University of Minnesota for its support of this investigation, and to Mr. George Werner for his assistance in the laboratory.

[15] J. A. Bearden and C. H. Shaw, Phys. Rev. **48**, 18 (1935).

[16] W. W. Beeman and H. Friedman, Phys. Rev. **56**, 392 (1939).

AUGUST 1, 1940 PHYSICAL REVIEW VOLUME 58

An Accurate Measurement of the Energy Released in the Disintegration of Li^6 by Protons

GILBERT J. PERLOW
Ryerson Physical Laboratory, University of Chicago, Chicago, Illinois

(Received May 21, 1940)

The energy release in the reaction $Li^6(p,\alpha)He^3$ has been determined by a comparison of the He^4 range with that of the alpha-particles from $Be^9(p,\alpha)Li^6$. The energy of the latter reaction is accurately known from electrostatic deflection measurements. The determination was carried out in a small, variable air pressure, absorption cell and ionization chamber, both being at the same pressure. The device had high dispersion, 1 mm of range corresponding to about 13 cm Hg. Calibration of the cell was carried out by a method which utilized this high dispersion. The Q value for the reaction was found to be 3.945 ± 0.06 Mev as compared to the previously accepted value due to Neuert of 3.72 ± 0.08. With the new Q value, H^3 is found to be unstable against β-decay by either 0.19 ± 0.09 or 0.10 ± 0.1 Mev depending on whether Bainbridge's or Aston's value for the deuterium-helium bracket is used. The mass of He^3 is found to be 3.01688 ± 0.00011 mass units.

INTRODUCTION

ONLY three nuclear reactions are known at the present time which lead to the formation of the He^3 nucleus. The one most studied has been $D^2 + D^2 \rightarrow He^3 + n^1$, and this chiefly through measurement of the neutron energy;[1] the alternative being to measure a 4-mm range. Another reaction is the recently discovered[2] beta-radioactivity of H^3. The third is the reaction $Li^6 + H^1 \rightarrow He^3 + He^4$, which is the subject of this paper. These short range particles were first found by Oliphant, Kinsey, and Rutherford.[3] The best measurement of the energy release hitherto published is that of Neuert,[4] who measured the

[1] T. W. Bonner and W. M. Brubaker, Phys. Rev. **49**, 19 (1936); T. W. Bonner, Phys. Rev. **52**, 686 (1937) and **53**, 711 (1938); E. Baldinger, H. Huber, and H. Staub, Helv. Phys. Acta **11**, [3] 245 (1938), and others.

[2] L. Alvarez and R. Cornog, Phys. Rev. **56**, 613 (1939) and **57**, 248A (1940).

[3] M. L. E. Oliphant, B. B. Kinsey, and Lord Rutherford, Proc. Roy. Soc. **141**, 722 (1933).

[4] H. Neuert, Physik. Zeits. **36**, 629 (1935).

range of the He^3 nuclei in a cloud chamber. This method is open to criticism chiefly because it depends directly on the range-energy curve in a region where it is not too well known. The method to be described here depends only on the slope of the range-energy curve over a narrow region. The percentage error in the Q value is 0.2 times the percentage error in the slope.

In this work the He^4 range from $Li^6(p,\alpha)He^3$ was compared by an absorption cell and ionization chamber method with that of the He^4's emitted in $Be^9(p,\alpha)Li^6$. The energy of the latter had been accurately determined in this laboratory by electrostatic deflection,[5] and since the expected difference in range was only of the order of a millimeter, it was felt that the measurements would be of high precision. The ranges were expected to be about 7 and 8 mm for the beryllium and lithium reaction, respectively. Thin targets were used in both cases.

Apparatus

The high voltage set used was the Cockcroft-Walton type circuit described by Hatch.[6] A low voltage ion source designed by Allison furnished the protons. The beam was magnetically separated and passed through two circular apertures 0.54 cm in diameter and 10 cm apart before striking the target. The disintegrations were observed at 90°. Figure 1 is a drawing of the target assembly and range measuring apparatus. The latter is seen to consist of two sections. The region from B to A acted as a variable air pressure absorption cell, that from A to the collecting electrode farther to the right as a parallel plate ionization chamber. The target spot and the opening A were the limiting apertures, each 0.54 cm in diameter. The screen B was covered on the higher pressure side by a collodion window with an air equivalent of about 3.5 mm. This was the only window in the apparatus. There was a fine perforated screen over A also, but nothing else, so that the pressures in the ionization chamber and absorption cell were the same. The screen had 26 holes per sq. cm, each hole being about 0.02 cm in diameter. The depth of the absorption cell was 0.54 cm and of the ionization chamber 0.45 cm. The collecting voltage for the latter was applied to the outside brass case of the entire device.

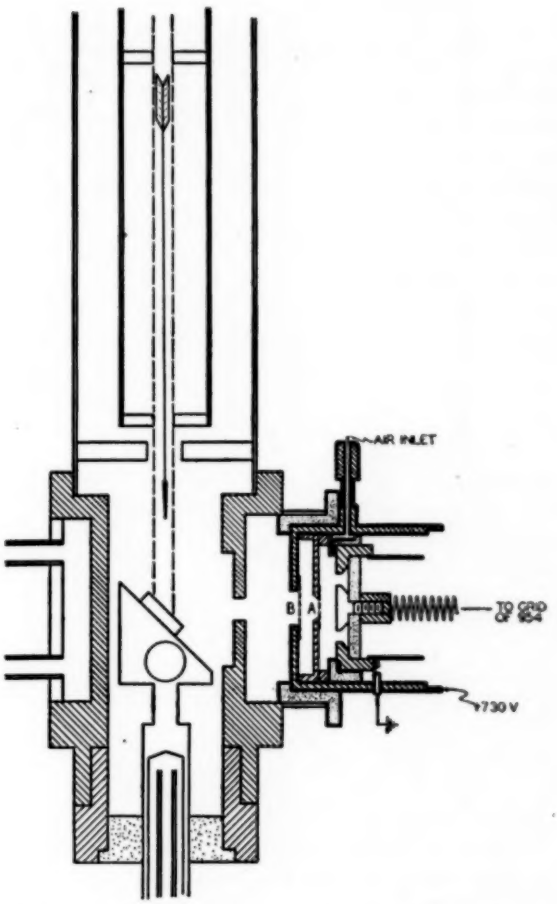

Fig. 1. Target assembly and range measurement apparatus. There was a collodion window on the right-hand side of screen B.

Performance of the Variable Pressure Range Comparison Device

The performance of the variable pressure ionization chamber will depend on the biasing of the counting circuit, that is, on the minimum number N_0 of ion pairs which must be formed between the plates to record a count. Preliminary trials showed that acceptable number-pressure curves of the short range particles from beryllium could be produced with a bias of 9 volts on the first stage of the vacuum-tube scale-of-sixteen counting circuit. By a method described later it

[5] S. K. Allison, L. S. Skaggs, and N. M. Smith, Jr., Phys. Rev. **54**, 171 (1938); L. S. Skaggs, Phys. Rev. **56**, 24 (1939); S. K. Allison, L. S. Skaggs, and N. M. Smith, Jr., Phys. Rev. **57**, 550 (1940).

[6] G. T. Hatch, Phys. Rev. **54**, 165 (1938).

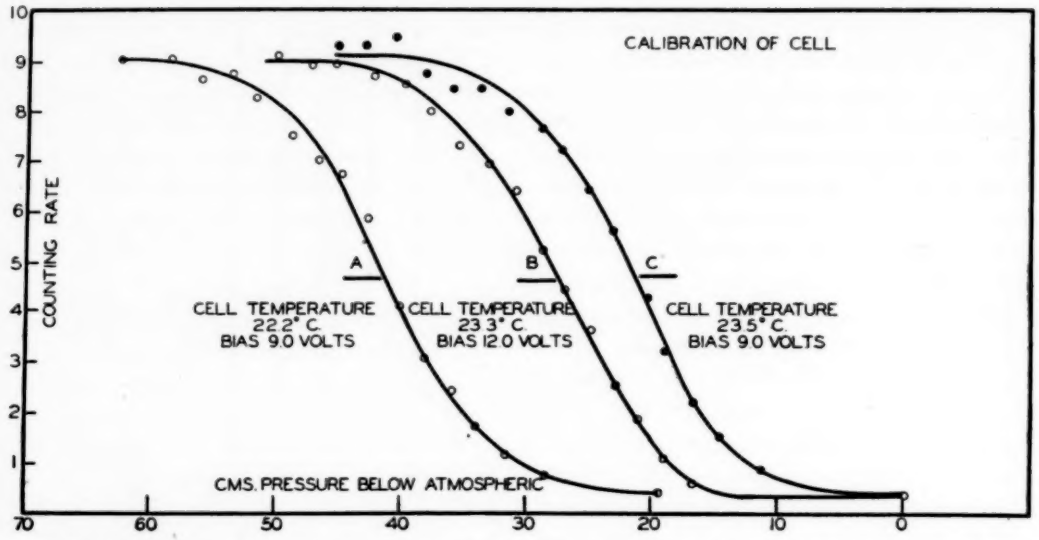

FIG. 2. Calibration of the cell with polonium alpha-particles. Curves A and C are separated by 1.5-mm motion of micrometer at the prevailing barometric pressure and at the temperatures indicated in the drawing. Curves B and C represent the effect of changing the bias three volts for groups of the same residual range. The ordinate 10 represents 1000 counts in 70 seconds.

was shown that this corresponded to the collection of 1900 ion pairs.

The range of a particle measured in the cell is a sum of three terms. The first is the air equivalent of the collodion window. This is assumed to be independent of the temperature and of the energy of the particle. The second term refers to the range expended in the first compartment of the device, i.e., the absorption cell proper. This will be the product of the cell length L with the air density ρ. In order to conform to the standard practice in range work, the unit of density is taken to be the density of dry air under 76 cm Hg pressure at a temperature of 15°C. The third term is the product of the penetration δ into the ionization chamber required to register a count with the corresponding air density. In the device used here, the latter is also ρ. Then for the difference in range of two separate groups of particles we have

$$R_1-R_2=L(\rho_1-\rho_2)+(\delta_1\rho_1-\delta_2\rho_2).$$

If now neither δ_1 nor δ_2 is greater than the ionization chamber depth D (=0.45 cm), the difference $(\delta_1\rho_1-\delta_2\rho_2)$ is zero since δ_1 and δ_2 are the linear path lengths required to produce N_0 ion pairs before losing ionizing power and these lengths vary inversely as the density. The device now acts like the conventional type in which the ionization chamber is at constant pressure. Then

$$R_1-R_2=\frac{288L}{76.0}\left[\frac{P_1}{T_1}-\frac{P_2}{T_2}\right], \qquad (1)$$

where P is the pressure and T the absolute temperature.

There is a certain critical pressure P_c, however, below which formula (1) becomes invalid. This is the pressure at which an alpha-particle will not produce enough ionization to record a count before reaching the end of the ionization chamber. It may be computed from:

$$N_0=\int_0^{D_c} I(x)dx$$

with $D_c=DP_c/76$. The abscissa $x=0$ corresponds to residual range zero in the specific ionization *versus* range curve $I(x)$. If it is assumed that $I(x)$ has the form of Fig. 9 in the paper of Holloway and Livingston,[7] and that the maximum ordinate represents the creation of 60,000 ion pairs per cm, one gets $P_c=17$ cm Hg for $N_0=1900$ ion pairs. Since none of the number-pressure curves started dropping off until somewhat above this pressure, formula (1) was applicable.

[7] M. G. Holloway and M. S. Livingston, Phys. Rev. **54**, 18 (1938).

The quantity N_0 was determined in the following way. A thin polonium source was placed so that its alpha-particles passed through the absorption compartment and entered the ionization chamber near the end of their range. The pressure was then reduced in the two-compartment device and the diminishing pulse heights on the oscillograph observed. (In order to reduce the pressure without rupturing the collodion film, a vacuum was created in an auxiliary chamber, temporarily attached.) The pressure was lowered until this rough evidence indicated that the particles traversing the ionization compartment were producing approximately the critical number of ion pairs corresponding to the selected bias. With the pressure held at this value, the distance of the polonium source was readjusted until the pulses showed a maximum height. Then an accurate measurement of the critical pressure was made by counting with the biased circuit and varying the pressure in this reduced region until the sharp low pressure cut-off of the number-pressure curve was found. Let the pressure at which the cut-off occurs be P_0. If the linear depth of the ionization chamber is D, then its equivalent depth at P_0 is $P_0D/76=D_0$. The critical number of ion pairs N_0 corresponding to the given bias may then be found from:

$$N_0=\left[\int_{\alpha}^{\alpha+D_0} I(x)dx\right]_{\max},$$

where α is to be chosen to give the greatest value for the integral. For the 9-volt bias, P_0 was measured to be 5.5 cm Hg. For $D=0.45$ cm D_0 becomes 0.033 cm, and graphical integration gives $N_0=1900$ ion pairs.

Calibration

Since the difference in range of two groups of particles as measured with an absorption cell is proportional to the product of the cell length by the pressure difference between the two number-pressure curves, the dispersion of the device may be made extremely large by choosing a short enough cell. Such was the case in the present measurements, each mm of range in standard air corresponding to about 13 cm difference in pressure. Now measurement of the cell dimensions is complicated by such things as the bulge of the screens, and the uncertainty of the boundary between absorption and ionization compartments. It is clear that a small absolute error in this measurement produces a large error in the range difference. Therefore the measured cell dimensions were given no weight in the calibration. Instead a method suggested to the author by Dr. N. M. Smith of this laboratory was employed. A thin polonium source was mounted on an accurate metric micrometer. The axis of the range measuring device was placed along the screw axis and the micrometer adjusted until particles ended their range in the cell at some particular pressure. The evacuated chamber mentioned previously was used to avoid rupturing the cell window.A number pressure curve was taken for a given position of the source. The micrometer was then turned an integral number of times and another number-pressure curve taken. In Fig. 2 curves A and C are separated by 1.5 mm motion of the micrometer at the prevailing barometric pressure. Table I gives the data of several such calibration runs suitably corrected for variations in temperature and barometric pressure during the run. The mean value is seen to be 12.95 ± 0.2 cm Hg difference in pressure at 15°C for each mm difference in range in air at 76.0 cm Hg and 15°C.

This method of calibration gives directly the range difference of two groups of alpha-particles measured with the cell. It automatically takes into account the irregularities of the screens, the variation of the air equivalent of window with the alpha-particle energy, any deviation from uniformity of the collecting field in the ionization chamber, the protruding of the collodion window through the screen apertures and any variation of this with pressure, and finally it minimizes any correction to the range difference due to change in obliquity of the two groups,—for although the geometry for the calibration was not

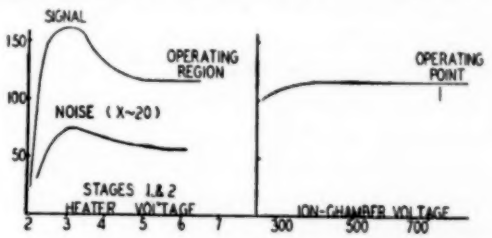

FIG. 3. Some operating characteristics of the amplifier and ionization chamber.

identical with that for the reactions investigated, it was not very different.

The geometry for the experiment was "good" according to the criteria of Livingston and Bethe[8] whose notation is used below. The ratio of the limiting aperture widths to the separation between them (one of them being the target spot) was $a/b=0.12$ while the quantity $\cos\theta_0$ was equal to 0.26 and 0.18 for the lithium and beryllium reactions, respectively. The obliquity correction was found to be less than 0.01 mm and was neglected. The angle straggling should be symmetrical and therefore not affect the mean range.

Pressure in the cell was measured with an open-tube mercury manometer. Atmospheric pressure was measured with an aneroid barometer frequently checked against the standard barograph at the U. S. weather bureau observatory a few hundred yards away. The temperature of the cell was read from a thermometer pressing against it. This temperature was usually about 2°C higher than that of the room because of heat conduction from the target chamber. Diffusion of cooler air into the cell was impeded by making the pressure lead of small bore.

Lithium targets were prepared by deposition of the fluoride from a flame upon a nickel button. For the beryllium targets, the fluoride was deposited from an oxygen flame. Because of the high yields from the beryllium reaction,[6] it was found necessary to rub the targets clean before the intensity was reduced enough to enable accurate measurement. A high intensity of particles produces an apparent shortening of the range as well as some straggling, due to particles crowding up on the "back-kick" of a given amplifier pulse.

Targets were heated after the fashion described by Hatch.[6] It is certain that the beryllium targets remained free of carbon. For the lithium ones, however, it was difficult to decide since alkali halides become discolored by bombardment with charged particles. It may have been the case that cohesive forces between the lithium fluoride and such organic materials as pump oil were stronger than those due to heat agitation. In such a case, a film of oil would be left, and would subsequently carbonize. This would reduce the measured range, and because of the irregularity of the carbonization, give increased straggling. To guard against this, no lithium target in the data reported was used for more than one run. However, bombardment of badly discolored targets showed no unidirectional shift of the mean range point, nor any appreciable change in the slope of the number-pressure curves.

The linear amplifier constructed for this research was of the usual resistance coupled type. A 954 acorn pentode was used in the first stage. There were two subsequent stages using 6J7 pentodes followed by two employing 6C5 triodes. Power for these was furnished by a power pack, except that the heater on the second stage was run in parallel with that on the first, a storage battery supplying the current. All stages but the last were self-biased. The power supplies for the amplifier and ionization chamber were of a simple sort, stabilization being achieved by a voltage regulator of the saturated core type placed on the a.c. line. Figure 3 gives some of the characteristics of the amplifier and ionization chamber. The curves on the left show the dependence of the gain and noise upon heater voltage of the first two stages. It is seen that there was a broad plateau in the neighborhood of 6 volts. This coincided with the discharge plateau of the storage battery, making stabilization automatic. The curve on the right shows that the ionization chamber was run at saturation. A scale-of-sixteen circuit similar to that described by Stevenson and Getting[9] was utilized. It was likewise stabilized by way of the a.c. line. The bias voltage was supplied by a battery and read with a good voltmeter.

Measurements

All data were taken with the bombarding beam at 370 kv as measured with a high resistance voltmeter calibrated some time before. This was safely above the observed 330-kev resonance in F^{19}. The deflecting magnet was set on the maximum of the mass 1 spot. Considerations of the ripple in a Cockcroft-Walton type circuit show that most of the beam has the average voltage, so that the energy of the protons at the target could be assumed quite close to 370 kv.

[8] M. S. Livingston and H. A. Bethe, Rev. Mod. Phys. 9, 245 (1937).

[9] E. C. Stevenson and I. A. Getting, Rev. Sci. Inst. 8, 414 (1937).

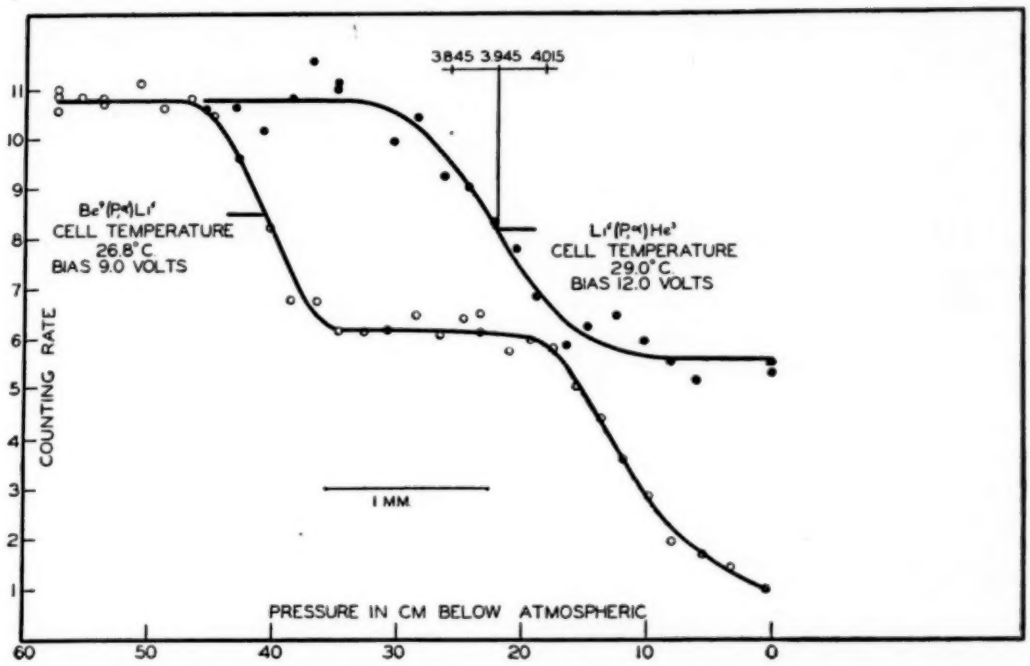

FIG. 4. Data for the computation of the Q value in $Li^6(p,\alpha)He^3$. Both the beryllium and lithium curves as plotted are corrected for barometric variation. Correction for the change in bias of the two curves has not been made. The extreme right of the beryllium curve shows the deuteron cut-off from $Be^9(p,d)Be^8$. The line marked 1 mm is from the calibration data of Table I. The numbers above the lithium curve indicate where the mean range point would have to occur to give various Q values if the alpha-particle energy from $Be^9(p,\alpha)Li^6$ is known exactly.

Care was taken to keep the magnet current constant during a run, and both the magnet and the generator supplying it were allowed to warm up for more than an hour before data were taken. Beams of between two and fifteen microamperes of protons were used, the measurement being made with a current integrator.

A considerable amount of adjustment of the absorption cell constants and the amplifier gain had to be made. Because of the high dispersion of the cell, and because it ran at pressures below atmospheric, only a small range interval could be measured. This interval had to be chosen to include the curves of interest and to exclude scattered protons (range $\sim$4 mm). It was also necessary that the deuterons from $Be^9(p,d)Be^8$ should have a threshold pressure sufficiently low that they might all be counted with the alphas from beryllium. It was found (Fig. 4) that the deuterons had more range in the cell than the alpha-particles and contributed more ionization at all pressures. Pains had then to be taken not to bias out the alphas. A satisfactory solution was achieved by increasing the amplifier gain and decreasing the bias as much as could be done safely. The curve of Fig. 4 marked Be shows the alpha-particles and the deuterons. This is taken at such a bias that at least 1900 ion pairs must be produced to record a count. The yield from the beryllium targets was so great that incidental noise had a negligible effect on these curves. For the lithium reaction, however, the situation was quite different. The only isotopic Li^6 target available was found to be too thick. The yield from the thin fluoride targets was quite small and comparable to the number of small disturbances. It was therefore necessary to count at a higher bias. The bias could not be made too much higher or the low pressure cut-off for the long range alpha-particles from Li^7 might fall in the pressure range being investigated and produce a rapid change in the background. A bias three volts higher (i.e., 12 volts) was found to be suitable. With this the He^3 particles and long range He^4's were counted at all pressures. Since the scaling circuit counted pulses of zero height for a 5.5-volt bias and 9.0 volts corresponded to 1900 ion pairs, 12 volts corresponds to

1900(12.0−5.5)/(9.0−5.5) or 3500 ion pairs. For this the critical pressure P_c is computed to be 25 cm Hg, which is safely below the region of interest.

In Fig. 4 both the beryllium and lithium curves are shown. The mean range of the lithium had to be corrected for the three-volt change in bias. This was done with the calibration apparatus, curves being taken at both biases without moving the micrometer. *B* and *C* of Fig. 2 are such a pair. Two runs judged to be of equal weight gave 5.80 and 6.00 cm Hg difference in pressure at 15°C for a three-volt bias change when suitable corrections were applied. The mean is then 5.90±0.04.

An interesting point concerning the lithium reaction is that there were not as many He^3 as He^4 particles observed. This is explicable if the reaction does not have spherical symmetry; for 90° in the laboratory system corresponds to different angles in the center of mass system for the two kinds of particles. A curve taken by varying the bias showed that there were about as many He^3's from Li^6 as long range He^4's from Li^7 and about as many short range He^4's as both together. A curve published by Neuert[4] shows the same inequality. This circumstance was quite helpful in that it reduced the probable error of the base-line on the number-pressure curves.

The energy of the alpha-particles from beryllium was computed from the 1940 revision of the electrostatic analyzer data of Allison, Skaggs, and Smith.[5] With a *Q* value of 2.115±0.04 Mev, the Be alpha-particle energy becomes 1.455±0.024 Mev at 370 kev proton energy. From Table II the pressure separation of the lithium and beryllium curves is 17.75±0.4 cm Hg. The bias correction is 5.90±0.04 cm Hg and addition to the uncorrected separation gives a true separation of 23.65±0.4 cm Hg. Table I gives the cell calibration as 12.95±0.4 cm Hg/mm range whence the true difference in range of the two groups is 1.83±0.04 mm in standard air. From the 1938 Cornell range-energy curve based, presumably, upon the work of Holloway and Livingston[7] the slope at 1.6 Mev is 0.190 Mev/mm. If we estimate a 2 percent uncertainty in this value we get the energy separation to be 0.347±0.009 Mev, the alpha-particles from Li^6 being more energetic. This gives 1.802 Mev for the lithium alpha-particles at 370-kv bombardment voltage. If a 10-kv uncertainty is assumed in both bombarding voltages, and exact masses are used in the computation, the *Q* value for the reaction becomes 3.945±0.06 Mev, practically the entire error being due to the quoted uncertainty of the electrostatic deflection determination of the beryllium reaction, an uncertainty which is probably not as large as assumed.

TABLE I. *Calibration of the absorption cell.*

Trial	Motion of Source (cm)	$\Delta P/\Delta R$ cm Hg per mm range	Weight
1*	0.100	12.65	10
2	0.150	12.45	10
3	0.100	14.40	3
4	0.150	13.38	8

Weighted average result: 12.95±0.2 cm Hg at 15°C is equivalent to 1-mm range at 76 cm Hg and 15°C

* Fig. 2, Curves *A*, *C*.

Application of Results

From the present measurements and certain others some information of interest may be deduced.

H^3-He^3 mass difference

Consider the reactions:

$$Li^6+H^1\rightarrow He^4+He^3+3.95\pm0.06, \quad (1)$$

$$D^2+D^2\rightarrow H^3+H^1+3.98\pm0.02, \quad (2)$$

$$Li^6+D^2\rightarrow He^4+He^4+22.20\pm0.04. \quad (3)$$

These three energies were determined with absorption cells, (1) and (3) were studied in this laboratory, (1) by the author and (3) by Smith.[10] Reaction (2) is described by Oliphant, Kempton and Rutherford,[11] and corrected by Livingston and Bethe.[8] From these three we get

$$(2D^2-He^4)-(2H^1-D^2)$$
$$=(H^3-He^3)+22.23 \text{ Mev}.$$

TABLE II. *Pressure separation of alpha-particles from* $Li^6(p,\alpha)He^3$ *and* $Be^9(p,\alpha)Li^6$.

Trial	ΔP in cm Hg	Weight
1	17.35	10
2	17.85	8
3	19.5	2

Weighted average result: ΔP = 17.75±0.4 cm Hg at 15°C

[10] N. M. Smith, Jr., Phys. Rev. **56**, 548 (1939).
[11] M. L. E. Oliphant, A. E. Kempton, and Lord Rutherford, Proc. Roy. Soc. **149**, 406 (1935).

The quantities on the left in parentheses are well-known mass-spectrograph brackets. If we use Bainbridge's values we get $H^3-He^3=0.19\pm0.09$ while Aston's predict $H^3-He^3=0.10\pm0.1$. That is we may expect H^3 to emit a low energy beta-ray. Neuert's value of 3.72 for reaction (1) would make H^3 stable by 50 and 130 kev for the two cases above. In the second case H^3 would be stable within the experimental error. The radioactivity of H^3 was recently observed by Alvarez and Cornog[2] who estimated the energy of the beta-ray to be about 10 Kev. Still more recently O'Neal and Goldhaber[12] have given evidence for the reaction $Be^9+D^2\rightarrow Be^8+H^3$ and detected beta-rays of about the same energy.

The present measurements give greater consistency than Neuert's with another series of reactions, suggested by Rumbaugh, Roberts, and Hafstad.[13] These reactions are

$$D^2+D^2\rightarrow H^1+H^3+Q_1,$$
$$D^2+D^2\rightarrow n^1+He^3+Q_2,$$
$$Li^6+n^1\rightarrow He^4+H^3+Q_3,$$
$$Li^6+H^1\rightarrow He^4+He^3+Q_4.$$

From these we get

$$(Q_2+Q_3)-(Q_1+Q_4)\equiv f(Q)=0.$$

Table III gives various values of the discrepancy $f(Q)$ for different determinations of the Q's. It is seen that the value $Q_4=3.95\pm0.06$ given by the author is in better agreement with all the different combinations chosen than that of Neuert. The smallest discrepancy (0.03 Mev) is obtained with Bonner's latest value of the energy of the neutrons from the D on D reaction, and with Livingston and Hoffman's earliest value of the Li^6 plus neutron reaction.

TABLE III. *Values of the discrepancy* $f(Q)=(Q_2+Q_3)-(Q_1+Q_4)$ *for various combinations of the values of* Q *from the reactions* $D(d,p)H^3$, Q_1; $D(d,n)He^3$, Q_2; $Li^6(n,\alpha)H^3$, Q_3; $Li^6(p,\alpha)He^3$, Q_4.

REACTION	Q	ERROR QUOTED	COMBINATION	$f(Q)$ MEV
†Q_1	3.98	0.02	$(Q_1Q_2Q_3Q_4')$	−0.08
†Q_2	3.18	0.13	$(Q_1Q_2Q_3'Q_4')$	+0.11
Q_2'	3.29	0.08	$(Q_1Q_2Q_3''Q_4')$	+0.22
†Q_3	4.67	0.05	$(Q_1Q_2'Q_3Q_4')$	+0.03
Q_3'	4.86	0.04	$(Q_1Q_2'Q_3'Q_4')$	+0.22
Q_3''	4.97		$(Q_1Q_2'Q_3''Q_4')$	+0.33
†Q_4	3.72	0.08	$(Q_1Q_2Q_3Q_4)$	+0.15
Q_4'	3.95	0.06	$(Q_1Q_2Q_3'Q_4)$	+0.34
			$(Q_1Q_2Q_3''Q_4)$	+0.45
			$(Q_1Q_2'Q_3Q_4)$	+0.26
			$(Q_1Q_2'Q_3'Q_4)$	+0.45
			$(Q_1Q_2'Q_3''Q_4)$	+0.56

† Corrected by Livingston and Bethe.[8]
Q_1, M. L. E. Oliphant, A. E. Kempton, and Lord Rutherford, Proc. Roy. Soc. **149**, 406 (1935).
Q_2, T. W. Bonner and W. M. Brubaker, Phys. Rev. **49**, 19 (1936).
Q_2', T. W. Bonner, Phys. Rev. **53**, 711 (1938).
Q_3, M. S. Livingston and J. G. Hoffman, Phys. Rev. **50**, 401 (1936).
Q_3', M. S. Livingston and J. G. Hoffman, Phys. Rev. **53**, 227 (1938).
Q_3'', L. H. Rumbaugh, R. B. Roberts and L. R. Hafstad, Phys. Rev. **54**, 657 (1938).
Q_4, H. Neuert, Physik. Zeits. **36**, 629 (1935).
Q_4', Present measurements.

Mass of He^3

In the absence of a good measurement of the upper limit of the β-ray spectrum from H^3, the best method of computing the mass of He^3 appears to be the following:

$$Li^6+H^1\rightarrow He^4+He^3+3.95\pm0.06 \text{ Mev},$$
$$Li^6+D^2\rightarrow He^4+He^4+22.20\pm0.04 \text{ Mev},$$
$$H^1=1.00812\pm0.000,02,$$
$$D^2=2.01472\pm0.000,02,$$
$$He^4=4.00388\pm0.000,07.$$

From this we obtain $He^3=3.01688\pm0.000,11$ mass units. This is to be compared with the value $3.01701\pm0.000,12$ quoted in the paper by Barkas.[14]

The 1.9-Mev excited state in He^3 reported by Bonner[1] would result in particles of too short range to be detected in this experiment.

The author wishes to express his indebtedness to Professor S. K. Allison for his extremely helpful direction of this research; also to Dr. L. S. Skaggs for the considerable time he spent aiding in the performance of the experiment. The author is also grateful to Miss M. R. Jones of the Chemistry Department for her aid in preparing a strong polonium source.

[12] R. D. O'Neal and M. Goldhaber, Phys. Rev. **57**, 1086 (1940).
[13] L. H. Rumbaugh, R. B. Roberts, and L. R. Hafstad, Phys. Rev. **54**, 657 (1938).
[14] W. H. Barkas, Phys. Rev. **55**, 691 (1939).

The Rotational Magnetic Moments of H_2, D_2, and HD Molecules*

The Rotational Radiofrequency Spectra of H_2, D_2, and HD in Magnetic Fields

N. F. RAMSEY, JR.**
Columbia University, New York, New York

(Received May 27, 1940)

The radiofrequency spectra of H_2, D_2, and HD molecules have been obtained for transitions corresponding to reorientations of the rotational angular momenta of the molecules. From these spectra the rotational magnetic moments of H_2, HD, and D_2 molecules in the first rotational states are found to be $+0.8787\pm0.0070$, $+0.6601\pm0.0050$, and $+0.4406\pm0.0030$ nuclear magneton, respectively, all of the moments being positive. The relative values are good to 0.2 percent and to this precision they are in the ratio 4 : 3 : 2 as expected theoretically. The rotational magnetic moment of H_2 in the second rotational state was found to be just twice that in the first. From the rotational moment values, the high frequency contribution to the diamagnetic susceptibility of H_2 is deduced to be $(0.093\pm0.007)\times10^{-6}$ per mole. Certain molecular interaction constants, including the interaction of the quadrupole moment of the deuteron with the inhomogeneous electric field of the molecule, are also obtained. The results are in complete agreement with similar measurements from the nuclear reorientation spectrum. Furthermore, the dependence upon orientation of the diamagnetic susceptibility of the hydrogen molecule in the first rotational state can be found. It is such that $\xi_{\pm1}-\xi_0=-(4.5\pm2.0)\times10^{-31}$ per molecule.

INTRODUCTION

THE molecular beam magnetic resonance method[1-3] was originally designed for the measurement of nuclear magnetic moments, but since rotational magnetic moments of molecules are of the same order of magnitude the method may be directly applied to the measurement of these moments as well. The chief difference is that a different ratio of frequency to magnetic field must be used so that resonance minima corresponding to reorientations of the rotational angular momenta instead of the nuclear spins may be observed. In addition to the rotational magnetic moments of the molecules, certain molecular interaction constants can be evaluated from the present experiments and compared with values of the same constants as found by Kellogg, Rabi, Ramsey, and Zacharias.[1,2] These constants measure the interaction energies of the nuclear magnetic moments with the rotational magnetic field of the molecule, the mutual interaction energy of the two nuclear magnetic moments with each other, and—most important of all—the interaction energy of the deuteron quadrupole moment[2,4] with the inhomogeneous electric field of the molecule. A still different constant measuring the dependence of the diamagnetic susceptibility of a hydrogen molecule upon its orientation can also be found.

The only previous measurements of rotational magnetic moments are those of Estermann and Stern,[5] who found by measurements on para-H_2 molecules in rotational state $J=2$ that the rotational magnetic moment was between 0.8 and 0.9 nuclear magneton per rotational quantum number. The present experiment not only pro-

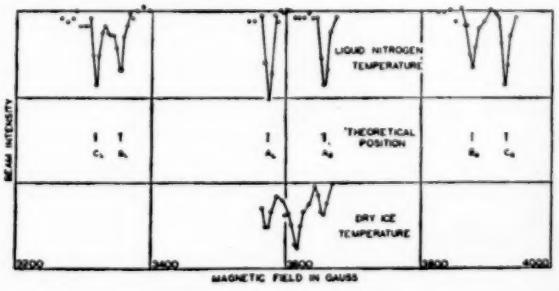

FIG. 1. The radiofrequency spectrum of H_2 corresponding to transitions in which the rotational angular momentum changes its orientation. The oscillator frequency is 2.4198 megacycles and the oscillating field about 10 gauss ($I_F=3.5$ amp.).

* Publication assisted by the Ernest Kempton Adams Fund for Physical Research of Columbia University.

** Now at the University of Illinois.

[1] J. M. B. Kellogg, I. I. Rabi, N. F. Ramsey, Jr., and J. R. Zacharias, Phys. Rev. **56**, 728 (1939).

[2] J. M. B. Kellogg, I. I. Rabi, N. F. Ramsey, Jr., and J. R. Zacharias, Phys. Rev. **57**, 677 (1940).

[3] I. I. Rabi, S. Millman, P. Kusch, and J. R. Zacharias, Phys. Rev. **55**, 526 (1939).

[4] J. M. B. Kellog, I. I. Rabi, N. F. Ramsey, Jr., and J. R. Zacharias, Phys. Rev. **55**, 318 (1939).

[5] I. Estermann and O. Stern, Zeits. f. Physik **85**, 17 (1933).

vides a much more accurate measurement of the rotational magnetic moment of H_2 by an entirely different method, but is also applied to D_2 and HD molecules and can be used to determine the signs as well as the magnitudes of the moments. Furthermore, the rotational magnetic moments of H_2 both in the first and in the second rotational states can be separately measured, whence the proportionality of the magnetic moment to the rotational angular momentum may be experimentally tested. This proportionality was assumed by Estermann and Stern[5] in their determination of the magnetic moment of the proton and is predicted theoretically by Wick,[6,7] but up to now no experimental evidence has been obtainable.

Method and Apparatus

The method used in this experiment is that described by RMKZ[3] and KRRZ.[1,2] As the latter authors have pointed out, the molecular beam magnetic resonance method may be regarded as a means of obtaining the absorption and stimulated emission spectra of molecules at radiofrequencies. Thus, the minima of beam intensity in the accompanying curves occur when the oscillator frequency f_0 is equal to the Bohr frequency, $\nu=\Delta E/h$, of the molecule, where ΔE is the energy difference corresponding to any two orientation states of the molecule between which the transitions are allowed, that is, states

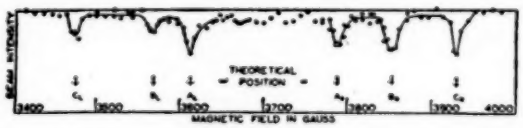

FIG. 2. The radiofrequency spectrum of D_2 corresponding to transitions in which the rotational angular momentum changes its orientation. The oscillator frequency is 1.2410 megacycles and the oscillating field about 14 gauss ($I_P=4.8$ amp.). The temperature is that of liquid nitrogen.

for which the total magnetic quantum numbers differ by an amount $\Delta M=\pm 1$. Hence by observations of the positions of these resonance minima the dependence of the energy of the molecule on its orientation may be deduced. When, as in the present experiment, the reorientation transitions occur in the presence of a homogeneous magnetic field, the energy depends upon the values of the nuclear and rotational magnetic moments of the molecule as well as upon certain interaction constants within the molecule; so, from the observed radiofrequency spectrum, the magnetic moments and the interaction constants may be deduced.

A group of resonance minima may be obtained corresponding to reorientations either of the nuclear or of the rotational angular momentum, i.e., to a change either of m_I or m_J. Experiments

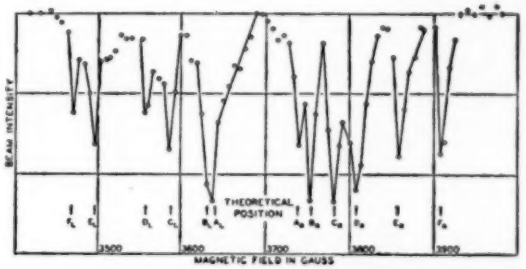

FIG. 3. The radiofrequency spectrum of HD corresponding to transitions in which the rotational angular momentum changes its orientation. The oscillator frequency is 1.850 megacycles and the oscillating field about 12 gauss ($I_P=4$ amp.). The temperature is that of liquid nitrogen.

of the former type have been done by KRRZ[1,2] in measuring nuclear moments, whereas the present experiments are limited to changes of m_J from which the rotational magnetic moments are obtainable.

The molecular beam apparatus used for this work is that which has already been fully described by KRRZ.[1] Since the present observations were taken with the same apparatus that was used in the proton and deuteron nuclear magnetic moment measurements the same magnet calibration could be used. As a check that the magnet had not changed, measurements of the nuclear magnetic moments were made during the course of the rotational measurements and were found to agree with the earlier measurements. In this way values of the rotational magnetic moments relative to a value of the proton moment of 2.785 nuclear magnetons were obtained to a greater precision than the precision of the absolute calibration of the magnetic field.

Results

The experimental results on the groups of resonance minima corresponding to $\Delta m_J=\pm 1$

[6] G. C. Wick, Zeits. f. Physik **85**, 25 (1933).
[7] G. C. Wick, Nuovo Cimento **10**, 118 (1933).

TABLE I. *Magnetic fields at which H_2 rotational resonances should occur for a fixed oscillator frequency $f_0=\mu_{R-H_2}H_0/h$. $H''=(\mu_P/r^3)_M$, $\alpha=\mu_{R-H_2}/2\mu_P$, and $k=(\xi_{+1}-\xi_0)/2\mu_{R-H_2}$. The numerical evaluations of the small second-order terms come from KRRZ's values of H' and H''.*

Δm_J	m_I	Magnetic Fields: First Order	Magnetic Fields: Second Order	Numerical Value of Second Order
0→1	1	$H_0-\frac{1}{\alpha}H'+\frac{3}{5\alpha}H''+kH^2+\frac{1}{\alpha}\frac{(3H''/5-H')^2}{H(1-\alpha)}$		$+\frac{338}{H}$
0→1	0	$H_0 \quad -\frac{6}{5\alpha}H''+kH^2+\frac{1}{\alpha}\frac{(3H''/5-H')^2}{H(1-\alpha)}$		$+\frac{338}{H}$
0→1	−1	$H_0+\frac{1}{\alpha}H'+\frac{3}{5\alpha}H''+kH^2+\frac{6H''}{5\alpha}\frac{(3H''/5+2H')}{H(1-\alpha)}$		$+\frac{23,180}{H}$
−1→0	1	$H_0-\frac{1}{\alpha}H'-\frac{3}{5\alpha}H''-kH^2+\frac{6H''}{5\alpha}\frac{(3H''/5+2H')}{H(1-\alpha)}$		$+\frac{23,180}{H}$
−1→0	0	$H_0 \quad +\frac{6}{5\alpha}H''-kH^2+\frac{1}{\alpha}\frac{(3H''/5-H')^2}{H(1-\alpha)}$		$+\frac{338}{H}$
−1→0	−1	$H_0+\frac{1}{\alpha}H'-\frac{3}{5\alpha}H''-kH^2+\frac{1}{\alpha}\frac{(3H''/5-H')^2}{H(1-\alpha)}$		$+\frac{338}{H}$

are shown in Figs. 1, 2, and 3 for H_2, D_2, and HD. Approximate values of the rotational magnetic moments (good to about 1.5 percent) can be obtained by merely using the values of the oscillator frequencies and of the magnetic fields at the centers of the groups of minima in the formula for the Larmor precession frequency ($\nu=\mu H/Jh$). However, because of the asymmetry of the curves, accurate determinations of the rotational magnetic moments as well as determinations of the interaction constants of the molecules depend on the detailed nature of the interaction functions as is discussed in subsequent paragraphs.

That the resonance minima shown in the accompanying diagrams correspond to changes of the rotational m_J is indicated by the following results: (1) that unlike the nuclear cases these groups of resonance minima do not correspond to magnetic moments common to either H_2 and HD or D_2 and HD, (2) that a new minimum arises in the center of the group of H_2 minima when the temperature is raised so that a higher rotational state is excited, (3) that the magnetic moments observed with H_2, HD, and D_2 are approximately inversely proportional to the moments of inertia of the molecules as expected theoretically for rotational magnetic moments, and (4) that this assumption makes possible a correct theoretical prediction of the separations of the various minima in a single group.

It is easily possible to account for the number of observed resonance minima in Figs. 1, 2, and 3. All but one of the curves are taken with the source at liquid nitrogen temperature at which, because of the low moments of inertia of hydrogen molecules, most of the molecules are in the zeroth or first rotational state.[1] Since it is impossible to change the value of m_J when the rotational quantum number, J, equals zero, the only molecules of interest are those for which J equals one. In the cases of H_2 and D_2, where the two nuclei are identical, the quantum-mechanical symmetry conditions require that the only varieties of molecules that can have $J=1$ are ortho-H_2 and para-D_2, for both of which the total nuclear spin, I, equals one. Therefore with H_2 and D_2 at liquid nitrogen temperature the only molecules concerned in the experiment are those with $I=1$ and $J=1$, whence there are nine energy levels corresponding to all allowed orientations of I and J and between these energy levels six different transitions corresponding to $\Delta m_J=\pm 1$ can occur. This is the reason that six resonance minima are observed for H_2 and D_2 at liquid nitrogen temperature. The additional H_2 minimum which appears when dry ice is placed in the source trap is due to molecules of para-H_2 with $I=0$ which are partially excited to rotational state two at the higher temperature. Since $I=0$, there is no spin-spin or spin-rotational interaction so only a single new peak is produced.

TABLE II. *Magnetic fields at which* D_2 *rotational resonances should occur for a fixed oscillator frequency* $f_0=\mu_{R-D_2}H_0/h$. $S_D=1/5(H''+H''')$, $H''=\langle\mu_D/r^3\rangle_{Av}$, $H'''=-5e^2qQ/4\mu_D$, $\alpha=\mu_{R-D_2}/\mu_D$, *and* $k=(\xi_{x1}-\xi_0)/2\mu_{R-D_2}$. *The* C_i*'s are as in KRRZ.*[2] *The numerical evaluations of the small second- and third-order terms come from KRRZ's values of* H' *and* S_D.

Δm_J	m_I	Magnetic Fields: First Order	Second Order	Third Order	Numerical Values of Second and Third Orders
$0\leftrightarrow1$	1	$H_0-\frac{1}{\alpha}H'+\frac{3}{\alpha}S_D+kH^2$		$+\frac{1}{\alpha}C_2'$	$+\frac{8{,}050}{H}$
$0\leftrightarrow1$	0	H_0	$-\frac{6}{\alpha}S_D+kH^2$	$+\frac{1}{\alpha}C_2'-\frac{2}{\alpha}C_3$	$+\frac{8{,}050}{H}+\frac{14{,}140{,}000}{H^2}$
$0\leftrightarrow1$	-1	$H_0+\frac{1}{\alpha}H'+\frac{3}{\alpha}S_D+kH^2+\frac{1}{\alpha}C_2$		$-\frac{1}{\alpha}C_2'-\frac{1}{\alpha}C_3$	$+\frac{41{,}300}{H}+\frac{7{,}070{,}000}{H^2}$
$-1\leftrightarrow0$	1	$H_0-\frac{1}{\alpha}H'-\frac{3}{\alpha}S_D-kH^2+\frac{1}{\alpha}C_2$		$-\frac{1}{\alpha}C_2'+\frac{1}{\alpha}C_3$	$+\frac{41{,}300}{H}-\frac{7{,}070{,}000}{H^2}$
$-1\leftrightarrow0$	0	H_0	$+\frac{6}{\alpha}S_D-kH^2$	$+\frac{1}{\alpha}C_2'+\frac{2}{\alpha}C_3$	$+\frac{8{,}050}{H}-\frac{14{,}140{,}000}{H^2}$
$-1\leftrightarrow0$	-1	$H_0+\frac{1}{\alpha}H'-\frac{3}{\alpha}S_D-kH^2$		$+\frac{1}{\alpha}C_2'$	$+\frac{8{,}050}{H}$

For HD where the nuclei are not identical, there is no symmetry restriction so the number of states with $J=1$ is eighteen, corresponding to all possible orientations of the spins of the two nuclei and of the rotational angular momentum. Between these eighteen states twelve different transitions with $\Delta m_J=\pm1$ can occur, which correspond to the twelve observed resonance minima.

By making the same assumptions as were made by KRRZ,[1,2] that is, by assuming the only interaction energies within the molecule to be a spin-spin magnetic interaction energy, a spin-rotational magnetic interaction energy, and the interaction of a deuteron electrical quadrupole moment with the inhomogeneous electric field of the molecule, it is possible to account not only for their results but also quite well for the present ones. Such agreement should be expected since the present experiments concern merely different transitions between the same set of energy levels. However, if in addition to their assumption, one takes into account the diamagnetic interaction energies of the molecules with the external field, the agreement between theory and experiment is even better, being perfect to well within the experimental error. This new assumption amounts to adding a term $-\frac{1}{2}\xi_{m_J}H^2$ to the Hamiltonian where ξ_{m_J} is the diamagnetic susceptibility of the molecule in the rotational state J when the rotational magnetic quantum number is m_J. This term gives rise to a displacement of the rotational resonance minima because of the dependence of the diamagnetic susceptibility ξ_{m_J} upon m_J, ξ_{m_J} clearly being least in magnitude when the line of the nuclei and hence the electron distributions are most nearly parallel to the field ($m_J=0$) and greatest when they are most nearly perpendicular to the field ($m_J=\pm J$). This added term of course does not affect the agreement already obtained by KRRZ,[1,2] since m_J and hence ξ_{m_J} is unaltered in these transitions whence its effect cancels out. With this assumption added to those of KRRZ the Hamiltonian of a diatomic molecule in a magnetic field $\mathbf{H}$ becomes (apart from terms independent of orientation)

$$\mathfrak{H}=-\boldsymbol{\mu}_1\cdot\mathbf{H}-\boldsymbol{\mu}_2\cdot\mathbf{H}-\boldsymbol{\mu}_R\cdot\mathbf{H}-H_1'(\boldsymbol{\mu}_1\cdot\mathbf{J})-H_2'(\boldsymbol{\mu}_2\cdot\mathbf{J})$$
$$+\frac{1}{r^3}\left\{\boldsymbol{\mu}_1\cdot\boldsymbol{\mu}_2-\frac{3(\boldsymbol{\mu}_1\cdot\mathbf{r})(\boldsymbol{\mu}_2\cdot\mathbf{r})}{r^2}\right\}-\tfrac{1}{2}\xi_{m_J}H^2 \qquad (1)$$
$$+\sum_{k=1}^{2}\frac{e^2q_kQ_k}{2I_k(2I_k-1)J(2J-1)}$$
$$\times\{3(\mathbf{I}_k\cdot\mathbf{J})^2+\tfrac{3}{2}\mathbf{I}_k\cdot\mathbf{J}-\mathbf{I}_k^2\mathbf{J}^2\},$$

where $\boldsymbol{\mu}_1$ and $\boldsymbol{\mu}_2$ are the nuclear magnetic moments, $\boldsymbol{\mu}_R$ the rotational magnetic moment, $\mathbf{J}$ the rotational angular momentum in units of

TABLE III. *Magnetic fields at which* HD *rotational resonances should occur for a fixed oscillator frequency* $f_0=\mu_{R\text{-HD}}H_0/h$. $S=(2\mu_P\mu_D/5r^3)_{Av}$, $E=H'''/5=+e^2qQ/4\mu_D$, $\alpha_P=\mu_{R\text{-HD}}/\mu_P$, $\alpha_D=\mu_{R\text{-HD}}/\mu_D$, *and* $k=(\xi_{+1}-\xi_0)/2\mu_{R\text{-HD}}$. *The numerical evaluations of the small second- and third-order terms come from KRRZ's values of* H_P', H_D', S, *and* E.

Δm_J	m_P	m_D	Magnetic Fields: First Order	Second Order	Third Order
$0\leftrightarrow 1$	$\frac{1}{2}$	1	$H_0-\frac{1}{\alpha_P}H_P'-\frac{1}{\alpha_D}H_D'+\frac{3}{\alpha_D}S-\frac{3}{\alpha_D}E+kH^2$	$+\frac{16,300}{H}$	$+\frac{2,650,000}{H^2}$
$0\leftrightarrow 1$	$\frac{1}{2}$	0	$H_0-\frac{1}{\alpha_P}H_P'+\frac{6}{\alpha_D}E+kH^2$	$+\frac{32,220}{H}$	$-\frac{590,000}{H^2}$
$0\leftrightarrow 1$	$\frac{1}{2}$	-1	$H_0-\frac{1}{\alpha_P}H_P'+\frac{1}{\alpha_D}H_D'-\frac{3}{\alpha_D}S-\frac{3}{\alpha_D}E+kH^2$	$+\frac{394}{H}$	$+\frac{2,470,000}{H^2}$
$0\leftrightarrow -1$	$-\frac{1}{2}$	1	$H_0+\frac{1}{\alpha_P}H_P'-\frac{1}{\alpha_D}H_D'-\frac{3}{\alpha_D}S-\frac{3}{\alpha_D}E+kH^2$	$+\frac{47,000}{H}$	$-\frac{7,150,000}{H^2}$
$0\leftrightarrow -1$	$-\frac{1}{2}$	0	$H_0+\frac{1}{\alpha_P}H_P'+\frac{6}{\alpha_D}E+kH^2$	$+\frac{35,300}{H}$	$-\frac{10,430,000}{H^2}$
$0\leftrightarrow -1$	$-\frac{1}{2}$	-1	$H_0+\frac{1}{\alpha_P}H_P'+\frac{1}{\alpha_D}H_D'+\frac{3}{\alpha_D}S-\frac{3}{\alpha_D}E+kH^2$	$+\frac{19,400}{H}$	$-\frac{9,850,000}{H^2}$
$-1\leftrightarrow 0$	$\frac{1}{2}$	1	$H_0-\frac{1}{\alpha_P}H_P'-\frac{1}{\alpha_D}H_D'-\frac{3}{\alpha_D}S+\frac{3}{\alpha_D}E-kH^2$	$+\frac{19,400}{H}$	$+\frac{9,850,000}{H^2}$
$-1\leftrightarrow 0$	$\frac{1}{2}$	0	$H_0-\frac{1}{\alpha_P}H_P'-\frac{6}{\alpha_D}E-kH^2$	$+\frac{35,300}{H}$	$+\frac{10,430,000}{H^2}$
$-1\leftrightarrow 0$	$\frac{1}{2}$	-1	$H_0-\frac{1}{\alpha_P}H_P'+\frac{1}{\alpha_D}H_D'+\frac{3}{\alpha_D}S+\frac{3}{\alpha_D}E-kH^2$	$+\frac{47,000}{H}$	$+\frac{7,150,000}{H^2}$
$-1\leftrightarrow 0$	$-\frac{1}{2}$	1	$H_0+\frac{1}{\alpha_P}H_P'-\frac{1}{\alpha_D}H_D'+\frac{3}{\alpha_D}S+\frac{3}{\alpha_D}E-kH^2$	$+\frac{394}{H}$	$-\frac{2,470,000}{H^2}$
$-1\leftrightarrow 0$	$-\frac{1}{2}$	0	$H_0+\frac{1}{\alpha_P}H_P'-\frac{6}{\alpha_D}E-kH^2$	$+\frac{32,220}{H}$	$+\frac{590,000}{H^2}$
$-1\leftrightarrow 0$	$-\frac{1}{2}$	-1	$H_0+\frac{1}{\alpha_P}H_P'+\frac{1}{\alpha_D}H_D'-\frac{3}{\alpha_D}S+\frac{3}{\alpha_D}E-kH^2$	$+\frac{16,300}{H}$	$-\frac{2,650,000}{H^2}$

$h/2\pi$, $\mathbf{I}_k$ the nuclear angular momentum in units of $h/2\pi$, $\mathbf{r}$ the radius vector between the two nuclei, Q_k the quadrupole moment of the kth nucleus, q_k the gradient of the electric field at the position of the kth nucleus divided by the charge of an electron, H_1' and H_2' the spin rotational interaction constants and essentially measures of the rotational magnetic fields at the positions of the nuclei, and ξ_{m_J} the diamagnetic susceptibility of the molecule in rotational state J, m_J.

From their Hamiltonian and the ordinary perturbation theory, KRRZ[1,2] have obtained expressions for the energies of the different molecular states when $J=1$ to the approximation of the third order perturbation theory. The energy expressions needed here are merely those of KRRZ with the above diamagnetic term added. These energy expressions may be differenced subject to the restriction $\Delta m_J=-1$ and from these differences and from the relation $hf_0=\Delta E$, expressions for the predicted fields at which resonance minima should occur may be obtained. These expressions for H_2, D_2, and HD molecules in the first rotational state are given in Tables I, II, and III, respectively, the notation being that of KRRZ[1,2] whenever possible. The numerical expressions for the small second- and third-order perturbations are based on the values of the interaction constants obtained by KRRZ. It should be noted that all the first-order corrections are symmetrical about H_0 so the second-order corrections are important in that they account for the observed asymmetry of the results.

From the expressions of the tables and from the values of the interaction constants found by KRRZ[1,2] in the nuclear resonance experiments,

the theoretical positions of the resonance minima may readily be predicted subject to the assumption of appropriate values for the μ_R's and $\xi_{\pm 1}-\xi_0$, the only remaining adjustable constants. When this is done, excellent agreement with the observations is obtained. This agreement makes possible an identification of the quantum numbers associated with each resonance minimum and shows the complete consistency of these results with those of KRRZ. The quantum numbers to be identified with each minimum are given in Tables IV, V, and VI, the correlation between these tables and the curves being the designation letters A_L, etc. The best determinations of the experimental positions of the resonances are also given in these tables.

After this identification has once been made, the process may be performed in the reverse direction and the experimental results used to evaluate the various interaction constants. The values so found not only provide a check upon the values of the same quantities as obtained from the nuclear resonance minima, but in some cases, like H_2 where the separations in gauss of the rotational minima are about seven times greater than the separations of the nuclear minima, the determinations can be made more accurately from the rotational than from the nuclear experiments. This evaluation has been performed by equating the theoretical resonance positions of Tables I, II, and III to the corresponding observed positions listed in Tables IV, V, and VI and by solving for the desired constants by the method of least squares. The values of the various quantities obtained in this way are as follows:

(a) For H_2 in the first rotational state when $f_0=2.420$ megacycles: $H_0=3613.1$ gauss, $H'=26.8\pm0.3$ gauss, $H''=33.9\pm0.3$ gauss, and

$$\xi_{\pm 1}-\xi_0=-(3.9\pm2.5)\times10^{-31}$$

per molecule;

(b) For D_2 in the first rotational state when $f_0=1.2410$ megacycles: $H_0=3696.2$ gauss, $H'=13.7\pm0.8$ gauss, $S_D=19.55\pm0.20$ gauss, and

$$\xi_{\pm 1}-\xi_0=-(5.1\pm2.5)\times10^{-31}$$

per molecule;

(c) For HD in the first rotational state when $f_0=1.850$ megacycles: $H_0=3677.4$ gauss, $H_D'=20.5\pm1.5$ gauss, $H_P'=20.23\pm0.5$ gauss, $S=11.70\pm0.5$ gauss, $E=17.30\pm0.3$ gauss, and

$$\xi_{\pm 1}-\xi_0=-(4.6\pm3.5)\times10^{-31}$$

per molecule.

The number of observed resonance minima exceeds the number of available parameters, but

TABLE IV. *Observed positions of* H_2 *rotational resonances and comparison with theory when* $f_0=2.420$ *megacycles. The theoretical positions are based on the values of* H_0, H', H'', *and k evaluated from these data by the method of least squares.*

Δm_J	m_I	Designation of Minimum	Experimental Position of Resonance (Gauss)	Theoretical Position (Gauss)
$0\leftrightarrow1$	1	A_L	3573.0	3572.9
$0\leftrightarrow1$	0	B_L	3354.3	3354.7
$0\leftrightarrow1$	−1	C_R	3920.3	3919.6
$-1\leftrightarrow0$	1	C_L	3319.3	3319.7
$-1\leftrightarrow0$	0	B_R	3871.3	3871.5
$-1\leftrightarrow0$	−1	A_R	3653.6	3653.5

TABLE V. *Observed positions of* D_2 *rotational resonances and comparison with theory when* $f_0=1.2410$ *megacycles. The theoretical positions are based on the values of* H_0, H', S_D, *and k evaluated from these data by the method of least squares.*

Δm_J	m_I	Designation of Minimum	Experimental Position of Resonance (Gauss)	Theoretical Position (Gauss)
$0\leftrightarrow1$	1	A_R	3787.3	3786.8
$0\leftrightarrow1$	0	C_L	3473.6	3473.9
$0\leftrightarrow1$	−1	B_R	3849.4	3849.5
$-1\leftrightarrow0$	1	B_L	3565.1	3565.2
$-1\leftrightarrow0$	0	C_R	3922.6	3922.8
$-1\leftrightarrow0$	−1	A_L	3610.5	3610.0

TABLE VI. *Observed positions of* HD *rotational resonances and comparison with theory when* $f_0=1.850$ *megacycles. The theoretical positions are based on the values of* H_0, H_P', H_D', S, E, *and k evaluated from these data by the method of least squares.*

Δm_J	m_P	m_D	Designation of Minimum	Experimental Position of Resonance (Gauss)	Theoretical Position (Gauss)
$0\leftrightarrow1$	$\frac{1}{2}$	1	D_L	3556.5	3557.1
$0\leftrightarrow1$	$\frac{1}{2}$	0	A_R	3737.7	3736.1
$0\leftrightarrow1$	$\frac{1}{2}$	−1	E_L	3499.6	3499.4
$0\leftrightarrow1$	$-\frac{1}{2}$	1	B_L	3631.8	3629.2
$0\leftrightarrow1$	$-\frac{1}{2}$	0	F_R	3906.5	3906.6
$0\leftrightarrow1$	$-\frac{1}{2}$	−1	C_R	3779.9	3780.8
$-1\leftrightarrow0$	$\frac{1}{2}$	1	C_L	3583.2	3584.9
$-1\leftrightarrow0$	$\frac{1}{2}$	0	F_L	3469.6	3467.9
$-1\leftrightarrow0$	$\frac{1}{2}$	−1	B_R	3750.0	3750.9
$-1\leftrightarrow0$	$-\frac{1}{2}$	1	E_R	3857.1	3855.6
$-1\leftrightarrow0$	$-\frac{1}{2}$	0	A_L	3631.8	3636.4
$-1\leftrightarrow0$	$-\frac{1}{2}$	−1	D_R	3806.5	3806.3

the consistency of the results is shown by a comparison of the experimental positions of the resonance minima with the theoretical positions predicted with the above values of the interaction constants. This comparison is given both on the graphs and in the last two columns of Tables IV, V, and VI. It will be seen that the agreement between theory and experiment is excellent—good to about one part in eight thousand for H_2 and D_2. Although the agreement in the case of HD is worse, it is still very good (about one part in two thousand). That the agreement should be worse in this case is not surprising since the experimental observations were by far the most difficult for HD. This was due to the fact that the rotational moment being reoriented was less than one-fourth the magnitude of the proton moment which occurred in the same molecule. Hence a sufficiently strong inhomogeneous field to throw out reoriented molecules caused all the molecules to make such large excursions because of the proton moment that many nonreoriented molecules were lost, which made the observable intensity of the resonance minima very weak. In fact, the average depth of an HD rotational resonance minimum of Fig. 3 was less than one percent of the total beam intensity. As this refocusing difficulty occurred for all the rotational measurements in a greater or lesser degree, here, unlike the nuclear case, no fundamental significance can be attached to the measured intensities of the resonances.

It will be noted that whereas most of the above quantities have been measured to a high precision, such is not true of $\xi_{\pm 1}-\xi_0$. This is due to the fact that at the magnetic fields of the experiments this term only slightly affects the positions of the resonance minima (1.8 gauss out of 3600 gauss at the most). At the time the experiments were performed it was not realized that such a quantity as $\xi_{\pm 1}-\xi_0$ could be obtained from the results, so there was no special effort to make the observations under the most favorable conditions. It is hoped that at some future date the experiments will be carried out at a much higher frequency and field where this diamagnetic effect, which varies as H^2, will be relatively much stronger.

From the frequencies, from the least-squares values of H_0 listed above, and from the relation

$$\mu_R = Jf_0h/H_0 \tag{2}$$

the values of the rotational magnetic moments of the molecules are obtained. These values are $\mu_{R-H_2}=0.8787\pm0.0070$, $\mu_{R-D_2}=0.4406\pm0.0030$, and $\mu_{R-HD}=0.6601\pm0.0050$ nuclear magneton. The moment values here quoted are relative to a value of the nuclear moment of the proton of 2.785 nuclear magnetons.[1] The relative values should be accurate to 0.2 percent although the absolute values of the moments, like the absolute value of the proton moment, are subject to an error of possibly 0.7 percent due to possible errors in the absolute calibration of the magnetic field.[1] Except for the evaluation of the effect of the second-order perturbations which slightly shift the centers of gravity of the groups of resonance minima, the determinations of the rotational magnetic moments are completely independent of the above detailed theory of the molecular interactions. So even if this theory were completely wrong, which is very highly improbable in view of the extensiveness of its experimental verification, the rotational magnetic moments should be correctly evaluated to an accuracy of at least 1.5 percent. Although the most accurate evaluation of the rotational magnetic moments comes as above from the observed value of H_0/f_0, an independent check of the values can be obtained from the separations of the different minima in the group. From Tables I, II, and III it will be noted that the separations of the minima depend on the ratios $\alpha=\mu_R/\mu_D$, etc. Therefore the agreement of the values of interaction constants obtained in this experiment with those obtained in the nuclear experiments indicates that the μ_R's have been correctly chosen.

It should be noted that, in the theoretical prediction of the resonance minima positions given above, it was implicitly assumed that the μ_R's were positive. Had the μ_R's been negative there would have been no change in the predicted positions as far as the first-order perturbations are concerned since by Tables I, II, and III the first-order energy perturbations are symmetrical about H_0. However, the direction of the shift due to the second-order perturbation and hence the nature of the asymmetry would have been

TABLE VII. *Summary of results. The notation is in agreement with Table XII of KRRZ.*[3] *The quantity in parenthesis in the μ_D/r^3 column is the value obtained by multiplying μ_P/r^3 by μ_D/μ_P. It is used in obtaining $5e^2qQ/4\mu_D$ from the D_2 observations. The first quantity for H' in* HD *is its value at the position of the proton and the second is at the position of the deuteron.*

MOLECULE	μ_R (N. M.)	$\langle\mu_P/r^3\rangle_{Av}$ (GAUSS)	$\langle\mu_D/r^3\rangle_{Av}$ (GAUSS)	SPIN-ORBIT CONSTANT $=H'$ (GAUSS)	$5e^2qQ/4\mu_D$ (GAUSS)	χ_{HF} (10^{-6} PER MOLE)	$\xi_{\Delta 1}-\xi_0$ (10^{-31} PER MOLECULE)
H_2 when $J=1$	0.8787 ± 0.0070	$33.9\ \pm0.3$		$26.8\ \pm0.3$		0.094 ± 0.007	-3.9 ± 2.5
H_2 when $J=2$	1.757 ± 0.014 or $2(0.8786\pm0.0070)$						
D_2 when $J=1$	0.4406 ± 0.0030		(10.42)	$13.7\ \pm0.8$	87.36 ± 1.2	0.093 ± 0.007	-5.1 ± 2.5
HD when $J=1$	0.6601 ± 0.0050	34.21 ± 1.5	10.26 ± 0.40	20.23 ± 0.5 $20.5\ \pm1.5$	86.50 ± 1.5	0.093 ± 0.007	-4.6 ± 3.5
Average of H_2, D_2, and HD						0.093 ± 0.007	-4.5 ± 2.0

reversed. Therefore, the existence of the slight second-order asymmetry of the experimental curves makes possible a determination of the sign of the rotational magnetic moments. In all three cases the rotational magnetic moments are found to be positive.

One of the most significant results of this experiment is obtained by a comparison of the H_2 resonance minima with the source at liquid nitrogen and at dry ice temperatures, respectively, as shown in Fig. 1. At dry ice temperatures, in addition to the six resonance minima found for H_2 at the lower temperature, where the only nonzero rotational state is the state one, a seventh minimum appears midway between the two central minima of rotational state one. This minimum may be assumed to be due to the second rotational state of H_2 which, though unexcited at liquid nitrogen temperature, is partially excited at dry ice temperature. Since only para-H_2 may be in the second rotational state and since para-H_2 has a zero resultant nuclear spin, there is no spin-spin or spin-rotational interaction so only a single unperturbed resonance minimum is obtained from which the rotational magnetic moment may be directly deduced from Larmor's formula. The magnetic moment as thus obtained is $1.757\pm0.014 = 2(0.8786\pm0.0070)$ nuclear magnetons or just twice the rotational moment of rotational state one. This result may also be obtained directly by observing that the new peak due to the second rotational state falls midway between the two central peaks of the first rotational state, which by Table I are unaffected by the second-order perturbations. Therefore, μ_R/J must be the same for $J=1$ and $J=2$ to within the experimental error of 0.2 percent in the determination of ratios of magnetic moments; in other words, as far as the first two rotational states of H_2 are concerned the rotational magnetic moment is proportional to the rotational angular momentum.

As a check upon the consistency of the results, observations were made upon H_2 at half the frequency and consequently at half the value of the magnetic field used in the published curves. The results are completely consistent with those at the higher frequency. Also the rotational magnetic moments of H_2 and D_2 molecules were measured with an earlier form of the present apparatus in which the path of the beam in the radiofrequency field was only 2.7 cm long in contrast to the present 13.5 cm length. Because of the shortness of the field and the smallness of the beam intensity, it was necessary to use a much stronger oscillating magnetic field whence the resolving power of the apparatus was much less (the half-widths of the resonance minima are proportional to the strength of the oscillating magnetic field[8]). For this reason it was impossible to resolve the individual peaks and there was consequently a much greater uncertainty in the evaluation of the magnetic moments than now. However, the moments could be determined with an estimated error of two percent and these values were reported.[9] The earlier measurements agree with the present ones to within the former's estimated error.

DISCUSSION OF RESULTS

A summary of the results obtained in this experiment is given in Table VII. Those quantities which have also been measured by KRRZ are $\langle\mu_P/r^3\rangle_{Av}$, $\langle\mu_D/r^3\rangle_{Av}$, H', and $5e^2qQ/4\mu_D$. The

[8] I. I. Rabi, Phys. Rev. **51**, 652 (1937).
[9] N. F. Ramsey, Jr., Phys. Rev. **55**, 595(A) (1939).

portion of Table VII pertaining to these quantities may be directly compared with Table XII of KRRZ.[2] It will be seen that the agreement is excellent, being well within the estimated experimental error in all cases. This agreement and the close agreement between theory and experiment in Tables IV, V, and VI provide very strong evidence for the validity of the theory on which this work is based and in particular for the quadrupole moment of the deuteron. A full discussion of this agreement, a final averaging of all the experimental results including those of this paper, and a computation of the deuteron quadrupole moment from the final average of the quantity $5e^2qQ/4\mu_D$ is contained in the paper of KRRZ[2] and will consequently not be discussed further here.

The observed value of the rotational magnetic moment of H_2 falls within the limits 0.8 to 0.9 nuclear magneton per rotational quantum number set experimentally by Estermann and Stern.[5] It also agrees with the much wider theoretical limits set by Wick.[6,7] The uncertainty of Wick's result arises from the sensitiveness of the computed rotational magnetic moment to the nature of the electron wave function of the molecule that is used, the predicted moment being $+0.36$ nuclear magneton with Wang wave functions and $+0.93$ nuclear magneton with another wave function of Wick's invention. It is perhaps worth emphasizing that the observed rotational magnetic moment for H_2 is much different from that which would be obtained if the electrons were a rigid charge distribution which rotated with the same angular velocity as the nuclei. Such a naive theory would predict[10] a rotational magnetic moment in the state $J=1$ of -3 nuclear magnetons which is much different in magnitude and opposite in sign from the observed result, the electron contribution to the magnetic moment from this theory being over thirty times greater than its experimental value. The necessity for a theory such as Wick's in which the electron contribution to the rotational magnetic moment is much less than on the rigid body model is thus evident.

The result that the rotational magnetic moment of H_2 is proportional to its angular momentum would be completely obvious if the electrons were assumed to behave as a rigid charge distribution, but, as just pointed out, this assumption is necessarily false. However, the proportionality of the rotational magnetic moment to J is also predicted by Wick's theory. As this prediction is the most important application[7] of the theory, its direct experimental proof in these experiments is particularly useful.

The experimental values of the rotational magnetic moments of H_2, HD, and D_2 as listed in the preceding section are in the ratio 3.994 : 3.000 : 2.003; that is, to within the experimental error of 0.2 percent they are in the ratio 4 : 3 : 2 or in the inverse ratio of the reduced masses of the molecules. Since the rotational angular velocities in the first rotational state are inversely proportional to the reduced masses the experiment shows that the rotational magnetic moments are proportional to the rotational angular velocities in a comparison of H_2, HD, and D_2 molecules. That such should be the case would certainly be expected in a comparison of H_2 and D_2 molecules; however, that it should be so in a comparison of H_2 with HD is not immediately apparent, for not only are the angular velocities of the two molecules different but so also are the positions of the axes about which the molecules rotate, since the center of mass of the HD molecule is not midway between the two nuclei. Still even for this case if the electrons behaved as a rigid charge distribution attached to the nuclei the rotational magnetic moment would be proportional to the rotational angular velocity, since for a rigid molecule with zero total charge and with central symmetry of the charge distribution the rotational magnetic moment is invariant to the position of the axis of rotation. That the magnetic moment should be inversely proportional to the reduced mass for unsymmetrical molecules like HD is on the basis of Wick's theory not immediately obvious. In fact, to make it so the electron contribution to the moment of HD must be more than twice as great as its contribution to H_2 even though the rotational angular velocity is less. This, however, may be proved as is shown in the appendix to the present paper where the general expression for the rotational magnetic moments of H_2, D_2, and HD molecules is derived.

[10] R. Frisch and O. Stern, Zeits. f. Physik **85**, 25 (1933).

Although the 4 : 3 : 2 ratio of the rotational magnetic moments holds to within the estimated experimental error of 0.2 percent in the determination of the ratios of moments, the discrepancy is very near the maximum experimental error and seems fairly persistent. It is in the direction that the moments of the lighter molecules are slightly less than would be expected. Such a discrepancy could probably be explained as the effect of the zero state vibrational motion of the molecule upon the mean separation of the nuclei. A quantitative calculation of the magnitude of the effect was not attempted.

From the theory of Wick or from the more general theory given in the appendix it is possible from the experimental measurement of the rotational magnetic moments to evaluate the high frequency term[11] of the ordinary diamagnetic susceptibility of H_2, D_2, and HD molecules. This is due to the fact that the summation in Eq. (6) of the appendix is just exactly the same as the summation which occurs in the theory of the diamagnetic susceptibility of molecules.[9] In fact, a comparison of the two shows that (in the notation of Van Vleck and the appendix)

$$\chi_{\text{mole-HF}}=\frac{e^2L\rho^2}{12mc^2}\left(1-\frac{2M_1M_2}{(M_1+M_2)M}\frac{\mu}{J}\right). \quad (3)$$

So with the observed values of the rotational moments, the high frequency term in the diamagnetic susceptibility of H_2, D_2, and HD are as listed in Table VII, the average value being

$$\chi_{\text{mole-HF}}=0.093\pm0.007\times10^{-6} \text{ per mole.}$$

This result may be subject to a somewhat larger error than 0.007 due to possible inaccuracies in the perturbation theories on which the calculation is based. The result calculated from Wang wave functions by Van Vleck and Frank[12] of $\chi_{\text{mole-HF}}=0.51\times10^{-6}$ thus appears to be about five times too big. However, if instead of the Wang wave function another H_2 wave function, used first by Wick,[6,7] is used in the calculation, the theoretical value for the high frequency part of the susceptibility may be made to drop even below the above experimental value.

[11] J. H. Van Vleck, *The Theory of Electric and Magnetic Susceptibility* (Oxford Press, 1932), p. 276.

[12] J. H. Van Vleck and A. Frank, Proc. Nat. Acad. Sci. **15**, 539 (1929).

The author wishes to thank Professor Rabi, under whose direction this work was carried out, for his interest and valuable advice. He also wishes to thank Professor Zacharias and Dr. Kellogg for their very great assistance in all phases of this work and Dr. F. G. Brickwedde of the National Bureau of Standards for purifying the HD used in this experiment. This research has been aided by grants from the Research Corporation and the Carnegie Institution of Washington.

Appendix

Theoretical expression for the rotational magnetic moments of H_2, D_2, *and* HD *molecules.*—Although Wick's treatment[6,7] applies only to a symmetrical molecule, it may readily be extended to the case of a molecule one of whose nuclei is of mass M_1 and the other of M_2 with the result that the rotational magnetic moment of the molecule in rotational state J is, in nuclear magnetons,

$$\mu=\frac{(M_2^2+M_1^2)M}{M_1M_2(M_1+M_2)}J$$
$$-\frac{2}{m\rho^2}\frac{(M_1+M_2)M}{M_1M_2}\left[\Sigma'\frac{|(0|M_{\xi 0}|n)|^2}{E_n-E_0}\right]J, \quad (4)$$

where M is the mass of the proton, m the mass of the electron, and ρ the distance between the nuclei. $(0|M_{\xi 0}|n)$ is a matrix element for the nonrotating molecule of the electronic angular momentum about an axis through the center of mass of the molecule and perpendicular to the internuclear line. Since the angular momentum is about the center of mass of the molecule and not about a point midway between the two nuclei, the quantity in brackets is different for HD than H_2 or D_2. The first term in the above expression is the nuclear contribution to the rotational magnetic moment and the second is the electron contribution, neither of which alone is inversely proportional to the reduced mass. To make possible a comparison of the H_2 and HD results the electronic angular momenta must be expressed about an axis which is the perpendicular bisector of the line joining the two nuclei. This transformation of the quantity in

the brackets can be performed with the aid of the invariance properties of the diamagnetic susceptibility shown by Van Vleck.[11] (It should be noted that the symmetry of the molecule is such that $|(0|M_{\xi 0}|n)|^2=\frac{1}{2}|P(0,n)|^2$ where $P(0,n)$ are the total angular momentum matrix elements used by Van Vleck.) The result is

$$\mu=\frac{(M_2^2+M_1^2)M}{M_1M_2(M_1+M_2)}J$$
$$-\frac{2}{m\rho^2}\frac{(M_1+M_2)M}{M_1M_2}\left[\Sigma'\frac{|(0|M_{\xi c}|n)|^2}{E_n-E_0}\right]J$$
$$-\frac{1}{\rho^2}\frac{(M_1+M_2)M}{M_1M_2}[\Sigma(\langle r_0^2\rangle_{Av}-\langle r_c^2\rangle_{Av})]J, \quad (5)$$

where $(0|M_{\xi c}|n)$ is the matrix element of electron angular momentum about an axis which is the perpendicular bisector of the line joining the two nuclei and is consequently the same for H_2, D_2, and HD except for second-order effects and where $\langle r_0^2\rangle_{Av}$ and $\langle r_c^2\rangle_{Av}$ are the mean square distances of the electron distribution from the center of mass and the midpoint of the molecule, respectively. However, if d is the separation of the midpoint from the center of mass $\langle r_0^2\rangle_{Av}-\langle r_c^2\rangle_{Av}=d^2$. From this and the value of $d=\frac{1}{2}(M_2-M_1)/(M_1+M_2)$ the above equation reduces to

$$\mu=\frac{(M_1+M_2)M}{2M_1M_2}$$
$$\times\left\{1-\frac{4}{m\rho^2}\left[\Sigma'\frac{|(0|M_{\xi c}|n)|^2}{E_n-E_0}\right]\right\}J, \quad (6)$$

whence μ_R should be inversely proportional to the reduced mass as found experimentally.

AUGUST 1, 1940 PHYSICAL REVIEW VOLUME 58

On the Spinor Equations for Particles with Arbitrary Spin and Rest Mass Zero

J. S. DE WET*
Institute for Advanced Study, Princeton, New Jersey
(Received April 20, 1940)

The spinor equations for arbitrary spin and rest mass zero are examined in some detail. Fierz has shown that for all values of the spin $f(>\frac{1}{2})$ there exists only two "really" independent plane wave solutions instead of $(2f+1)$ when the rest mass is not zero. Fierz later showed, in rather a complicated way, that these two plane waves correspond to components of spin $\pm f$ along the momentum vector of the wave. We will arrive here at the same result but in a much simpler and more direct way.

INTRODUCTION

M. FIERZ[1] has given a detailed discussion of the spinor wave equations for particles with arbitrary spin proposed by Dirac.[2] Fierz showed that when the rest mass is zero there is a certain degeneracy of the equations, and that for a given spin f there are only two really independent plane wave solutions instead of $(2f+1)$. The interpretation of this was not given in his first paper. In a subsequent paper,[3] however, he discusses the rest mass zero case in more detail, and arrives at the result that the two plane waves correspond to axial spins $\pm f$ about the momentum vector of the plane waves. His work is rather complicated. Here we will arrive at the same result in a much simpler way. For coherence it is necessary to give here some of the work appearing in Fierz's paper. The first section will be largely a restatement of Fierz's results, although the notation I will use will be slightly different. The second section will contain a detailed study of the rest mass zero case. In the present discussion no distinction will be made between the cases of integral and half-odd spin.

* Now in the Applied Mathematics Department, University of Cape Town, South Africa.
[1] M. Fierz, Helv. Phys. Acta **12**, 3 (1939).
[2] P. A. M. Dirac, Proc. Roy. Soc. **A155**, 47 (1936).
[3] M. Fierz, Helv. Phys. Acta **13**, 45 (1940).

Such a distinction is quite unnecessary, since the work is exactly the same for both. The only essential difference between the two cases is the form of the energy momentum tensor and charge current vector, but these do not enter in the present work.

The spinor notation which I shall use is that of Veblen. A very good concise account of this formalism has been given by A. H. Taub,[4] to which the reader is referred.

The present work was developed during the course of a number of reports on Fierz's paper that I gave to a seminar on spinor theory, conducted by Professors O. Veblen and J. von Neumann. I am much indebted to Professors Veblen and von Neumann for helpful discussion.

1. The Spinor Equations for Particles with Arbitrary Spin and Rest Mass Nonzero

The equations are stated most simply for our purposes in the following form:

$$g^{\sigma\tau}\psi^{A_1A_2\cdots A_r\dot{B}_1\dot{B}_2\cdots\dot{B}_s}(0)_{;\sigma\tau}=\kappa^2\psi^{A_1A_2\cdots A_r\dot{B}_1\dot{B}_2\cdots\dot{B}_s}(0) \qquad (\sigma,\tau=1,2,3,4),\quad (A,B=1,2), \tag{1}$$

where $\psi^{A_1A_2\cdots A_r\dot{B}_1\dot{B}_2\cdots\dot{B}_s}(0)$

is a spinor field of the type indicated by its indices and is symmetrical in all its dotted and undotted indices, $g^{\sigma\tau}$ is the metric tensor which has the components

$$\|g^{\sigma\tau}\|=\begin{Vmatrix}1&0&0&0\\0&1&0&0\\0&0&1&0\\0&0&0&-1\end{Vmatrix}$$

in all Galilean frames, and $\kappa=mc/\hbar$ where m is the rest mass of the particle. Furthermore

$$\psi^{A_1A_2\cdots A_r\dot{B}_1\dot{B}_2\cdots\dot{B}_s}(0)_{;\sigma\tau} \quad \text{means} \quad \frac{\partial^2\psi^{A_1A_2\cdots A_r\dot{B}_1\dot{B}_2\cdots\dot{B}_s}(0)}{\partial x^\sigma\partial x^\tau}.$$

In addition to (1) the spinor $\psi(0)$ (spinor indices are omitted when not necessary) is to satisfy the following condition:

$$\psi^{A_2\cdots A_r\dot{B}_1\cdots\dot{B}_{s+1}}(1)$$

defined by

$$\psi^{A_2\cdots A_r\dot{B}_1\cdots\dot{B}_{s+1}}(1)=g^{\sigma\dot{B}_{s+1}}{}_{A_1}\psi^{A_1A_2\cdots A_r\dot{B}_1\cdots\dot{B}_s}(0)_{;\sigma} \tag{2}$$

is symmetric in all its dotted and undotted indices, where the $g^{\sigma\dot{A}}{}_B$ are the components of the four basic spinor matrices. (See Taub, reference 4.)

For the case of *integral* spin $f=r$, we must have $s=r$ in the above equations.

For the case of *half-odd spin* $f=r+\frac{1}{2}$, we must have $s=r+1$ in the above equations.

The above two statements will become clearer in the later work.

The most important property of the matrices $\|g^{\sigma\dot{A}}{}_B\|$ is

$$\tfrac{1}{2}(g^{\sigma\dot{A}}{}_{B}g^{\tau\dot{B}}{}_{C}+g^{\tau\dot{A}}{}_{B}g^{\sigma\dot{B}}{}_{C})=g^{\sigma\tau}\delta^{\dot{A}}{}_{\dot{C}} \tag{3}$$

and the complex conjugate of (3). From this it follows that

$$g^{\rho\dot{A}_1}{}_{B_{s+1}}\psi^{A_2\cdots A_r\dot{B}_1\cdots\dot{B}_{s+1}}(1)_{;\rho}=\kappa^2\psi^{A_1\cdots A_r\dot{B}_1\cdots\dot{B}_s}(0). \tag{4}$$

The second-order equation (1) may thus be replaced by the first-order equations (2) and (4) where the $\psi(1)$ and $\psi(0)$ are spinors symmetric in all their dotted and undotted indices. This is the usual form in which the equations are given.

We can now define in general a $\psi(m)$ $(m=1, 2, \cdots r)$ by

$$\psi^{A_{m+1}\cdots A_r\dot{B}_1\cdots\dot{B}_{s+m}}(m)=g^{\sigma_m\dot{B}_{s+m}}\psi^{A_m\cdots A_r\dot{B}_1\cdots\dot{B}_{s+m-1}}(m-1)_{;\sigma_m}$$
$$=g^{\sigma_1\dot{B}_{s+1}}{}_{A_1}\cdots g^{\sigma_m\dot{B}_{s+m}}{}_{A_m}\psi^{A_1\cdots A_r\dot{B}_1\cdots\dot{B}_s}(0)_{;\sigma_1\sigma_2\cdots\sigma_m}. \tag{5}$$

It is easily seen that $\psi(m)$ is symmetric in all its dotted and undotted indices in virtue of the like symmetry of $\psi(1)$ and $\psi(0)$. Furthermore the $\psi(m)$ all satisfy equations like (4), *viz.*,

$$g^{\rho\dot{A}_{m+1}}{}_{B_{s+m+1}}\psi^{A_{m+2}\cdots A_r\dot{B}_1\cdots\dot{B}_{s+m+1}}(m+1)_{;\rho}=\kappa^2\psi^{A_{m+1}\cdots A_r\dot{B}_1\cdots\dot{B}_{s+m}}(m). \tag{6}$$

We note that in particular

$$\psi^{\dot{B}_1\cdots\dot{B}_{s+r}}(r)$$

[4] A. H. Taub, Ann. of Math. **40**, 937 (1939). For typographical reasons the usual dotted indices will here be replaced by indices with dots put in front of the indices.

has only dotted indices and is symmetric in all these indices.

In a similar way we can define spinors $\psi(-m)$ $(m=1, 2, \cdots s)$ by

$$\psi(-m)^{A_1\cdots A_{r+m}\dot{B}_{m+1}\cdots\dot{B}_s} = \bar{g}^{\sigma_m\dot{A}_{r+m}}{}_{B_m}\psi(-[m-1])^{A_1\cdots A_{r+m-1}\dot{B}_m\cdots\dot{B}_s}{}_{;\sigma_m}$$

$$= \bar{g}^{\sigma_1\dot{A}_{r+1}}{}_{B_1}\cdots\bar{g}^{\sigma_m\dot{A}_{r+m}}{}_{B_m}\psi(0)^{A_1\cdots A_r\dot{B}_1\cdots\dot{B}_s}{}_{;\sigma_1\cdots\sigma_m}$$

$$= \frac{1}{\kappa^2}\bar{g}^{\sigma_1\dot{A}_{r+1}}{}_{B_1}\cdots\bar{g}^{\sigma_m\dot{A}_{r+m}}{}_{B_m}\bar{g}^{\sigma\dot{A}_1}{}_{B_{s+1}}$$
$$\times\psi(1)^{A_2\cdots A_r\dot{B}_1\cdots\dot{B}_{s+1}}{}_{;\sigma_1\sigma_2\cdots\sigma_m\sigma}, \quad (7)$$

using (4) to get the last part of the equation. Again from the symmetry of $\psi(1)$ and $\psi(0)$ in all their dotted and undotted indices, it follows from (7) that $\psi(-m)$ has like symmetry.

In particular

$$\psi(-s)^{A_1A_2\cdots A_{r+s}}$$

is a spinor with undotted indices only, and is symmetric in all of them. The $\psi(-m)$ satisfy the following equations (analogous to (6)) in virtue of (1):

$$g^{\rho\dot{B}_m}{}_{A_{r+m}}\psi(-m)^{A_1\cdots A_{r+m}\dot{B}_{m+1}\cdots\dot{B}_s}{}_{;\rho} = \kappa^2\psi(-[m-1])^{A_1\cdots A_{r+m-1}\dot{B}_m\cdots\dot{B}_s} \quad (8)$$

We can write the above equations (dropping the spinor indices) as follows:

$$g^\sigma\psi(0)_{;\sigma}=\psi(1), \quad \bar{g}^\sigma\psi(1)_{;\sigma}=\kappa^2\psi(0),$$
$$g^\sigma\psi(1)_{;\sigma}=\psi(2), \quad \bar{g}^\sigma\psi(2)_{;\sigma}=\kappa^2\psi(1),$$

and so on up to

$$g^\sigma\psi(r-1)_{;\sigma}=\psi(r), \quad \bar{g}^\sigma\psi(r)_{;\sigma}=\kappa^2\psi(r-1),$$

and (9)

$$\bar{g}^\sigma\psi(0)_{;\sigma}=\psi(-1), \quad g^\sigma\psi(-1)_{;\sigma}=\kappa^2\psi(0),$$
$$\bar{g}^\sigma\psi(-1)_{;\sigma}=\psi(-2), \quad g^\sigma\psi(-2)_{;\sigma}=\kappa^2\psi(-1),$$

up to

$$\bar{g}^\sigma\psi(-[s-1])_{;\sigma}=\psi(-s),$$
$$g^\sigma\psi(-s)_{;\sigma}=\kappa^2\psi(-[s-1]).$$

The notation will be clear if we note that the first two equations of (9) are Eqs. (2) and (4).

From any of the above pairs of equations, together with the symmetry in dotted and undotted indices of the two ψ's involved, can be deduced all the other equations as well as the symmetry of the rest of the ψ's in dotted and undotted indices. From this it appears that we could have started with Eq. (1) involving a ψ with any number of dotted and undotted indices, rather than the $\psi(0)$ we started with, having either $r=s$ or $r=s+1$. One reason why the $\psi(0)$ has a preferred position is that the physical quantities like the energy momentum tensor and charge current vector are most simply expressed in terms of $\psi(0)$. As we will see later, when the rest mass is zero the ψ that we start with definitely has a preferred position. If we start with any ψ other than $\psi(0)$, the energy momentum tensor and charge current vector formed from it is identically zero. This follows from the fact that these tensors defined in terms of ψ's other than $\psi(0)$ involve second and higher derivatives, i.e., terms like

$$g^{\sigma\tau}\psi_{;\sigma\tau\rho}$$

say, and these are zero in virtue of (1) with $\kappa=0$.

Let us now consider plane wave solutions of the equations.

$$\psi(0)^{A_1\cdots A_r\dot{B}_1\cdots\dot{B}_s} = \Psi(0)^{A_1\cdots A_r\dot{B}_1\cdots\dot{B}_s}\, e^{i\kappa_\sigma x^\sigma} \quad (10)$$

will be a solution if

$$-g^{\sigma\tau}\kappa_\sigma\kappa_\tau=\kappa^2 \quad (11)$$

and the components of $\Psi(0)$ are constants.

In addition $\Psi(1)$ given by

$$\Psi(1)^{A_2\cdots A_r\dot{B}_1\cdots\dot{B}_{s+1}} = i\kappa_\sigma g^{\sigma\dot{B}_{s+1}}{}_{A_1}\Psi(0)^{A_1\cdots A_r\dot{B}_1\cdots\dot{B}_s} \quad (12)$$

must be symmetric in all its dotted and undotted indices. $\Psi(0)$ has $(r+1)\cdot(s+1)$ independent components, considering only its symmetry in its spinor indices. The symmetry of the right-hand side of (12) imposes $r\cdot s$ conditions on the components of $\Psi(0)$, however, so that it has $(r+1)(s+1)-rs=r+s+1$ independent components.

The same reasoning applies to all the $\Psi(m)$ $(m=r, r-1, \cdots 1, 0, -1, -2, \cdots -s)$. Each has $r+s+1$ independent components, and any

$\Psi(m)$ is expressible in terms of

$$\Psi(r)^{\dot{B}_1\cdots\dot{B}_{s+r}}$$

by the following relation:

$$\Psi(r-m)^{A_1\cdots A_m\dot{B}_1\cdots\dot{B}_{s+r-m}} = \frac{1}{\kappa^{2m}}\bar{g}^{A_1}{}_{\dot{B}_{s+r}}\cdots \times \bar{g}^{\dot{A}_m}{}_{B_{s+r-m+1}}\Psi(r)^{\dot{B}_1\cdots\dot{B}_{s+r}} \quad (m=0, 1, 2, \cdots, r+s), \quad (13)$$

where

$$g^{\dot{A}}{}_B = i\kappa_\sigma g^{\sigma\dot{A}}{}_B. \quad (14)$$

By (13) the components of any $\Psi(m)$ are expressed in terms of the $(r+s+1)$ independent components of $\Psi(r)$.

Let us now choose a special coordinate system in such a way that

$$\kappa_1=\kappa_2=\kappa_3=0, \quad \kappa_4=\pm\kappa.$$

Then

$$g^{\dot{A}}{}_B = i\kappa_4 g^{4\dot{A}}{}_B.$$

If we now apply a space rotation to the system (rotation of the x^1, x^2, x^3, leaving x^4 invariant) the corresponding spinor transformation is a unimodular linear transformation leaving $g^{4\dot{A}}{}_B$ numerically invariant, i.e., a unitary transformation; since in a special spin coordinate system the matrix $g^{\dot{A}}{}_{\dot{A}B}$ (obtained from $g^{4\dot{A}}{}_B$ by lowering the dotted index) has the components

$$\left\|\begin{matrix}1 & 0\\ 0 & 1\end{matrix}\right\|.$$

Thus under a space rotation for a system with zero momentum ($\kappa_1=\kappa_2=\kappa_3=0$) the connection between the $(r+s+1)$ independent components of $\Psi(r)$ and the components of $\Psi(r-m)$ is numerically invariant. Now the components of $\Psi(r)$ transform according to the irreducible representation $D_{\frac{1}{2}(r+s)}$ of the rotation group under the unitary spin transformation associated with a space rotation. Further since the $g^{4\dot{A}}{}_B$ are numerically invariant under the unitary spin transformation, the $(r+s+1)$ independent components of $\Psi(r-m)$—and in particular $\Psi(0)$—also transform according to $D_{\frac{1}{2}(r+s)}$.[5]

[5] See B. L. van der Waerden, *Gruppentheoretische Methode in der Quantenmechanik* (Springer, Berlin, 1932), Chap. III.

Hence the equations correspond to a spin $\frac{1}{2}(r+s)$. From this follows the earlier statement that when $s=r$, the corresponding spin is $f=r$, and when $r=s+1$, the corresponding spin is $r+\frac{1}{2}$.

2. Rest Mass Zero Case

The work of the preceding section has been largely a restatement of Fierz's results. We now consider the rest mass zero case. Fierz showed that when the rest mass is zero, the $\Psi(0)$ had only two "really independent" components, since it was possible to add to $\psi(0)$ a set of plane wave solutions of the equations depending on $(r+s-1)$ independent constants, without changing the energy momentum tensor or charge current vector for the system. The transformation of the ψ's by the addition of these terms he calls "gauge transformations." The supposition was that by a suitable choice of the gauge transformation one could reduce all but two of the components of $\Psi(0)$ to zero. Here we will investigate the nature of the two components of $\Psi(0)$ which are not zero. Working in a special coordinate system for which $\kappa_2=\kappa_3=0$ we will show that there are two components of $\Psi(0)$ which are "gauge invariant" and nonzero, i.e., by no choice of the gauge transformation can these two components be reduced to zero. These two components then are the two "really" independent components of $\Psi(0)$. We will then show that under axial rotations about the x^1 axis through an angle θ, these two components are multiplied by

$$e^{\frac{1}{2}i(r+s)\theta} \quad \text{and} \quad e^{-\frac{1}{2}i(r+s)\theta},$$

so that they correspond to components of spin $\pm f=\pm\frac{1}{2}(r+s)$ along the x^1 axis. But the momentum vector lies along the x^1 axis (since we have chosen coordinates in such a way that $\kappa_2=\kappa_3=0$). Thus the two gauge invariant states correspond to components of spin $\pm f$ in the direction of the momentum vector. Thus we here arrive at the result of Fierz's second paper in a simple and direct manner.

The equation for the rest mass zero case is (1) with $\kappa=0$, together with the condition that $\psi(1)$ defined by (2) is symmetric in all its dotted and undotted indices. Then $\psi(1)$ satisfies (4) with

$\kappa=0$. The $\psi(m)$ $(m=1, 2, \cdots, r)$ are defined as before by (5) and satisfy (6) with $\kappa=0$.

The $\psi(-m)$ $(m=1, 2, \cdots, s)$ are defined as before in terms of $\psi(0)$ by the first part of Eqs. (7), but the symmetry of $\psi(-m)$ in dotted and undotted indices no longer follows by our previous argument, since there the last part of (7) (which no longer applies since $\kappa=0$) was used. It is still true, however, as we will see later, that $\Psi(-m)$ is symmetric in dotted and undotted indices in virtue of the like symmetry of $\Psi(0)$ and $\Psi(1)$. So that for the rest mass zero case the equations (9) are replaced by similar equations with $\kappa=0$.

Let us now consider plane wave solutions of the equations as before

$$\psi(0)^{A_1\cdots A_r\dot{B}_1\cdots\dot{B}_s} = \Psi(o)^{A_1\cdots A_r\dot{B}_1\cdots\dot{B}_s} e^{i\kappa_\sigma x^\sigma} \tag{15}$$

where now

$$g^{\sigma\tau}\kappa_\sigma\kappa_\tau=0. \tag{16}$$

We then have the following state of affairs: $\Psi(0)$ still has $(r+s+1)$ independent components —as before a result of the symmetry of $\Psi(1)$ and $\Psi(0)$ in their dotted and undotted indices. We will show that for a special coordinate system all the remaining components of $\Psi(0)$ are zero. Further, in this coordinate system $\Psi(m)$ has $(r+1-m)$ nonzero components and in particular $\Psi(r)$ has only *one* nonzero component. Similarly $\Psi(-m)$ has $(s+1-m)$ nonzero components and in particular $\Psi(-s)$ has only *one* nonzero component.

In what follows we wish to be quite explicit and give the actual matrices $\|g^{\sigma\dot{A}}{}_{B}\|$ in a particular spin coordinate system. Let the

$$\|g^{\sigma\dot{A}}{}_{B}\| = \begin{Vmatrix} g^{\sigma\dot{1}}{}_{1} & g^{\sigma\dot{1}}{}_{2} \\ g^{\sigma\dot{2}}{}_{1} & g^{\sigma\dot{2}}{}_{2} \end{Vmatrix}$$

be given by

$$\begin{aligned} \|g^{1\dot{A}}{}_{B}\| &= \begin{Vmatrix} 0 & 1 \\ 1 & 0 \end{Vmatrix}, \quad \|g^{2\dot{A}}{}_{B}\| = \begin{Vmatrix} 1 & 0 \\ 0 & -1 \end{Vmatrix}, \\ \|g^{3\dot{A}}{}_{B}\| &= \begin{Vmatrix} i & 0 \\ 0 & i \end{Vmatrix}, \quad \|g^{4\dot{A}}{}_{B}\| = \begin{Vmatrix} 0 & -1 \\ 1 & 0 \end{Vmatrix}. \end{aligned} \tag{17}$$

Then let us choose a special space time frame of reference in such a way that

$$\kappa_2=\kappa_3=0, \quad \kappa_1^2=\kappa_4^2. \tag{18}$$

Then we have

$$\begin{aligned} \|i\kappa_\sigma g^{\sigma\dot{A}}{}_{B}\| &= \begin{Vmatrix} 0 & 0 \\ 2i\kappa_1 & 0 \end{Vmatrix} \quad (\kappa_1=+\kappa_4) \\ &= \begin{Vmatrix} 0 & 2i\kappa_1 \\ 0 & 0 \end{Vmatrix} \quad (\kappa_1=-\kappa_4). \end{aligned} \tag{19}$$

For definiteness let us take $\kappa_1=\kappa_4$ and denote the matrix

$$\|i\kappa_\sigma g^{\sigma\dot{A}}{}_{B}\| = \begin{Vmatrix} 0 & 0 \\ 2i\kappa_1 & 0 \end{Vmatrix} \text{ by } \|g^{\dot{A}}{}_{B}\|.$$

Now $\Psi(1)$ is by definition given by

$$\Psi(1)^{A_2\cdots A_r\dot{B}_1\cdots\dot{B}_{s+1}} = i\kappa_\sigma g^{\sigma\dot{B}_{s+1}}{}_{A_1}\Psi(0)^{A_1\cdots A_r\dot{B}_1\cdots\dot{B}_s}. \tag{20}$$

In the special coordinate system, we have from (19) and (20)

$$\Psi(1)^{A_2\cdots A_r\dot{B}_1\cdots\dot{B}_s\dot{1}} = 0. \tag{21}$$

Now $\Psi(1)$ is symmetric in all its dotted indices. Hence the only nonzero components of $\Psi(1)$ are:

$$\Psi(1)^{A_2\cdots A_r\dot{2}\dot{2}\cdots\dot{2}}$$

and there are r such nonzero components.* It follows further from (20) and (19) and the dotted and undotted index symmetry of $\Psi(1)$ that the following components of $\Psi(0)$ are zero in our special coordinate system:

$$\begin{aligned} &\text{all terms} \quad \Psi(0)^{1A_2\cdots A_r\dot{B}_1\cdots\dot{B}_s} \\ &\qquad\qquad (A, B=1, 2). \\ &\text{excepting} \quad \Psi(0)^{1A_2\cdots A_r\dot{2}\dot{2}\cdots\dot{2}} \end{aligned} \tag{22}$$

The number of terms of $\Psi(0)$ that are zero is thus $r\cdot(s+1)-r=rs$. Since the total number of terms of $\Psi(0)$ is $(r+1)(s+1)$ the number of nonzero terms is $(r+s+1)$, i.e., just the number of independent components of $\Psi(0)$.

* In the following we shall frequently use *component* and *term* for *independent component* and *independent term*.

Similarly we have (in the special coordinate system)

$$\Psi(m)^{A_{m+1}\cdots A_r \dot{B}_1\cdots\dot{B}_{s+m}} = g^{\dot{B}_{s+1}}{}_{A_1}\cdots g^{\dot{B}_{s+m}}{}_{A_m}\Psi(0)^{A_1\cdots A_r\dot{B}_1\cdots\dot{B}_s} \tag{23}$$

and it follows from the form of $\|g^{\dot{A}}{}_{B}\|$ and the symmetry of $\Psi(m)$ in all dotted and undotted indices, that the only nonzero terms of $\Psi(m)$ are

$$\Psi(m)^{A_{m+1}\cdots A_r\dot{2}\dot{2}\cdots\dot{2}}, \quad (r+1-m) \text{ in number.}$$

In particular the *only* nonvanishing term of $\Psi(r)$ is

$$\Psi(r)^{\dot{2}\dot{2}\cdots\dot{2}} = (2i\kappa_1)^r \Psi(0)^{11\cdots1\dot{2}\cdots\dot{2}}. \tag{24}$$

Similar results will hold for the $\Psi(-m)$ provided $\Psi(-1)$ is symmetric in all dotted and undotted indices. That this is so is easily verified in the special coordinate system. For

$$\Psi(-1)^{A_1\cdots A_{r+1}\dot{B}_2\cdots\dot{B}_s} = \hat{g}^{\dot{A}_{r+1}}{}_{B_1}\Psi(0)^{A_1\cdots A_r\dot{B}_1\cdots\dot{B}_s}. \tag{25}$$

Now from (25)

$$\Psi(-1)^{A_1\cdots A_{r-1}1\,2\,\dot{B}_2\cdots\dot{B}_s} = -2i\kappa_1\Psi(0)^{A_1\cdots A_{r-1}1\dot{1}\dot{B}_2\cdots\dot{B}_s}$$

$$= 0 \text{ from (22)} \quad \text{and}$$

$$\Psi(-1)^{A_1\cdots A_{r-1}2\,1\,\dot{B}_2\cdots\dot{B}_s} = 0 \quad \text{from (25) and (19).}$$

So the symmetry of $\Psi(-1)$ in dotted and undotted indices follows in a special coordinate system, and hence in any spin coordinate system.

The rest of the argument then proceeds as before. $\Psi(-m)$ has $(s+1-m)$ nonzero components and in particular $\Psi(-s)$ has only *one* nonzero component given by

$$\Psi(-s) = (-2i\kappa_1)^s \Psi(0)^{22\cdots2\,\dot{2}\cdots\dot{2}\dot{1}\cdots\dot{1}} \tag{26}$$

Let us now consider the effect of the "gauge transformations" of Fierz on the $\Psi(0)$, $\Psi(m)$ and $\Psi(-m)$.

Fierz showed that the energy momentum tensor and charge current vector for the system was unchanged if one replaced the plane waves

$$\Psi(0)e^{i\kappa_\sigma x^\sigma} \quad \text{by} \quad [\Psi(0)+\Psi'(0)]e^{i\kappa_\sigma x^\sigma},$$

where the $\Psi'(0)$ is given by

$$\begin{aligned}\Psi'(0)^{A_1A_2\cdots A_r\dot{B}_1\cdots\dot{B}_s} &= i\kappa_\sigma g^{\sigma\dot{B}_1A_1}\,\Phi(0)^{A_2\cdots A_r\dot{B}_2\cdots\dot{B}_s}\\ &+ i\kappa_\sigma g^{\sigma\dot{B}_1A_2}\,\Phi(0)^{A_1A_3\cdots A_r\dot{B}_2\cdots\dot{B}_s} + \cdots\\ &+ i\kappa_\sigma g^{\sigma\dot{B}_2A_1}\,\Phi(0)^{A_2\cdots A_r\dot{B}_1\dot{B}_3\cdots\dot{B}_s}\\ &+ i\kappa_\sigma g^{\sigma\dot{B}_2A_2}\,\Phi(0)^{A_1A_3\cdots A_r\dot{B}_1\dot{B}_3\cdots\dot{B}_s} + \cdots\\ &+ \cdots\cdots\cdots\cdots\cdots\cdots\cdots\\ &+ i\kappa_\sigma g^{\sigma\dot{B}_sA_1}\,\Phi(0)^{A_2\cdots A_r\dot{B}_2\cdots\dot{B}_{s-1}\dot{B}_1}\\ &+ i\kappa_\sigma g^{\sigma\dot{B}_sA_2}\,\Phi(0)^{A_1A_3\cdots A_r\dot{B}_2\cdots\dot{B}_{s-1}\dot{B}_1} + \cdots,\end{aligned} \tag{27}$$

where

$$\Phi(0)^{A_2\cdots A_r\dot{B}_2\cdots\dot{B}_s}$$

is symmetric in all its dotted and undotted indices and in addition $\Phi(1)$ defined by

$$\Phi(1)^{A_2A_4\cdots A_r\dot{B}_2\cdots\dot{B}_{s+1}} = i\kappa_\sigma g^{\sigma\dot{B}_{s+1}}{}_{A_2}\Phi(0)^{A_2\cdots A_r\dot{B}_2\cdots\dot{B}_s} \tag{28}$$

is symmetric in all its dotted and undotted indices.

We must verify that $\Psi'(0)$ and $\Psi'(1)$ are symmetric in all their dotted and undotted indices. For $\Psi'(0)$ this is apparent from the definition (27). $\Psi'(1)$ is given by

$$\begin{aligned}\Psi'(1)^{A_2\cdots A_r\dot{B}_1\cdots\dot{B}_{s+1}} &= i\kappa_\sigma g^{\sigma\dot{B}_{s+1}}{}_{A_1}\Psi'(0)^{A_1\cdots A_r\dot{B}_1\cdots\dot{B}_s}\\ &= i\kappa_\sigma g^{\sigma\dot{B}_1A_2}\,\Phi(1)^{A_3\cdots A_r\dot{B}_2\cdots\dot{B}_{s+1}}\\ &+ i\kappa_\sigma g^{\sigma\dot{B}_1A_3}\,\Phi(1)^{A_2A_4\cdots A_r\dot{B}_2\cdots\dot{B}_{s+1}} + \cdots\\ &+ i\kappa_\sigma g^{\sigma\dot{B}_2A_2}\,\Phi(1)^{A_3\cdots A_r\dot{B}_1\dot{B}_3\cdots\dot{B}_{s+1}}\\ &+ i\kappa_\sigma g^{\sigma\dot{B}_2A_3}\,\Phi(1)^{A_2A_4\cdots A_r\dot{B}_1\dot{B}_3\cdots\dot{B}_{s+1}} + \cdots\\ &+ \cdots\cdots\cdots\cdots\cdots\cdots\cdots\end{aligned} \tag{29}$$

In deriving the above we use (3) and (16). Thus $\Psi'(1)$ is given in terms of $\Phi(1)$ in the same way as $\Psi'(0)$ in terms of $\Phi(0)$, and is symmetric in all its dotted and undotted indices. The same applies for all $\Psi'(m)$ for $m \leqslant r-1$. All the $\Psi'(m)$ are given by means of a relation like (29) in terms of $\Phi(m)$, where $\Phi(m)$ is defined in terms of $\Phi(0)$ in the same way as $\Psi(m)$ in terms of $\Psi(0)$.

For $m=r$, however, $\Psi'(r)=0$. This is perhaps most easily seen from (27), considering the definition of $\Psi'(r)$ in terms of $\Psi'(0)$ and noting (3) and (16).

The position then is as follows: $\Psi(0)$ has $(r+s+1)$ independent nonzero components. To this may be added $\Psi'(0)$ depending on $\Psi(0)$ which has $(r+s-1)$ independent nonzero components, so that by a suitable choice of $\Phi(0)$ all but two of the components of $\Psi(0)$ can be made zero.

Further $\Psi(m)$ $(m=1, 2, \cdots, r)$ has $(r+1-m)$ nonzero independent components and $\Phi(m)$ has $(r-m)$ nonzero independent components, so that each $\Psi(m)$ has only *one* "really" independent component. In particular $\Psi(r)$ has only one nonzero component, and $\Psi'(r)=0$ as was shown earlier. A similar state of affairs holds for the $\Psi(-m)$.

It is now clear that the single nonzero components of $\Psi(r)$ and $\Psi(-s)$ cannot be transformed away by a gauge transformation. But these nonzero components are given in terms of the components

$$\overset{11\cdots1'2\cdots'2}{\Psi(0)} \quad \text{and} \quad \overset{22\cdots2'1\cdots'1}{\Psi(0)}$$

of $\Psi(0)$ by (24) and (26).

Hence it is clear that these two components of $\Psi(0)$ are gauge invariant and are the two really independent components of $\Psi(0)$.

All that remains is to interpret these states. With the choise of the matrices $\|g^{\sigma'A}{}_B\|$ that we have made, an axial rotation about the x^1 axis through an angle θ corresponds to the spin transformation $\Gamma^A{}_B$ given by

$$\|\Gamma^A{}_B\| = \begin{Vmatrix} e^{\frac{1}{2}i\theta} & 0 \\ 0 & e^{-\frac{1}{2}i\theta} \end{Vmatrix}.$$

Under this spin transformation

$$\overset{1\cdots1'2\cdots'2}{\Psi(0)}$$

is multiplied by a factor $e^{\frac{1}{2}i(r+s)\theta}$, while

$$\overset{2\cdots2'1\cdots'1}{\Psi(0)}$$

is multiplied by a factor $e^{-\frac{1}{2}i(r+s)\theta}$.

From this follows that the two components of $\Psi(0)$ correspond to components of spin $\pm\frac{1}{2}(r+s)$ along the x^1 axis. But we have chosen the frame of reference in such a way that the x^1 axis coincides with the momentum vector. So that the two states correspond to components of spin $\pm f$ along the momentum vector (where $f=\frac{1}{2}(r+s)$). This is the result given by Fierz. A further result of Fierz is that the (total angular momentum)^2 for the system is always $\geqslant f(f+1)$. The reason for this is easily seen. The orbital angular momentum for the system always has component zero along the momentum vector. Thus it follows that the total angular momentum always has the components $\pm f$ along the momentum vector, and thus the (magnitude)^2 of the total angular momentum must always be $\geqslant f(f+1)$.

The Scattering of 50-Kilovolt Electrons by Aluminum

C. T. CHASE AND R. T. COX
New York University, University Heights, New York, New York

(Received May 15, 1940)

Apparatus is described for scattering electrons with thin foils and measuring the intensity of scattering in a narrow pencil making any angle from 30° to 120° with the direction of incidence. Electrons with energies below 95 percent of the energy on incidence are excluded by a retarding voltage. The theory of nearly single scattering is discussed, and a general expression is found for the error introduced by slight plural scattering. In the case of Rutherford scattering this expression gives for the fractional error the value $\epsilon^2|\csc^2(\theta/2)-\frac{1}{2}|$ where θ is the angle at which scattering is measured and ϵ^2 is the mean square deflection of particles traversing in the foil the same length of path as those scattered at the angle θ. The relation of this result to Wentzel's criterion is shown. Electrons accelerated by 50 kv were scattered by thin composite foils of Al on collodion. A difference was found, though not explained, between the intensities of scattering at 90° on the two sides of the foil, which was inclined at 45° to the direction of incidence. With allowance made for this asymmetry in comparing the scattering at angles above and below 90°, relative intensities at angles from 30° to 120° were within 5 percent of those predicted by Mott. Comparison of the observed and predicted absolute intensities of the scattering from Al was subject to an uncertainty of about 20 percent, principally in the determination of the thickness of the Al film. Within this uncertainty, the observation agreed with the prediction. If the actual scattering differs from the predicted, it appears from these observations to be more probably less than greater.

INTRODUCTION

IF a beam of electrons of speed v is incident normally on a thin foil of thickness t, having, per unit volume, n atoms of atomic number Z, then the fraction scattered into a small solid angle Ω around a direction making an angle θ with the direction of incidence may conveniently be written

$$i=nt\Omega(Ze^2/2mv^2)^2(1-\beta^2)\csc^4(\theta/2)R. \quad (1)$$

For the factor R, Mott[1] has calculated from the Dirac equations, assuming a Coulombian field, the expression

$$R=1-\beta^2\sin^2(\theta/2)+(Z\beta\pi/137)\cos^2(\theta/2)\sin(\theta/2)$$
$$+\text{terms of the second and higher powers in } Z/137. \quad (2)$$

The results of several experiments have indicated exceptions to this equation and to the closely related prediction of an asymmetry in double scattering, and it has been suggested that they show an actual invalidity of the Dirac equations in a range of electron speeds where it is hardly to be expected on other evidence.[2] On the other hand, the experiments offer difficulties in technique, and not all the experimental results are in mutual agreement. It seems desirable therefore to have more observation on the subject.

In the present experiment tests were made of Eq. (2) with 50-kv electrons scattered at angles between 30° and 120° by thin composite foils of Al evaporated on collodion.

APPARATUS AND EXPERIMENTAL PROCEDURE

The chamber in which the electrons were scattered is shown in Fig. 1(a) in vertical section and in Fig. 1(b) in horizontal section. Its vertical wall is a short section of 1-ft. steel pipe, supported for insulation on a glass cylinder of the same diameter and 2 feet high. The beam of electrons enters the chamber, as shown by the arrow, through a sylphon bellows and ground joint from the accelerating tube (not shown). This beam, already rendered parallel by the distribution of voltage among the electrodes of the accelerating tube, is defined by the diaphragm D_1. This diaphragm is at the end of a steel tube set in a bracket fastened to the top of the scattering chamber. The bracket is flanked by blocks of lead to absorb x-rays. The electrons passing the diaphragm strike the foil, which is mounted on one of two diaphragms carried by a cylindrical rod projecting through the top of the scattering

[1] N. F. Mott, Proc. Roy. Soc. **A124**, 425 (1929).
[2] A general discussion of theory and experiment is given in an article by M. E. Rose, Phys. Rev. **57**, 280 (1940).

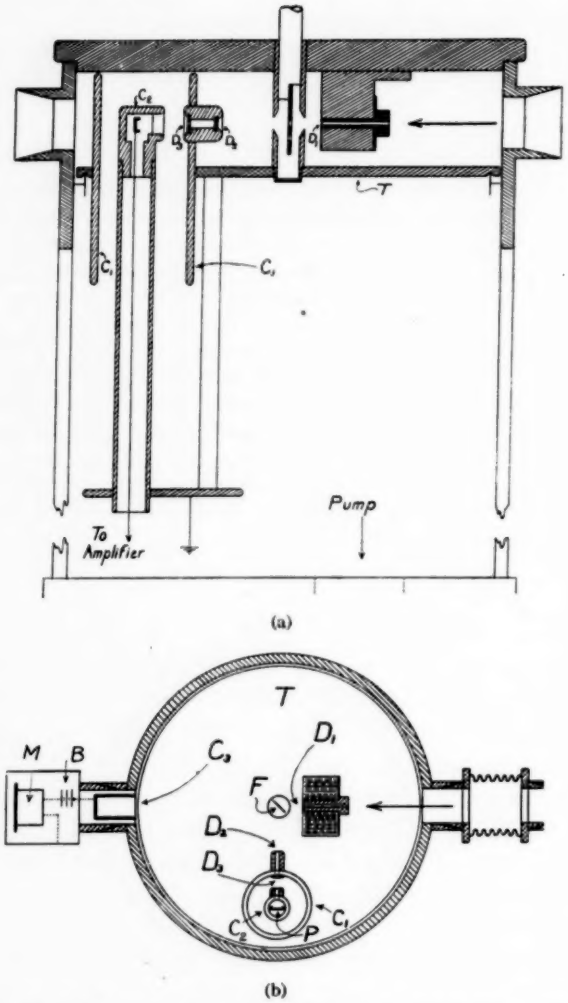

FIG. 1 (a) vertical section and (b) horizontal section of scattering chamber. The wall of the chamber is 1-ft. steel pipe. The support is a glass cylinder. Arrow shows direction of incident beam. T, turning floor of chamber. D_1, diaphragm defining incident beam. D_2, diaphragm defining scattered beam. D_3, larger diaphragm behind D_2. C_1, brass cylinder enclosing region of retarding voltage. C_2, collecting chamber for scattered beam. C_3, collecting chamber for incident beam. B, collecting voltage for primary beam. M, microammeter for measuring incident current. F, scattering foil. P, collecting electrode for scattered beam.

chamber. The rod is attached to a mechanism (not shown) housed in sylphon bellows above the top of the scattering chamber and evacuated with it. This mechanism permits placing either of the two diaphragms in the electron beam and also setting their plane for incidence at 45° to either side of normal, all by manipulation outside the vacuum.

The floor of the scattering chamber is a steel disk with a circular groove on the under side near the rim. This groove rides on three small wheels set on axles 120° apart on the inner wall of the scattering chamber. Two of the wheels are idlers; the third can be driven from outside the vacuum by a crank housed in a flexible metal tube. In this way the floor can be rotated about a vertical axis through the center of the scattering foil.

A brass pipe C_1 projects through the floor from below almost to the top of the chamber. In the wall of this pipe is a copper cylinder carrying two steel diaphragms D_2 and D_3. Inside C_1 but insulated from it by three supporting Pyrex glass rods is the copper chamber C_2 for the collection of the beam of scattered electrons.

The potentials of the parts of the apparatus are shown schematically in Fig. 2. The chamber C_2 was at ground potential. The pipe C_1 and all the parts of the scattering chamber outside it were at a potential V which was the highest positive potential of the apparatus. It was maintained by a transformer and electron-tube rectifier with a large condenser to eliminate ripple. The voltage was found by measuring with a microammeter the current through a calibrated high resistance.

The filament was maintained below ground potential by means of a power pack producing a voltage V_R which was a small fraction of the total voltage used to accelerate the electrons. The electrons were thus incident on the foil with an energy corresponding to the total voltage $V+V_R$. The scattered beam was defined in field-free space at high potential by the diaphragm D_2 (which was considerably smaller than D_3). Passing through D_3 the electrons were retarded by the voltage V, applied between D_3 and a grid of fine tungsten wire in the opening of C_2. Hence only the energy corresponding to the voltage V_R could be retained by any electron passing through the grid. For this reason V_R may be called the residual voltage. Any electron which lost in being scattered an energy as great as that corresponding to this residual voltage was repelled before reaching the grid.

Not only these electrons were excluded by the retarding voltage V but also secondary electrons ejected from the foil by the primary beam and any that may have been ejected by x-rays from any part of the apparatus except the interior of C_2.

Electrons passing the grid of C_2 were collected on the plate P. This was maintained at a positive potential of 270 volts with respect to the grid to prevent the escape of electrons by recoil or the escape of secondary electrons ejected from P. The current to P passed thence to an amplifier of the Barth type, described by Penick[3] and the amplified current was measured by a shunted Leeds and Northrup Type R galvanometer.

The current incident on the foil was commonly about 10 μa. With the precautions taken against slow electrons and x-rays it was possible to measure scattered currents as small as 10^{-6} μa. This allowed the diaphragm D_2 to be made small enough to give a rather high angular resolution. It subtended a plane angle of about 3° at the foil, its solid parallax, Ω in Eq. (1), being 0.00223 rad.[2]

In measuring the fraction of the incident electrons scattered at any angle through the diaphragm D_2, readings of the incident and scattered currents were alternated. To measure the incident current, the foil was removed from the incident beam by the mechanism above the scattering chamber, which was operated from a distance by gas pressure, without impairing the insulation of the scattering chamber or jarring the apparatus. The incident current then passed directly to the chamber C_3 and was measured by the microammeter M, which could be read from a distance. When the diaphragm carrying the foil was removed from the incident beam it was replaced by an open diaphragm carefully made to be as nearly as possible identical with it. This diaphragm was used for "blank" readings to detect any current to C_2 other than that of electrons scattered by the foil. Whatever such current there was, it was too small to measure.

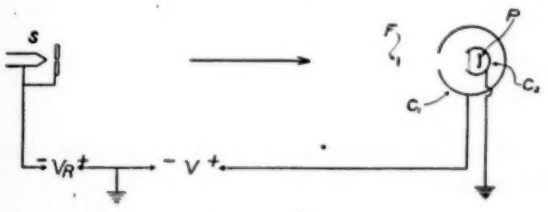

FIG. 2. Schematic diagram of apparatus showing potentials of different parts. S, source of electrons, filament of accelerating tube. F, scattering foil. C_1, chamber enclosing region of retarding voltage. C_2, collecting chamber. P, collecting electrode. V_R+V, total accelerating voltage. V, retarding voltage. V_R, residual voltage.

[3] D. B. Penick, Rev. Sci. Inst. **6**, 115 (1935).

The zero of the galvanometer was subject to some drift. To eliminate the effect of this each reading made with the beam of electrons incident on the foil was bracketed between two readings with the beam cut off.

RETARDATION OF ELECTRONS IN THE FOIL

Any electron traversing the foil must lose some energy in remote collisions with other electrons. It would obviously be a mistake to set the residual voltage so low as to exclude from the measured scattered current any electrons which had lost only such energy as this. To find a proper value for the residual voltage, the current scattered to the collecting electrode was measured with various values of the residual voltage. Figure 3 shows the result of observations made with one foil (foil II of the later discussion). The scattered current was measured at 90°, with the electrons emerging from the same face of the foil as that on which they were incident. Incidence was at 45°, so that an electron traversing almost the whole oblique thickness of the foil and being reflected through 90° at the far side would have a length of path in the foil $2\sqrt{2}$ times the thickness of the foil. No other conditions of observation would provide so great a possible length of path and hence so great a possible retardation.

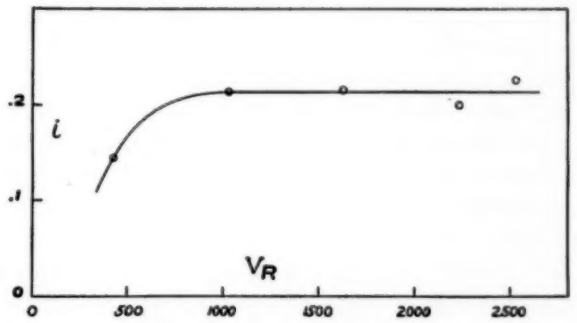

FIG. 3. Variation with residual voltage of current to collecting electrode (in units of 1 cm galvanometer deflection per microampere incident on foil). Scattering at 90° on side of incidence. Foil II.

It is evident from the figure that the energy lost by ordinary retardation was less than 1 kev, since the current was not increased by the increase of residual voltage from 1 to 2.5 kev. The thickest foil used in the observations on scattering was about twice as thick as the one used here.

The residual voltage employed was 2.5 kv, which is judged more than enough to compensate for the ordinary retardation of the electrons.

Tests of Single Scattering

Wentzel[4] has given as a criterion for single scattering of the Rutherford type that the angle θ at which scattering is observed shall be several times greater than 4ω, where

$$\omega = 2\cot^{-1}\frac{2V}{Ze}\left(\frac{2}{\pi nt}\right)^{\frac{1}{2}},$$

eV being the kinetic energy of the electron. It has been customary to consider scattering as single at angles above 12ω. In the present experiment ω, as reckoned from the oblique thickness of the foil, was about 2° for the thinner foils used and something less than 3° for the thickest. Consequently the criterion would be satisfied at angles around 30° and higher. Instead of depending wholly on Wentzel's criterion, however, we have applied a more empirical test of single scattering derived from the following considerations.

When the foil is thin enough for most of the electrons to pass through with only small deflections, it is very improbable that one electron should undergo two large deflections. The deviations from strictly single scattering at any large angle will rather be due almost entirely to the combination of a single deflection through an angle nearly equal to this one with one or more much smaller deflections.

In Fig. 4 let OP be the direction of the beam of electrons incident on the foil. Let OQ be the direction of the observed scattered ray making an angle θ with the direction of incidence, OP. Let it be assumed that an electron observed in the ray OQ entered the ray not by a single deflection from OP to OQ through the angle θ but by the combination of two deflections, one from OP to OP' through a small angle ϵ and another from OP' to OQ through the angle θ' nearly equal to θ. The angle Φ between the planes of ϵ and θ may be taken at random. Also the sequence of the two deflections has no significance in the result; ϵ may even be considered as the resultant of several small deflections of which some may precede and some follow the large deflection.

[4] G. Wentzel, Ann. d. Physik **69**, 333 (1922).

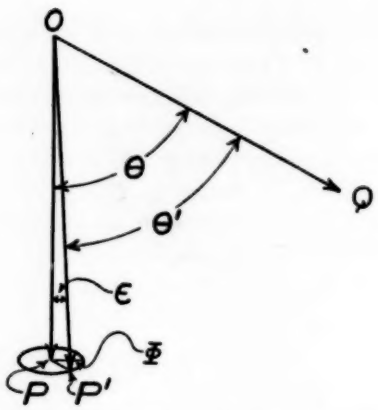

Fig. 4. Combination of small deflection ϵ with large deflection θ' to produce deflection at angle of observation θ. OP, direction of incidence. OP', direction after deflection ϵ. OQ, direction after deflections ϵ and θ'. Φ, angle, assumed random, between planes of ϵ and θ.

If powers of ϵ above the second are neglected,

$$\theta' = \theta - \epsilon\cos\Phi + \tfrac{1}{2}\epsilon^2\cot\theta\sin^2\Phi.$$

Let $p(\theta)$ be the probability of single deflection through the angle θ from the ray OP to the ray OQ, and let $p(\theta')$ be the probability of single deflection through the angle θ' from the ray OP' to the ray OQ. Then to the same degree of approximation as before

$$p(\theta') = p(\theta) - \frac{\partial p}{\partial\theta}(\epsilon\cos\Phi - \tfrac{1}{2}\epsilon^2\cot\theta\sin^2\Phi) + \frac{1}{2}\frac{\partial^2 p}{\partial\theta^2}\epsilon^2\cos^2\Phi.$$

Let $p'(\theta)$ denote the average probability of deflection into the ray OQ of an electron initially incident in the direction OP but deflected through the angle ϵ, the average to be taken with all values of Φ equiprobable. Then

$$p'(\theta) = \frac{1}{\pi}\int_0^{\pi} p(\theta')d\Phi.$$

With the expression given above for $p(\theta')$, we obtain

$$p'(\theta) - p(\theta) = \tfrac{1}{4}\epsilon^2\left(\cot\theta\frac{\partial p}{\partial\theta} + \frac{\partial^2 p}{\partial\theta^2}\right). \qquad (3)$$

To find the error made when the actual, approximately single scattering is taken as strictly single, it is necessary to average this expression

over all values of ϵ. The error is thus the right-hand member of the equation with ϵ^2 denoting the mean square deflection of electrons having a mean length of path in the foil equal to that of the electrons deflected at the angle θ from the direction of incidence. In our experiment, incidence being at 45°, the mean length of path was not very different among the electrons observed and was not greater at any angle than that of an electron passing undeflected through the foil. Consequently ϵ^2 was not greater than the mean square deflection of all the electrons incident on the foil, which could be estimated experimentally. Equation (3) is valid for any law of scattering provided the observed large deflections may be ascribed to the combination of a single large deflection only with much smaller deflections. The derivatives of p may in this case be replaced without serious error by those of the experimentally determined function p'. Thus the experimental data furnish all the means of the test.

The observations in this experiment show p' varying very nearly as $\csc^4(\theta/2)$. In this case Eq. (3) gives for the fractional error caused by plural scattering:

$$\{p'(\theta)-p(\theta)\}/p(\theta)=\epsilon^2\{\csc^2(\theta/2)-\tfrac{1}{2}\}. \quad (4)$$

To estimate ϵ^2, the scattering at small angles was observed with the movable collecting chamber. The observations made with one foil (foil II of the later discussion) are shown in Fig. 5, the current collected in the chamber being plotted against the angle. Since the diaphragm in the front of the chamber subtended approximately 3°, the resolution was low at these small angles, and ϵ^2 could not be determined accurately. But since the collected current at 0° was 0.3 of the incident current, it is clear that 0.3 of the incident electrons were not scattered through more than 1.5°, half the angle subtended by the diaphragm. From this and the shape of the curve, it seems reasonable to take 2° or 0.035 rad. as the value of ϵ. With this value, the error caused by plural scattering would be 1.8 percent at 30° and 0.18 percent at 90°. With the thickest foil used, the errors would be not quite twice as large as with this one.

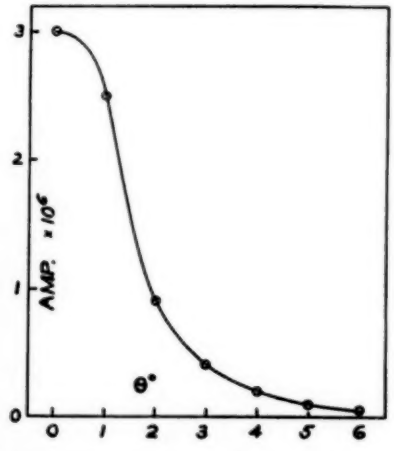

FIG. 5. Scattered current at small angles, in microamperes. Foil II. The incident current was 10 μa.

From the preceding calculation it may be seen why the simple form of Wentzel's criterion, which states that θ shall be at least equal to about 12ω, serves as well as it does. From Eq. (4) it follows that, if the fractional error is not to exceed a certain value δ, then it is necessary that

$$\frac{\theta}{\epsilon} \geq \frac{1}{\delta^{\frac{1}{2}}}\theta[\csc^2(\theta/2)-\tfrac{1}{2}]^{\frac{1}{2}}.$$

Now $\theta[\csc^2(\theta/2)-\frac{1}{2}]^{\frac{1}{2}}$ varies only slowly with θ. From the value 2 when θ is zero it goes to a minimum of 1.9 when θ is about 0.6π and rises to 2.2 when θ is π. To set a maximum for the fractional error is thus approximately the same as to set a minimum for θ/ϵ (about 14 for a maximum error of 2 percent).

If the coherence of the scattering is not important, ϵ is proportional to $(nt)^{\frac{1}{2}}$. So also is ω if it is small. Hence setting a maximum value for the fractional error is also approximately setting a minimum value for θ/ω, as is done in applying Wentzel's criterion.

If Wentzel's criterion is to be valid, however, ω must be reckoned with t taken as the mean length of path in the foil of the electrons scattered at the angle θ, not as that of an undeflected electron. A similar point has already been made in regard to ϵ. The exceptions to Wentzel's criterion reported by Neher[5] may probably be ascribed to the fact that the average path of the scattered electrons in his experiment was much greater than the foil thickness, from which ω was computed.

[5] H. V. Neher, Phys. Rev. **38**, 1321 (1931).

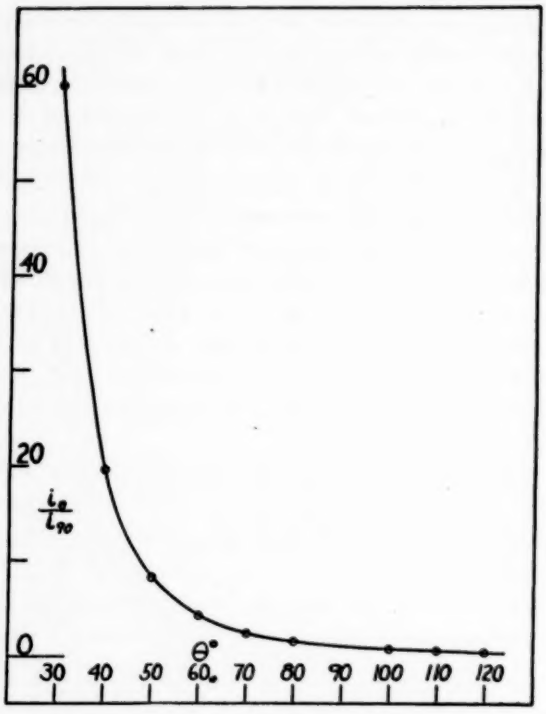

FIG. 6. Variation with angle of relative scattered current. Plotted points show averages of measurements with three foils. Curve shows Mott's theory.

RELATIVE SCATTERING AT VARIOUS ANGLES

Three foils were used in the final observations, all made in the same way. Al wire was wrapped around a tungsten filament and evaporated in vacuum by heating the filament. Some of the Al was allowed to condense on the very thin collodion film used as the support for the scattering foil.

The collodion film was too thin to allow a measurement of its thickness, but it was not so thin that its contribution to the scattering could be ignored. Consequently in order to compare the absolute intensity of the scattered current with that predicted it was necessary to determine the difference in the scattering by a film before and after a known layer of Al was deposited on it. Moreover the scattering by the collodion alone could not be measured directly, for uncoated films of collodion were quickly destroyed by the beam of electrons. Probably they became so highly charged that they were torn apart by electrostatic forces.

Foils I and II were collodion films thinly coated with Al. Foil III was the same foil as II but with an additional coating of Al of about the same thickness as the first. The difference in the scattering by foils II and III was ascribed to the second layer of Al. The determination of this difference was thus subject to the inaccuracies of the observations with both foils. The measurement of all absolute intensities is also subject of course to inaccuracies of calibration and to the considerable uncertainty in the determination of the thickness of the Al layer.

The comparison of the relative scattering at different angles with the prediction of the theory was free from several of the errors of calibration and from the error in measuring the thickness of the foil. Also it did not require taking the difference between the intensities observed with foils II and III. For elements of atomic number as low as those of Al and the constituents of collodion, the third term in the expression for R, Eq. (2), is small, and the difference in its extreme values between 30° and 120° does not amount to more than 2 percent of R. Since the probable errors of even the relative intensities at different angles were greater than this, the third term in R was ignored in the comparison. The other two terms do not involve Z and are the same for collodion as for Al. Hence the data obtained with the three foils could be averaged together.

With these three foils and others used in preliminary observations, an effect was observed for which we have as yet no explanation. It appeared in a comparison of the intensities of the beams scattered at 90° on the two sides of the foil, the side on which the beam was incident and the opposite side. Single nuclear scattering should be equally intense on both sides. But the observed scattering was consistently more intense on the side on which the beam was incident. The ratio of the two intensities was 1.1 for the thinner foils I and II and 1.2 for the thicker foil III.

It is hard to see what sort of scattering could combine with the nuclear scattering to cause such a difference. Some kind of boundary reflection, if it could be imagined great enough to be

TABLE I.

θ	30°	40°	50°	60°	70°	80°	100°	110°	120°
i_θ/i_{90} obs.	60	19.5	8.2	4.1	2.31	1.50	0.69	0.53	0.44
i_θ/i_{90} pred.	60	19.6	8.3	4.2	2.38	1.49	0.71	0.54	0.42

detectable, might produce a difference in this sense, but the absolute value of this difference should remain constant once the boundary was established, and the relative value should diminish with increasing thickness of the foil. The observed difference varied in the opposite way. Any effect of the coherence of the scattering at different scattering centers might increase in its relative value with increasing thickness of the foil, but it is hard to imagine either that coherence would be important at 90° with 50-kv electrons or that coherent scattering would be asymmetrical.

On the other hand we have not been able to ascribe the asymmetry to any defect of the experiment. Tests already described seem to make it unlikely that it was caused by scattering from parts of the apparatus other than the foil, or by a selective action of the retarding voltage on electrons traversing different lengths of path in the foil, or by plural scattering. To test for any accidental asymmetry in the apparatus, the foil was turned through 90°, so that its sides of incidence and emergence were reversed with respect to the two sides of the scattering chamber, but the asymmetry persisted.

Measurement of the scattering on both sides of the foil could only be made around 90°. Over the higher range of angles, scattering could be measured only on the side of incidence, and over the lower range only on the other side. Consequently in comparing the scattering above 90° with that below allowance for the observed asymmetry could only be made in some rather arbitrary way.

We have followed the simplest procedure possible by comparing the scattering measured at every angle with that observed at 90° and using the scattering measured at 90° on the side of incidence for the comparison at angles above 90° and the scattering measured at 90° on the side of emergence for the comparison at angles below 90°.

Table I shows the observed values of i_θ/i_{90} with those predicted by Eqs. (1) and (2). The observed values are averages for all the readings with the three foils in which every reading was given the same weight except that 7 out of 260 were discarded, either because they were very far from the mean or because of some suspicious circumstance in the behavior of the apparatus noted when they were made.

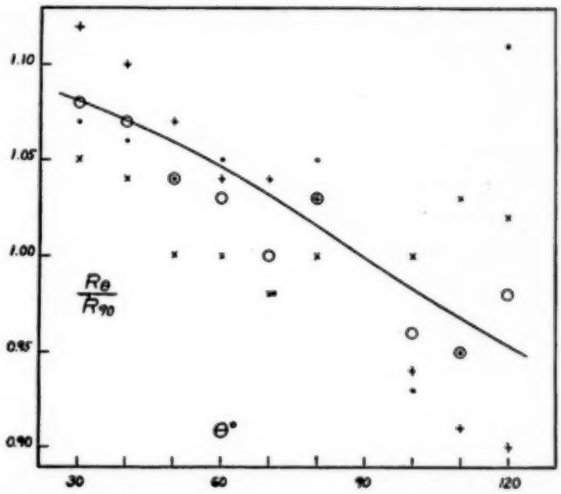

FIG. 7. Variation with angle of R_θ/R_{90}, Eq. (1). Dots, foil I. xxx, foil II. Crosses, foil III. Circles, average. Curve, Mott's theory.

The same data are shown in Fig. 6, in which the points show the observations and the curve shows the prediction. To the scale of this figure only the average values obtained with the three foils can be shown, as the points representing the separate observations fall too near together to be plotted. Although the deviations of the plotted points from the curve are scarcely discernible, it should be noted that the graph of i_θ/i_{90} against θ does not give a very critical comparison of observation with prediction, since the factor $\csc^4(\theta/2)$ must provide the dominant variation in any theory of scattering in a Coulombian field. A stricter comparison is made in Fig. 7, in which R_θ/R_{90} is plotted against θ. The curve is plotted from Eq. (2) with neglect of terms after the second. The plotted points show the observations made with the three foils and their average. The curve passes about as near to the open circles, which show the average values of the measurements, as any smooth curve could. The agreement is, indeed, perhaps closer than can be considered significant in view of the spread of the measurements with the foils separately.

Absolute Intensity of Scattering

To obtain the scattered intensity as a fraction of the incident current, it was necessary to find what part of the current passing through the

diaphragms D_2 and D_3 was intercepted by the grid in front of the collecting plate P. This was done by swinging the diaphragm D_2 into the incident beam with the scattering foil removed and measuring the current to P with a microammeter, and alternately swinging the chamber C_1 out of the beam and measuring the current to the fixed collecting chamber C_3. The current to P was found to be 90 percent of that to C_3.

To compare the absolute values of i_θ observed and predicted, it was necessary to determine the thickness or, more directly, the mass per unit area, of the second Al layer deposited on foil II to produce foil III. Two estimates were made. The first was by assuming that all the Al wire wrapped around the tungsten filament was evaporated, as it appeared to be, and that the fraction deposited per unit area on the foil was $1/(4\pi r^2)$, where r is the distance from the filament to the foil. The surface density of the foil so estimated was 16.2 micrograms per cm^2, which would make the thickness 6.0×10^{-6} cm. Two factors may have made this estimate too high. The Al may not have been entirely evaporated from the filament and some of the atoms striking the foil may not have adhered. Of course some atoms may have reached the foil after rebounding from other surfaces, but this possibility was limited by baffle-plates above the foil. The values of i_θ predicted from this estimate of the surface density are for these reasons more likely to be high than low, and the ratio of the observed i_θ to that predicted more likely to be low than high.

The other estimate was kindly made for us by Mr. Hermann Yagoda by a colorimetric microchemical method applied to a layer of Al deposited on a blank collodion film by the evaporation of the same quantity of Al wire and under the same conditions as in the preparation of foil III.

A disk of this foil 4.8 mm in diameter was immersed in 0.5 cm^3 of 10-percent hydrochloric acid, which was then warmed over steam until the film lost its metallic luster. The solution, together with water used in two subsequent washings of the collodion film, was transferred to a micro-Nessler tube. The contents of the tube were treated with 0.4 cm^3 of 50-percent ammonium acetate and 0.1 cm^3 of freshly prepared 0.5-percent solution of the ammonium salt of aurin tricarboxylic acid. The solution was diluted to 2 cm^3 and, 15 minutes later, when the pink of the Al lake became fully developed, the sample was compared in color with a set of standards made by treating standardized Al-ion solutions in the same way as the solution of the Al of the foil had been treated.

The surface density of the foil found by this method was 13.6 micrograms per cm^2, which would make the thickness 5.0×10^{-6} cm.

Other samples of the Al layer meant to be measured by another chemical method were unfortunately destroyed in the process without yielding a result.

In reckoning the difference in the currents scattered by foil III and foil II, which is to be ascribed to the additional layer of Al, only the readings at angles from 30° to 60° have been used, since the random errors of the measurements were relatively larger at the higher angles. The ratio of the observed scattering to the predicted is 0.80 if the surface density of the foil is reckoned by the inverse-square calculation and 0.96 if it is taken as given by the colorimetric method. Both values would be lower if the readings at larger angles were included. The first and smaller of these values might be expected to be low, as was explained before. Either one is uncertain by as much as the difference between them. It would appear, however, from these observations that if the actual scattering is different from that predicted by Mott it is more likely lower than higher.

Comparison with Neher's Observations

Among the many experiments on the scattering of electrons, a part of the work of Neher[5] seems most nearly comparable to ours in respect to the experimental conditions. He measured the scattering by Al of electrons at voltages around that of our experiment and at higher angles above 90°. He found, as we do, that the relative scattering at different angles is in agreement with Mott's theory, though because of the small difference between Mott's distribution and Rutherford's he could not discriminate between them. He found the ratio of the observed to the predicted scattering to be 1.32, an apparent differ-

ence from our result given above. Since all his observations were made above 90°, where ours are least accurate, the two results may not be strictly comparable. If they may be compared, then our observation of the asymmetry between the scattering on the side of incidence and on the other side may perhaps be relevant. All of his observations were on the side of incidence, and if the excess scattering to this side is a general characteristic of scattering by foils and not a peculiarity of our apparatus, the difference between his observations and ours might be explained.

We wish to thank Mr. A. C. Weid for help in the construction of the apparatus and in making preliminary observations, Mr. Hermann Yagoda for measurements on the foil thickness, our colleagues Professors F. E. Myers and O. Halpern and Dr. R. D. Huntoon for helpful discussions, and Mr. William Werker for technical assistance.

AUGUST 1, 1940 PHYSICAL REVIEW VOLUME 58

Partially Inverted Multiplets in MgI

LEO PINCHERLE
King's College, London, England

(Received December 11, 1939)

With the use of Fermi-Thomas statistical eigenfunctions the separations of the $3s3d\ ^3D$ term of MgI are evaluated, taking into account all the magnetic interactions in the atom and the electrostatic interactions with other configurations. The smallness of the observed separations is found to be due to the large value of the exchange integrals of the magnetic actions.

1. INTRODUCTION

THIS note discusses some remarkable fine structures found by Meissner[1] in the magnesium spectrum (MgI), namely partially inverted multiplets showing very small separations. It will be shown that they arise from several causes whose importance can be evaluated; the exact calculation is, however, impossible because of the approximations which one is compelled to introduce and because of the unavailability of accurate atomic eigenfunctions. In any case the study of these phenomena in a particular example may be interesting in view of conclusions that are generally valid in similar cases.

We shall discuss the $3s3d\ ^3D$ term, placed at 13,712 cm^{-1}, whose levels, relative to the center of gravity of the term, are, respectively:

$$^3D_3 \text{ at } +0.0032 \text{ cm}^{-1}; \quad ^3D_2 \text{ at } -0.0140 \text{ cm}^{-1};$$

$$^3D_1 \text{ at } +0.0157 \text{ cm}^{-1}.$$

These positions are those which would be expected according to the theory if only the spin-spin interaction of the two outer electrons, and no other magnetic energy, existed. In fact, according to this hypothesis, the positions of the levels would be:

$$^3D_3 \text{ at } +\tfrac{1}{14}L\alpha^2; \quad ^3D_2 \text{ at } -\tfrac{1}{2}L\alpha^2; \quad ^3D_1 \text{ at } +\tfrac{1}{2}L\alpha^2,$$

(α = fine structure constant;

$$L=\int_0^\infty R_{3s}^2(r_1)r_1^2dr_1\int_{r_1}^\infty R_{3d}^2(r_2)\frac{dr_2}{r_2};$$

R_{3s}, R_{3d} = radial eigenfunctions of the $3s$ and $3d$ electron, respectively). Thus the ratios between the experimental values are very near to the theoretical ones, and also the value of the integral L, evaluated with Fermi statistical eigenfunctions, is

$$L\alpha^2=0.055 \text{ cm}^{-1},$$

leading to the correct order of magnitude of the separations.

Now the interaction considered is only one, and not the most important, of the causes which contribute to the splitting of the term. We have now to discuss all these causes.

[1] K. W. Meissner, Ann. d. Physik **31**, 518 (1938).

First of all the splitting is determined by the magnetic interactions in the atom. As is known, usually a sufficient approximation is obtained by considering only the "spin-orbit interaction" for the outer electrons

$$H=\frac{\alpha^2}{2}\frac{1}{r}\frac{\partial U(r)}{\partial r}\mathbf{L}\cdot\mathbf{S},$$

neglecting all the other magnetic interactions and the exchange, and assuming for the potential U a suitable expression that takes into account the screening of the nuclear field by the inner electrons. This approximation would give in our case, again using statistical eigenfunctions, the value $+0.41$ for $z(^3D)$ (the "parameter of the spin-orbit interaction"), namely a *normal* triplet with separations larger by a factor 30 or 50 than the observed ones.

That means that the approximation is not sufficient, as could of course be expected, and we have to calculate directly the energies of all the magnetic interactions of the electrons outside closed shells with the other electrons (and with the nucleus) and between themselves. The results of these calculations, whose particulars are given in Section 2, have no great significance because of the inadequate approximation (the use of statistical eigenfunctions), but it appears that the value of $z(^3D)$ is very much lowered by the exchange integrals of the magnetic actions, whose contribution to the parameter is negative, and which has a relatively large value (-0.27 cm^{-1}), practically equal to the contribution of the classical integrals. (We can introduce a parameter analogous to the ordinary parameter of the spin-orbit interaction because all the non-vanishing magnetic energies (excepting the above-mentioned spin-spin interaction of the two outer electrons) cause the triplet to be a normal one.)

Among the other causes that can contribute to the splitting of the multiplet, hyperfine structures do not occur for the atom in question and, as the magnetic interactions are very small compared with the Coulomb interactions, the Russell-Saunders approximation is strictly valid. On the other hand, it is found in Section 3 that an electrostatic configuration interaction causes separations comparable with those produced by the magnetic actions. Also this cause produces a normal separation of the triplet and we must therefore conclude that, in order to obtain as a resultant the observed practically null separation, the sum of the magnetic actions must in reality produce a completely inverted multiplet and then that the value of the exchange integrals of these actions should be larger than the above given value. Then the calculation does not lead to definite conclusions about the observed positions of the levels. It is, however, likely that the sum of all the causes, which would make the term a normal one, happens to be zero, and so the observed features are due mainly to the spin-spin interaction of the two outer electrons, and possibly to minor causes which produce, for the other interactions, small deviations from Landé's interval rule.

2. Evaluation of the Magnetic Integrals

As an expression for the interaction of two electrons the best approximation is Breit's formula,[2] namely

$$H_{12}=\alpha^2\left\{\left(\left[\frac{\mathbf{r}_1-\mathbf{r}_2}{r_{12}^3},\frac{2\mathbf{p}_2-\mathbf{p}_1}{2}\right]\cdot\mathbf{s}_1\right)+\left(\left[\frac{\mathbf{r}_1-\mathbf{r}_2}{r_{12}^3},\frac{\mathbf{p}_2-2\mathbf{p}_1}{2}\right]\cdot\mathbf{s}_2\right)\right\}$$

$$+\frac{\alpha^2}{r_{12}^5}\{-3((\mathbf{r}_1-\mathbf{r}_2)\cdot\mathbf{s}_1)((\mathbf{r}_1-\mathbf{r}_2)\cdot\mathbf{s}_2)+r_{12}^2(\mathbf{s}_1\cdot\mathbf{s}_2)\}$$

$+$ terms not dependent on the spin,

where $\mathbf{r}_1$, $\mathbf{r}_2$ are the coordinates of the two electrons, $\mathbf{p}_1$, $\mathbf{p}_2$ their momenta, $\mathbf{s}_1$, $\mathbf{s}_2$ their spins and r_{12} their separation.

We have to consider the interaction between the nuclear field and the spin of the $3d$-electron

$$H_n=\alpha^2Z([\mathbf{r}/r^3,\mathbf{p}/2]\cdot\mathbf{s}),$$

which gives the first-order perturbation energy

$$E_n=\int\psi_{3d}^*H_n\psi_{3d}d\tau,$$

and the interaction between all the inner electrons and the $3d$-electron; besides the classical

[2] G. Breit, Phys. Rev. **34**, 553 (1929).

integrals E_c of these interactions

$$E_c=\sum_k \int \psi_k^*(1)\psi_{3d}^*(2)H_{12}\psi_k(1)\psi_{3d}(2)d\tau_1 d\tau_2,$$

we have to consider also the exchange integrals E_s

$$E_s=\sum_k \int \psi_k^*(1)\psi_{3d}^*(2)H_{12}\psi_k(2)\psi_{3d}(1)d\tau_1 d\tau_2.$$

In the preceding sums we include the spin-orbit interaction of the two outer electrons which, like the other interactions, produces a normal triplet; on the contrary their spin-spin interaction, treated already, which produces another kind of separation is not included. The sum of the interactions of the $3s$-electron with the inner electrons vanishes.

The calculations are rather long: they require mainly the use of well-known formulas on spherical harmonics; for the details we may refer to a note of David[3] on the doublets of lithium; they are simplified by sum theorems. For instance, the integral with respect to the spin coordinates, when we sum over the pair of inner electrons with equal space eigenfunctions and opposite spins, is in every case simply m_s multiplied by a numerical factor (m_s refers to the $3d$-electron); the result of the integration with respect to the angular coordinates, when we sum over all the inner electrons with the same n and the same l, is likewise m_l multiplied by a numerical factor; and so for instance E_c becomes

$$E_c=-\alpha^2 m_s m_l \sum_{n'l'}(2l'+1) \times \int_0^\infty R_{3d}^2(r_2)r_2^{-1}dr_2 \int_0^{r_2} R_{n'l'}(r_1)r_1^2 dr_1$$

(n', l' = quantum numbers of the inner electrons). The exchange integrals are more complicated, especially for $l'=1$; besides the R's they contain also the dR/dr's.

All the integrals have a factor $m_s m_l$; thus the diagonalization of that portion of the matrix E which corresponds to a given configuration n, l is obtained exactly as in the ordinary theory: in particular the parameter z_{3d} (corresponding to the ordinary parameter of the spin-orbit interaction for the $3d$ electron) is obtained by substituting formally in all the integrals $l+\frac{1}{2}$ ($=5/2$ in our case) in place of $m_s m_l$. The required separation parameter of the ^3D term is $z(^3D)=\frac{1}{2}z_{3d}$. Table I summarizes the results, giving the contribution to $z(^3D)$ of the various integrals. It is difficult to estimate the size of the error produced by the use of the statistical eigenfunctions. It can even be rather large, but it probably affects the classical and the exchange integrals in the same way. In any case, even if the results obtained, especially the value of $z(^3D)$, are uncertain, the large value of the exchange integrals is ascertained. If we neglect these integrals, we obtain for $z(^3D)$ the value

$$z(^3D)=+0.032 \text{ cm}^{-1}$$

in fair agreement with the value $+0.41$ given by the ordinary calculation of the spin-orbit interaction.

TABLE I. *Contributions to the separation parameter of the $3s3d\,^3D$ term of* MgI.

Interaction E_n with the nuclear field		$=+1.62$ cm
Classical interaction E_c with the inner electrons		$=-1.30$ cm
Exchange interaction E_s with the inner electrons		$=-0.27$ cm
Total	$z(^3D)$	$=+0.05$ cm

3. CONFIGURATION INTERACTION

The term we are studying is $3s3d\ ^3D$. It can interact only with other even ^3D terms; the nearest is $3p4p\ ^3D$. It is a negative term to which we can ascribe a position[4] of about $-22{,}000$ cm^{-1}, and it is almost the only one responsible for the perturbation. As it is a normal triplet, it produces a normal separation also for the term we are studying.

It may seem strange that there can be an appreciable perturbation by such a distant term, but it depends essentially on the very small value of the required separations; moreover Bacher[5] has shown that in the same MgI spectrum the $3s3d\ ^1D$ term is greatly displaced from its normal

[3] E. David, Zeits. f. Physik **91**, 289 (1934).

[4] This is the position observed by F. Paschen (Ann. d. Physik **12**, 509 (1932)), for $3p3d\,^3D$ which should have about the same energy.

[5] R. F. Bacher, Phys. Rev. **43**, 264 (1933); **56**, 385 (1939). As I had the necessary eigenfunctions at my disposal, I have calculated again the integral R_s of Bacher's note, and I have found the value 23,060 cm^{-1} instead of 21,353 as found by Bacher with another kind of eigenfunction.

position by the perturbation of a notably distant term. Another case of configuration interaction has been treated by Hartree and Swirles.[6]

As we have a complete Russell-Saunders coupling, each of the levels of the terms interacts only with the level of the other configuration with the same J, and the interaction is independent of J, as follows from the fact that the electrostatic interaction commutes with all components of $\boldsymbol{L}$ and $\boldsymbol{S}$.

The matrix element connecting the two configurations is[7]

$$T=(2/15)^{\frac{1}{2}}[R^1(3s3d,\ 3p4p)-R^1(3s3d,\ 4p3p)].$$

Let A be the difference between the wave numbers of the centers of gravity of $3s3d\ {}^3D$ and $3p4p\ {}^3D$, and let z be the separation parameter of the $3p4p$ term; then, neglecting the very small separation of the $3s3d$ term, we obtain three similar secular equations for the three levels, e.g., for the ${}^3D_3$ term:

$$\begin{vmatrix} -x & T \\ T & -A-2z-x \end{vmatrix}=0.$$

From these equations we obtain as displacements of the $3s3d\ {}^3D$ levels:

$${}^3D_3:\ \frac{T^2}{A+2z}\approx\frac{T^2}{A}\left(1-\frac{2z}{A}\right),$$

$${}^3D_2:\ \frac{T^2}{A-z}\approx\frac{T^2}{A}\left(1+\frac{z}{A}\right),$$

$${}^3D_1:\ \frac{T^2}{A-3z}\approx\frac{T^2}{A}\left(1+\frac{3z}{A}\right).$$

[6] D. R. Hartree and B. Swirles, Proc. Camb. Phil. Soc. **33**, 240 (1937).

[7] Notations as in Condon and Shortley, *The Theory of Atomic Spectra* (Cambridge, 1935).

Again using statistical eigenfunctions:

$$R^1(3s3d,\ 3p4p)=-3290\ \text{cm}^{-1};$$
$$R^1(3s3d,\ 4p3p)=+4620\ \text{cm}^{-1};$$
$$T=-2890\ \text{cm}^{-1}.$$

The experimental value of A is $\sim$36,000 and that of z is 10.8 cm^{-1}.[8] We have then a displacement of the center of gravity of the term

$$T^2/A=232\ \text{cm}^{-1},$$

and the separation parameter of the perturbed $3s3d\ {}^3D$ term is

$$zT^2/A^2=0.069\ \text{cm}^{-1}.$$

It is of the same order of magnitude as the separations due to the magnetic actions.

Terms such as $3p5p\ {}^3D$ and higher ones produce only negligible perturbations as compared with that now studied. The $(2p)^5(3s)^2 3p\ {}^3D$ term has a very large separation and is inverted, so that its action is in the opposite sense to, that of $3p4p\ {}^3D$; but, owing to its great distance (>3 Ry), it has no appreciable effect.

4. Conclusion

The smallness of the separations of the $3s3d\ {}^3D$ term of MgI is due to the large value of the exchange integrals of the magnetic interactions between the $3d$ electron and the inner electrons. They probably compensate also the separation produced by the electrostatic interaction of $3s3d\ {}^3D$ with $3p4p\ {}^3D$ which is found to be comparable with that due to the magnetic actions.

The particular position of the levels seem to be due only to the spin-spin interaction of the two outer electrons.

[8] We deduce this value from the experimental separations of the $2s3p\ {}^3P$ and $2s4p\ {}^3P$ triplets, remembering that for $npn'p\ {}^3D$ terms $z({}^3D)=\frac{1}{4}(z_{np}+z_{n'p})$.

The Absorption of Praseodymium Ion in Solutions and in the Solid State

F. H. SPEDDING
Chemistry Department, Iowa State College, Ames, Iowa

(Received May 9, 1940)

Following the methods outlined in Condon and Shortley's *Theory of Atomic Spectra*, the energy states of praseodymium IV were calculated. It was assumed in the solid and liquid phases that the sharp absorption spectrum would arise from transitions within the incomplete $4f$ shell, in other words from states arising from the f^2 configuration. Excellent agreement was found with the experimentally observed values of Pr IV.

THE absorption spectrum of praseodymium ion in solutions and in the solid state has been studied by a great many investigators during the past forty years. The spectrum always consists of three narrow bands in the blue-green region and an additional band in the red. These bands show some structure at room temperatures and resolve into many extremely sharp lines at low temperatures. While the positions of these bands in the spectrum remain approximately constant regardless of the praseodymium compound and are therefore to be attributed to electronic transitions involving the Pr ion, they do shift slightly, and the fine structure of the bands may vary considerably.

On account of the weak intensity and extreme sharpness of these bands Van Vleck[1] concluded on theoretical grounds that they must be due to transitions between electronic states arising from rearrangement of the $4f$ electrons of the rare earth ion. In other words they are transitions entirely within the incomplete $4f$ shell. If this is true and if Russell-Saunders coupling is assumed, it can readily be shown by the application of Pauli's principle that the only states allowed for Pr^{+++} are ^3H, ^3F, ^3P, ^1I, ^1G, ^1D and ^1S and that the absorption bands must arise from transitions between these states. Hund's[2] work on magnetic susceptibilities shows that at least for the lowest state Russell-Saunders coupling is closely approximated.

From analogy with the La II spectrum Ellis[3] concluded that the blue bands of praseodymium arose from a $^3H_4-{}^3P_{0,1,2}$ and that the red band arose from the $^3H_4$-$^1I_6$ transition. Bethe and Spedding[4] next showed that the spectrum of Tm IV could be completely accounted for on theoretical grounds. This is the companion rare earth to Pr IV and has the same energy states except that they are inverted due to the incomplete $4f$ shell being more than half completed. They assumed that the bands were due to transitions between states arising from the $4f^{12}=4f^2$ configuration. Following the methods outlined in the book by Condon and Shortley,[5] they calculated the separation of the levels due to electrostatic interaction and then took into account the spin-orbital interactions including *perturbations*. It was found for the upper states that Russell-Saunders coupling was far from being obeyed, since in some cases the perturbations amounted to as much as 10,000 cm^{-1}. The theoretically predicted bands, however, are in excellent agreement with the experimentally observed ones, the discrepancies in all cases being much smaller than might reasonably be expected when one considers the very simple assumptions which were made in the theoretical calculations. This holds also for the four new bands[6] which now have been observed, but which were not reported at the time the predictions were made.

[1] J. H. Van Vleck, J. Phys. Chem. **41**, 67 (1937).
[2] F. Hund, Zeits. f. Physik **33**, 855 (1925).
[3] C. B. Ellis, Phys. Rev. **49**, 875 (1936).

[4] H. Bethe and F. H. Spedding, Phy. Rev. **52**, 454 (1937).
[5] E. U. Condon and G. H. Shortley, *The Theory of Atomic Spectra* (Cambridge 1935), p. 207.
[6] Selection rules state that the $^3H_6-{}^3P_1$ $^3H_6-{}^3P_0$ should be absent or at least very faint. Gobrecht, Ann. d. Physik **31**, 600 (1935), finds bands between 34,000 cm^{-1} and 38,000 cm^{-1} which he attributes to Tm IV but states his salts contained Gd as an impurity. Meehan and Nutting, J. Chem. Phys. **7**, 1001 (1939), fail to report any bands in this region. Spedding and Gladrow in work now in progress have photographed $Tm_2(SO_4)_3 \cdot 8H_2O$ crystals 2.5 mm in thickness and find no trace of these bands. They are planning to photograph much thicker crystals in the near future to see if any trace of them exists.

Lueg,[7] Freyman and S. Takavorian,[8] Gobrecht[9] and Rosenthal,[10] have investigated the infra-red spectrum of praseodymium and have reported bands at about 5200, 6500 and 9800 cm^{-1}. Lange[11] by arbitrarily evaluating the F constants in the formulae for the f^2 configuration given by Condon and Shortley[12] in their electrostatic-interaction calculations, forces a rough fit with experimentally obtained levels. It is tacitly assumed that good Russell-Saunders coupling is obeyed by all levels, and that the perturbations can be neglected. Gobrecht[13] extending Lange's work does the same thing for Tm and also obtains a forced agreement. He objects to the spectroscopic designations given the bands by Bethe and Spedding[4] on the grounds that they used the wrong screening constant. This objection is groundless, since Bethe and Spedding calculated the spacing of the levels for various values of Condon and Shortley's[12] ζ which is directly related to the screening constant σ and chose the best value of ζ to fit with experiment. This value is in excellent agreement with the σ determined from x-ray measurements. Further the designations given by Gobrecht must obviously be wrong since he has levels with the same J quantum number crossing each other which arose from the same electronic configuration. Therefore, the perturbations which he neglected must be extremely large and in fact do amount to as much as 10,000 wave numbers. It also follows that most of the conclusions in these papers regarding screening constants of the rare earths are invalid on account of the neglected perturbations.

TABLE I. *Electrostatic interaction.*

	LaII cm^{-1}	PrIV cm^{-1}	TmIV cm^{-1}
^3H	0	0	0
^3F	1,718	4,120	5,670
^1G	2,750	6,600	9,080
^1D	3,260	7,820	10,750
^1I	5,964	14,330	19,700
^3P	8,015	19,230	26,450
^1S	13,756	33,000	45,400

Mukherji[14] also gives a designation to the transitions of Pr IV and has done this by extrapolating the spacings of the observed levels of La II to the larger spacings which they would occupy in the stronger fields of Pr IV. He has therefore taken into account the perturbations as they exist for La II, but has neglected the greatly increased perturbations which would occur for some levels in Pr IV, and therefore gives the wrong designation for them.

In this paper the levels for the free ion of Pr IV were calculated as follows. For the electrostatic interaction, between the electrons, the calculated value of La II which is analogous to Pr IV was taken as a basis. It was assumed that the spacing between the energy levels without spin orbital interaction is simply multiplied by a constant factor on going from La II to Pr IV. This arises from (a) the higher degree of ionization (b) the greater internal nuclear charge. Assuming Ellis's designation to be correct this turns out to be about 2.4 (Table I).

The constant ζ[12] characteristic of the spin-orbit interaction was calculated for La II from the splitting of the H level which has most nearly Russell-Saunders coupling and was found to be about 170 cm^{-1}. It is assumed that ζ increased again by a factor of 2.4 from La II to Pr IV and should therefore be about 400 cm^{-1} for Pr IV. In column 2 of Table II the positions of the Pr levels are given for this value of ζ when the perturbations are omitted, in other words, pure Russell-Saunders coupling is assumed to exist. In column 3, the positions of the levels are given

TABLE II. *Spin orbital interaction with and without perturbations.*

	ζ = 400 cm^{-1} PrIV WITHOUT	PrIV WITH	Δ	ζ = −1,400 cm^{-1} TmIV WITHOUT	TmIV WITH	Δ
$^3H_4$	−2,400	−2,639	+239	$^3H_6$	−7,000	−7,490	+490
$^3H_5$	−400	−400	0	$^3H_5$	1,400	1,400	0
$^3H_6$	2,000	+1,923	+77	$^3H_4$	8,400	−1,925	+10,325
$^3F_2$	2,520	1,857	+663	$^3F_4$	1,470	5,780	− 4,310
$^3F_3$	3,720	3,720	0	$^3F_3$	7,070	7,070	0
$^3F_4$	5,320	4,391	+929	$^3F_2$	11,270	3,250	+8,020
$^1G_4$	6,600	7,767	−1,167	$^1G_4$	9,080	15,090	−6,010
$^1D_2$	7,820	8,239	−419	$^1D_2$	10,750	16,240	−5,490
$^1I_6$	14,330	14,407	−77	$^1I_6$	19,700	20,190	−490
$^3P_0$	18,430	17,921	+509	$^3P_2$	25,000	27,530	−2,530
$^1P_1$	18,830	18,830	0	$^3P_1$	27,800	27,800	0
$^3P_2$	19,630	19,873	−243	$^3P_0$	29,200	24,665	+4,535
$^1S_0$	33,000	33,509	−509	$^1S_0$	45,400	49,935	−4,535

[7] P. Lueg, Zeits. f. Physik **39**, 391 (1926).
[8] R. Freyman and S. Takavorian, Comptes rendus **194**, 963 (1932).
[9] H. Gobrecht, Ann. d. Physik **28**, 673 (1937).
[10] Gottfried Rosenthal, Physik. Zeits. **40**, 508 (1939).
[11] H. Lange, Ann. d. Physik **31**, 609 (1938).
[12] E. U. Condon and G. H. Shortley, reference 5, p. 207.
[13] H. Gobrecht, Ann. d. Physik **31**, 600 (1938).
[14] P. C. Mukherji, Ind. J. Phys., January, 1938, p. 399.

after perturbations are taken into account. This was done according to the methods outlined by Condon and Shortley[15] or M. H. Johnson, Jr.[16] The secular equations for the f^2 configuration are given below.

		$^1I_6$	$^3H_6$
$J=6$	$^1I_6$	I	$6\frac{1}{2}\zeta$
	$^3H_6$	$6\frac{1}{2}\zeta$	$H+5\zeta$

		$^3H_5$
$J=5$	$^3H_5$	$H-\zeta$

		$^3H_4$	$^1G_4$	$^3F_4$
$J=4$	$^3H_4$	$H-6\zeta$	$-2(10/3)^{\frac{1}{2}}\zeta$	0
	$^1G_4$	$-2(10/3)^{\frac{1}{2}}\zeta$	G	$2(11/3)^{\frac{1}{2}}\zeta$
	$^3F_4$	0	$2(11/3)^{\frac{1}{2}}\zeta$	$F+3\zeta$

		$^3F_3$
$J=3$	$^3F_3$	$F-\zeta$

		$^3F_2$	$^1D_2$	$^3P_2$
$J=2$	$^3F_2$	$F-4\zeta$	$-2(6)^{\frac{1}{2}}\zeta$	0
	$^1D_2$	$-2(6)^{\frac{1}{2}}\zeta$	D	$3(2)^{\frac{1}{2}}\zeta$
	$^3P_2$	0	$3(2)^{\frac{1}{2}}\zeta$	$P+\zeta$

		$^3P_1$
$J=1$	$^3P_1$	$P-\zeta$

		$^3P_0$	$^1S_0$
$J=0$	$^3P_0$	$P-2\zeta$	$-4(3)^{\frac{1}{2}}\zeta$
	$^1S_0$	$-4(3)^{\frac{1}{2}}\zeta$	S

These equations were solved for ζ equals 350 cm^{-1}, 400 cm^{-1} and 450 cm^{-1}, and the results compared with experiment. The best agreement was found for a value of $\zeta=400$ in good agreement with our preliminary assumption. The agreement with experiment was exceptionally good (see Table III), the deviations in every case being much smaller than one might expect considering the simple assumptions used. Further in every case where a band was predicted one was found except for the $^3H_4-{}^3H_5$ transition which occurs so far in the infra-red that that region of the spectrum has not yet been investigated. In no case was a band found where none was predicted. Also the interpretation of the spectrum of praseodymium is completely consistent with the interpretations of the spectrum of La II and Tm IV. By shifting the arbitrary constants slightly (2.4 for the electrostatic interaction and 400 cm^{-1} for ζ) an apparently better fit with experiment might have been obtained. It would not, however, have had any real meaning unless the fine structure of the multiplets due to crystal splitting had been investigated and other possible perturbations taken into account.[17]

TABLE III. *Comparison of calculated and observed terms.*

	PrIV Calc. cm^{-1}	PrIV Ob. cm^{-1}		TmIV Calc.	TmIV Ob.
$^3H_4$	0	0	$^3H_6$	0	0
$^3H_5$	2,239		$^3H_4$	5,565	
$^3F_2$	4,496	4,750	* $^3H_5$	8,490	8,248†
$^3H_6$	4,562	5,650	$^3F_2$	10,740	12,750†
$^3F_3$	6,359	5,950	** $^3F_4$	13,270	14,600
$^3F_4$	7,030	7,250	$^3F_3$	14,560	15,150
$^1G_4$	10,406	9,469	$^1G_4$	22,580	21,500
$^1D_2$	10,878	10,200	$^1D_2$	23,730	21,100
$^1I_6$	17,046	16,630	$^1I_6$	27,680	28,000
		17,480			
$^3P_0$	20,560	20,660	$^3P_0$	32,155	35,000†
		20,910			
$^3P_1$	21,469	21,150	$^3P_2$	35,020	36,300†
		22,305			
$^3P_2$	22,512	22,810	$^3P_1$	35,290	38,000†
		24,050			
$^1S_0$	36,144		$^1S_0$	57,425	

*Maximum at 5180 cm^{-1}.
**Maximum at 6557 cm^{-1} shows a distinct indentation on short wave side.
† These bands were not observed when levels were first calculated. See reference 6.

[15] E. U. Condon and G. H. Shortley, reference 5, p. 267.
[16] M. H. Johnson, Jr., Phys. Rev. **38**, 1628 (1931).

[17] The multiplets due to crystal splitting are always associated with superimposed crystal and molecular frequencies. This causes the multiplets to be composed of many lines. As the sharp absorption spectra are obtained at low temperatures, the observed associated lines are usually due to vibrations superimposed on the excited or upper state and therefore the lines usually occur on the violet side of the multiplets.

Effect of Hyperfine Structure upon the Magnetic Rotation of the Plane of Maximum Polarization of Resonance Radiation

BERTRAND J. MILLER
State University of Iowa, Iowa City, Iowa

(Received April 23, 1940)

An equation has been developed for the polarization, and the angle of maximum polarization of resonance radiation as observed along a magnetic field perpendicular to the electric vector and the direction of propagation of the incident beam. Explicit application has been made to the polarization and the angle for the line $^1S_0-{}^1P_1$ for various values of the ratio of the hyperfine separation constant to the natural breadth of the levels, for a nuclear moment of $\frac{1}{2}$. It was noted here that the form of the curves might differ widely from that to be expected from classical considerations. The polarization, and the angle of maximum polarization for the sodium D lines, for several values of the same ratio, were computed and compared with experimental observations. Thus a range of possible values of A was determined, which is not in disagreement with previous figures, and a value for τ established which agrees well with that calculated from optical dispersion data.

INTRODUCTION

THE polarization of resonance radiation in magnetic fields has been extensively studied, and since the realization of the role played by hyperfine structure, most of the early discrepancies between theoretical predictions and experimental results have been removed. However, one experiment of some interest has not yet been compared with modern theory; i.e., the rotation of the plane of polarization by a magnetic field perpendicular to both the direction of propagation and the electric vector of the exciting beam, the emitted radiation being observed along H.

Experimental data for the polarization and the azimuth of the plane of maximum polarization are available for the D lines of sodium;[1] a theoretical equation for the effect has also been published,[2] but needs some extending, as it is based on the assumption of a separation constant large in comparison with the natural breadth of the levels, whereas, in this experiment, they are of the same order.

It seemed worthwhile to undertake the comparison of this experiment with theory, as it should lead to values of the hyperfine separation constant A, and the mean life, τ which could be compared with those available from other sources.

THEORY

The most convenient starting place is Breit's[2] Eq. (159)

$$I_\xi=(C/g_a)\sum_{\mu,\mu'}^{m,m'}(e\dot{x})_{\mu m}(e\dot{x})_{m\mu'}(e\dot{\xi})_{\mu' m'}(e\dot{\xi})_{m'\mu}/[1-2\pi i\tau\nu_{\mu'\mu}].$$

Here I_ξ is the intensity of radiation polarized in the direction ξ, C is a constant depending on the experimental conditions, μ and m represent sub-levels of the upper state (b) and the lower (a), respectively, and g_a is the statistical weight of the lower state, and is also a constant throughout this paper. τ is the mean life of b, and $\nu_{\mu'\mu}$ is the energy difference between the states μ' and μ expressed, of course, as a frequency. The incident radiation is supposed to be broad compared to the emitted; and is polarized in the x direction.

Let us equip the matrices with more descriptive subscripts; e.g., if the states μ and m are those which would, in a weak field, be characterized by the quantum numbers $F=\varphi$, $M_F=\mu$ and $F=f$, $M_F=m$, the matrix element $e\dot{x}_{\mu m}$ is written $e\dot{x}_{\mu m}^{\varphi f}$. Further, let the axis of z be that of the magnetic field, and y be the direction of propagation of the exciting beam. We choose the standard representation for the matrix elements, $e\dot{z}$ being diagonal, and $e(\dot{x}\pm i\dot{y})$ is zero unless $\mu=m\pm1$. Finally, let θ be the angle between x and ξ.

[1] A. Ellett, J. Opt. Soc. Am. and Rev. Sci. Inst. **10**, 427 (1925).
[2] G. Breit, Rev. Mod. Phys. **5**, 91 (1933), especially Art. 4, p. 117 *et seq.*

Substitution into (1) and simplification gives

$$I_\xi=\sum_\mu^{\varphi\varphi'}[\alpha_\mu^{\varphi\varphi'}/1+(2\pi\tau\nu_{\mu\mu}^{\varphi'\varphi})^2]+\sum_\mu^{\varphi\varphi'}\beta_\mu^{\varphi\varphi'}\left\{[e^{2i\theta}/(1+2\pi i\tau\nu_{\mu+2,\mu}^{\varphi'\varphi})]+[e^{-2i\theta}/(1-2\pi i\tau\nu_{\mu+2,\mu}^{\varphi'\varphi})]\right\},$$

$$P_x=2\left\{\sum_\mu^{\varphi\varphi'}\beta_\mu^{\varphi\varphi'}/[1+(2\pi\tau\nu_{\mu+2,\mu}^{\varphi'\varphi})^2]\right\}\left\{\sum_\mu^{\varphi\varphi'}\alpha_\mu^{\varphi\varphi'}/[1+(2\pi\tau\nu_{\mu\mu}^{\varphi'\varphi})^2]\right\}^{-1}\left(=\frac{I_x-I_y}{I_x+I_y}\right). \tag{1}$$

Differentiating I_ξ with respect to θ, and equating to zero, one has, for the angle of maximum polarization

$$\tan 2\theta=\left\{\sum_\mu^{\varphi\varphi'}\gamma_\mu^{\varphi\varphi'}/[1+(2\pi\tau\nu_{\mu+2,\mu}^{\varphi'\varphi})^2]\right\}\left\{\sum_\mu^{\varphi\varphi'}\beta_\mu^{\varphi\varphi'}/[1+(2\pi\tau\nu_{\mu+2,\mu}^{\varphi'\varphi})^2]\right\}^{-1}, \tag{2}$$

where

$$\alpha_\mu^{\varphi\varphi'}=(C/g_a)\,|\sum_f(e\dot{x})_{\mu,\mu+1}^{\varphi f}(e\dot{x})_{\mu+1,\mu}^{f\varphi'}+(e\dot{x})_{\mu,\mu-1}^{\varphi f}(e\dot{x})_{\mu-1,\mu}^{f\varphi'}|^2,$$

$$\beta_\mu^{\varphi\varphi'}=(C/g_a)\,|\sum_f(e\dot{x})_{\mu,\mu+1}^{\varphi f}(e\dot{x})_{\mu+1,\mu+2}^{f\varphi'}|^2, \quad \gamma_\mu^{\varphi\varphi'}=2\pi\tau\nu_{\mu+2,\mu}^{\varphi'\varphi}\beta_\mu^{\varphi\varphi'}. \tag{3}$$

As is customary, the frequency differences and matrix elements required will be obtained from the Goudsmit-Bacher[3] modification of the Darwin[4] method. It is necessary to calculate the amplitudes of the electric moments themselves, however, rather than the transition probabilities, owing to the appearance of quantities such as $(ex)_{\mu m}^{\varphi f}(ex)_{m\mu'}^{f\varphi'}$ which are not transition probabilities.

A formal simplification is perhaps not effected, but calculation is facilitated if the sum in the denominator of P_x is split into two parts. Noting that $\alpha_\mu^{\varphi\varphi'}$ is symmetric in φ and μ, we may write

$$\sum_\mu^{\varphi\varphi'}\alpha_\mu^{\varphi\varphi'}/[1+(2\pi\tau\nu_{\mu\mu}^{\varphi'\varphi})^2]=\sum_\mu^{\varphi}\alpha_\mu^{\varphi\varphi}+2\sum_\mu^{\varphi>\varphi'}\alpha_\mu^{\varphi\varphi'}/1+(2\pi\tau\nu_{\mu\mu}^{\varphi'\varphi})^2.$$

Introducing the definition $2\delta=\sum_\mu^{\varphi}\alpha_\mu^{\varphi\varphi}$ we have

$$P_x=\left\{\sum_\mu^{\varphi\varphi'}\beta_\mu^{\varphi\varphi'}/[1+(2\pi\tau\nu_{\mu+2,\mu}^{\varphi'\varphi})^2]\right\}\left\{\delta+\sum_\mu^{\varphi\varphi'}\alpha_\mu^{\varphi\varphi'}/[1+(2\pi\tau\nu_{\mu+2,\mu}^{\varphi'\varphi})^2]\right\}^{-1}. \tag{4}$$

The Transition $^1S_0-{}^1P_1$

To illustrate the method and to lend support to a peculiar feature of the D line curves, calculations have been made on the simpler transition $^1S_0-{}^1P_1$, and the assumption of a nuclear moment of $\frac{1}{2}$. Following Goudsmit and Bacher, we assume that the perturbed functions may be written

$$\psi_{M_F}^{JF}=\sum_{M_J+M_I=M_F}X_{M_JM_I}^{JF}\psi_{M_J}^{J}P_I^{M_I}(\cos\theta)e^{iM_I\Phi},$$

where the $\psi_{M_J}^J$ are the characteristic functions of the atom with no nuclear spin. The energy differences and the X's are then determined by the chains of equations,

$$-X_{M_J-1,M_I+1}^{JF}(\tfrac{1}{2}A)(J-M_J+1)(I+M_I+1)+X_{M_JM_I}^{JF}(\nu_{M_F}^{JF}-AM_JM_I-M_J\omega)$$
$$-X_{M_J+1,M_I-1}^{JF}(\tfrac{1}{2}A)(J+M_J+1)(I-M_I+1)=0, \tag{5}$$

together with the normalizing equation,

$$\sum_{M_J+M_I=M_F}(X_{M_JM_I}^{JF})^2(I+M_I)\,!(I-M_I)\,!(J+M_J)\,!(J-M_J)\,!=1. \tag{6}$$

[3] S. Goudsmit and R. F. Bacher, Phys. Rev. **34**, 1499 (1929).
[4] C. G. Darwin, Proc. Roy. Soc. **A115**, 1 (1927).

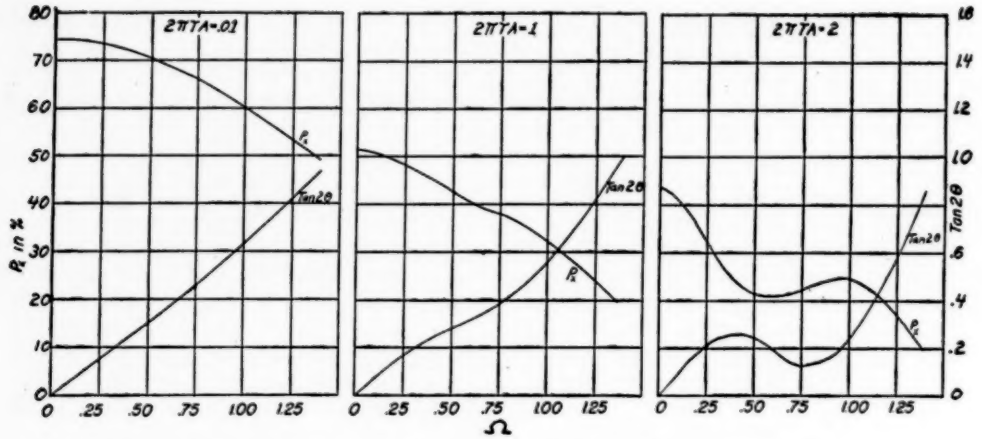

FIG. 1. P_z and angle of rotation of plane of maximum polarization of line ${}^1S_0-{}^1P_1$, as functions of Ω.

The matrix elements are now given in terms of the X's by the equations

$$(e\dot{x})^{\varphi f}_{M_F,M_F\pm1}=\tfrac{1}{2}\sum_{M_J+M_I=M_F}X^{J\varphi}_{M_JM_I}X^{J'f}_{M_J\pm1,M_I}(J+M_J)!(J-M_J)!(I+M_I)!(I-M_I)!. \tag{7}$$

In the above equations, $\omega=g(J)eH/4\pi mc$.

By equating the determinants of the chains to zero one obtains the quantities $\nu^{JF}_{M_F}/A$ as functions of $\Omega(=\omega/A)$. The $\nu^{JF}_{M_F}/A$ will hereafter be donated by $E^{F}_{M_F}$, the J superscript being unnecessary, as the only energies needed are those of the upper level, and these will all have the same J in the cases treated.

The chains and the normalizing equation, together with the E's found from the determinants, determine the X's, and from these last, the matrix elements may be calculated.

Inserting the quantum numbers of the lower (${}^1S_0$) level in Eqs. (5), (6), and (7), one gets no splitting with H, and all the $X^{JF}_{M_JM_I}=1$ independently of H, because the coupling of M_I and H has been neglected.

The upper level chains contain two members at most, so that the E's are the roots of quadratic equations, making a calculation in closed form possible. Inserting the values of the E's and the X's in (7), and the resulting matrix elements in (3), one has

$$\sum_\mu{}^{\varphi\varphi'}_{\mu}\alpha^{\varphi\varphi'}_{\mu}/1+(2\pi\tau\nu^{\varphi'\varphi}_{\mu\mu})^2=\tfrac{1}{2}+\tfrac{1}{8}a_+^{-4}+\tfrac{1}{8}a_-^{-4}+\tfrac{1}{8}a_+^{-4}[1+K^2a_+^2]^{-1}+\tfrac{1}{8}a_-^{-4}[1+K^2a_-^2]^{-1},$$

$$\sum_\mu{}^{\varphi\varphi'}_{\mu}\beta^{\varphi\varphi'}_{\mu}(1+2\pi\tau\nu^{\varphi'\varphi}_{\mu+2,\mu})^2=\tfrac{1}{8}a_+^{-2}[1+K^2b_-^2]^{-1}+\tfrac{1}{8}a_+^{-2}[1+K^2c_-^2]^{-1}$$
$$+\tfrac{1}{8}a_-^{2}[1+K^2b_+^2]^{-1}+\tfrac{1}{8}a_-^{2}[1+K^2c_+^2]^{-1},$$

$$\sum_\mu{}^{\varphi\varphi'}_{\mu}\gamma^{\varphi\varphi'}_{\mu}/1+(2\pi\tau\nu^{\varphi'\varphi}_{\mu+2,\mu})=\tfrac{1}{8}Ka_+^{-2}c_-[1+K^2c_-^2]^{-1}+\tfrac{1}{8}Ka_+^{-2}b_-[1+K^2b_-^2]^{-1}+\tfrac{1}{8}Ka_-^{2}c_+[1+K^2c_+^2]^{-1}$$
$$+\tfrac{1}{8}Ka_-^{2}b_+[1+K^2b_+^2]^{-1}$$

where
$$K=2\pi\tau A,$$
$$a_\pm=E^{1\frac{1}{2}\frac{1}{2}}_{\pm\frac{1}{2}\pm\frac{1}{2}}=(\Omega^2\mp\Omega+\tfrac{9}{4})^{\frac{1}{2}},\quad b_\pm=E^{1\frac{1}{2}1\frac{1}{2}}_{-1\pm\frac{1}{2},1\pm\frac{1}{2}}=\tfrac{1}{2}[3(\tfrac{1}{2}\pm\Omega)-E^{1\frac{1}{2},\frac{1}{2}}_{\mp\frac{1}{2}\mp\frac{1}{2}}],$$
$$c_\pm=E^{1\frac{1}{2},\frac{1}{2}}_{\pm1\frac{1}{2},\mp\frac{1}{2}}=\tfrac{1}{2}[3(\tfrac{1}{2}\mp\Omega)+E^{1\frac{1}{2},\frac{1}{2}}_{\pm\frac{1}{2},\pm\frac{1}{2}}].$$

It will be observed that the terms in the β sum, which is the numerator of P_z and the denominator of tan 2θ may have sharp maxima, while those in the γ sum, which is the numerator of tan 2θ may have both maxima and minima. The maxima for the terms in the β sum occur approximately where the frequency difference in the denominator vanishes (an impossible occurrence in the terms of the α sum, since the frequency differences there are between levels of the same M_F); these maxima are

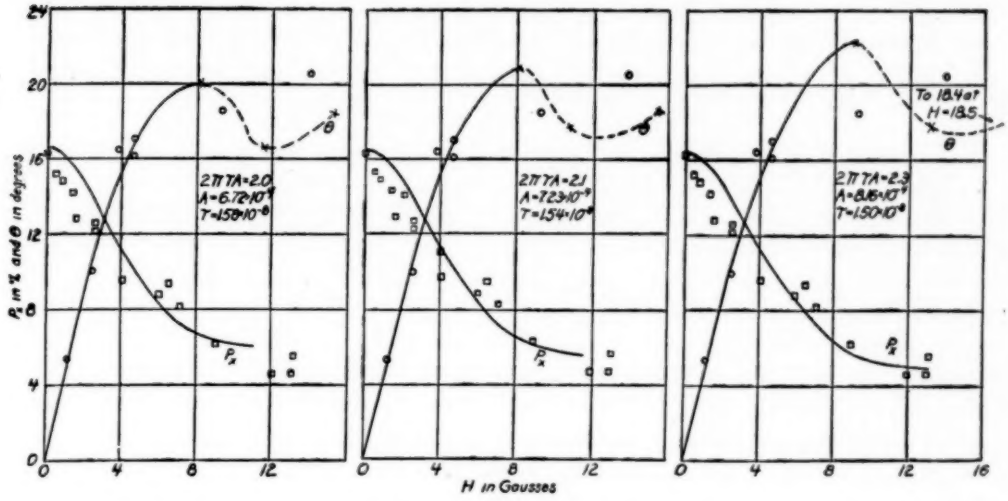

FIG. 2. P_z and angle of rotation of plane of maximum polarization of lines ${}^2S_{\frac{1}{2}}-{}^2P_{1\frac{1}{2},\frac{1}{2}}$ as functions of H.

very sharp for large K. The γ terms have maxima approximately at $KE^{FF'}_{MFMF'}=1$ and minima at -1, and pass through zero where the frequency differences vanish. Observing the roles of these sums in P_z and $\tan 2\theta$, one might be led to expect "humps" in the curves in the neighborhood of values of Ω at which two levels cross, especially for large values of K.

This expectation is borne out, as is shown in Fig. 1. The term responsible for the behavior is that connected with b_+ which vanishes at $\Omega=1$.

The scales for $\tan 2\theta$ are not the same in the various curves; in the curve for $2\pi\tau A=0.01$, the ordinates of $\tan 2\theta$ have been multiplied by 50, and in the curve for $2\pi\tau A=2$, these ordinates have been divided by two, to facilitate comparison of the curves. In Fig. 2, however, all curves have the same scales.

THE D LINES

Considerably more labor is involved in the calculations for these transitions; fortunately, much of it had already been accomplished. Thus, it had already been shown[5] that D_1 was unpolarized for all fields and any value of I that might be assumed, so that D_2 alone needed to be considered. In the same paper, a closed expression was given for the X's of the lower levels; this enabled their elimination from the expressions for the probability amplitudes. The energies and the X's were available for $\Omega=1$ and $\Omega=\sqrt{2}$. The secular determinants of the chains give rise to a quartic, two cubics, two quadratics, and two linear equations; solutions of the cubics for $\Omega=\frac{1}{2}$ were also available.

By eliminating the lower level X's and considering D_2 alone, it is possible to omit the superscript J from the X's, and write

$$\alpha_\mu^{\varphi\varphi'}=(C/g_a)[9(\mu)!(3-\mu)!X^{\varphi}_{1\frac{1}{2},\mu-1\frac{1}{2}}X^{\varphi'}_{1\frac{1}{2},\mu-1\frac{1}{2}}+9(-\mu)!(3+\mu)!X^{\varphi}_{-1\frac{1}{2},\mu+1\frac{1}{2}}X^{\varphi'}_{-1\frac{1}{2},\mu+1\frac{1}{2}}$$
$$+(1+\mu)!(2-\mu)!X^{\varphi}_{\frac{1}{2},\mu-\frac{1}{2}}X^{\varphi'}_{\frac{1}{2},\mu-\frac{1}{2}}+(1-\mu)!(2+\mu)!X^{\varphi}_{-\frac{1}{2},\mu+\frac{1}{2}}X^{\varphi'}_{-\frac{1}{2},\mu+\frac{1}{2}}]^2,$$

$$\beta_\mu^{\varphi\varphi'}=(C/g_a)[(2+\mu)!(1-\mu)!X^{\varphi}_{-\frac{1}{2},\mu+\frac{1}{2}}X^{\varphi'}_{1\frac{1}{2},\mu+\frac{1}{2}}+(3+\mu)!(-\mu)!X^{\varphi}_{-1\frac{1}{2},\mu+1\frac{1}{2}}X^{\varphi'}_{\frac{1}{2},\mu+1\frac{1}{2}}]^2.$$

The equation for the polarization in zero field takes a very simple form, *viz.*;

$$P_0=\frac{Y+0.81}{\frac{1}{3}Y+4.27},\quad Y=\frac{0.45}{1+4K^2}+\frac{1.425}{1+9K^2}+\frac{0.315}{1+25K^2}.$$

[5] A. Ellett and N. Heydenburg, Phys. Rev. **46**, 583 (1934).

TABLE I. *Polarization in percent of D_2 and of the doublet.*

$2\pi\tau A$	0	1	2	2.1	2.2	2.3	3	
$P_x(D_2)$	60	24.24	20.46	20.32	20.21	20.11	19.65	18.97
$P(D_1+D_2)$	50	19.71	16.59	16.48	16.39	16.31	15.93	15.37

The polarization in zero field is seen to be determined by the product $2\pi\tau A$ which may be considered the ratio of the separation of the lines to their natural breadth. Table I shows the polarization of D_2, excited by D_2 and of the doublet, excited by the doublet. The theoretical intensity ratio of two to one in the incident beam is assumed.

The energies, or rather the quantities $E^F_{M_F}$, and the quantities $\alpha_\mu^{\varphi\varphi'}$, $\beta_\mu^{\varphi\varphi'}$ and $\gamma_\mu^{\varphi\varphi'}$ which depend on H and A only through Ω have been calculated[6] for $\Omega=0.05$, 0.15, 0.25, 0.50, 0.75, 1, $\sqrt{2}$. The E's are known to one part in the fifth place; the others are probably not significant beyond the fourth figure. To calculate P_x or θ, it is necessary to assume a value for $2\pi\tau A$; these calculations have been made for $2\pi\tau A=2$, 2.1, 2.3, another significant figure probably being lost in the process, because of the number of terms summed. The polarizations for zero field corresponding to these values are, as seen from Table I, 16.6 percent, 16.5 percent, and 16.3 percent. The observations of Ellett[1] and Larrick[7] show that the most probable value of the initial polarization lies within this range. These curves are graphed as functions of H and compared with the experimental points in Fig. 2. Here one has another parameter to adjust for the best fit; $2\pi\tau A$ having been chosen, one can still select a value for A, which governs the scale of abscissae of the theoretical curves, since $\Omega=g(J)eH/4\pi mcA$. The values of A used in the graphs shown range from 6.72 to 8.16×10^{-4} cm^{-1}. Since, in all cases but one, the polarization predicted for zero field was higher than that observed in this experiment (which seems likely in the light of later observations); and since the theoretical curve has a horizontal tangent at $H=0$; and finally, since the curve is insensitive to small variations in A in the region of small H, it is impossible to fit the theoretical curve to the experimental for any reasonable value of A. Thus, this parameter has been chosen in each case primarily to give a good fit with the rotation curve in the region of small H.

The curves for the rotation of the plane of polarization may be said to fit within the experimental error, which is admittedly quite large for $H>4$ gausses. The same behavior is noted as in the simpler case, the levels which cross in this instance being those characterized by the quantum numbers $F=1$, $M_F=0$, and $F=2$, $M_F=-2$. It is perhaps worthy of mention that the hump in the curve disappears for smaller values of $2\pi\tau A$. The form of the curve is not well determined for large H, due to the paucity of calculated points. This is of little importance, however, as the theoretical and experimental curves are not being compared in this region.

Theory and experiment agree to approximately the same degree for all the values of $2\pi\tau A$ presented here; thus these experimental data will not fix A with any precision. Qualitative agreement is indicated, however, with the value of 6×10^{-4} cm^{-1} obtained by Ellett and Heydenburg,[5] from calculations for the case in which the magnetic field is parallel to the exciting beam.

The curves are much more sensitive to variations in τ. The total range of τ is from 1.50 to 1.58 $\times10^{-8}$ sec., which value is in excellent agreement with that which can be calculated from optical dispersion data,[8] namely 1.54×10^{-8}.

In conclusion the author wishes to thank Professor A. Ellett for helpful suggestions throughout the progress of the work.

[6] The α's for $\Omega=\sqrt{2}$ have not been calculated.
[7] L. Larrick, Phys. Rev. **40**, 1041A (1932).
[8] S. A. Korff and G. Breit, Rev. Mod. Phys. **4**, 471 (1932), especially Table XX, p. 499.

Optical Dispersion and Molar Refraction at Zero Frequency for Compressed Nitrogen, Argon, and Carbon Dioxide Measured as Functions of Density

CLARENCE E. BENNETT
University of Maine, Orono, Maine

(Received May 25, 1940)

Data obtained by displacement interferometry have been reduced to give the variation of refractive index at infinite wave-length with density for pure nitrogen up to 0.01656 gram per cc. Precise data are also presented for dispersion in pure argon, and the Cauchy constants under NTP conditions are evaluated as follows for this gas: $A_0-1=0.0002771\pm0.0000008$, $B_0=1.477\times10^{-14}$. It is also noted that the Lorentz-Lorenz function, and hence the molar refraction at zero frequency, are independent of density for these two gases; the density range for argon extending up to 0.03342 gram per cc. The values of molar refraction are found to be 4.369 ± 0.003 cc for nitrogen and 4.138 ± 0.012 cc for argon. Preliminary work on carbon dioxide indicates a slight negative deviation from linearity for $(A-1)$ with density, and a marked negative variation of the Lorentz-Lorenz function with density. The latter means a decrease in the molar refraction at zero frequency, and suggests a decrease in the molar polarization with density. This is not in accord with the findings of Keyes and Oncley who report an increase of molar polarization with density for this gas. The NTP values of the Cauchy constants for CO_2 are also evaluated as follows: $(A_0-1)=0.0004419\pm0.0000036$, and $B_0=2.791\times10^{-14}$. The extrapolated value of the molar refraction at zero frequency is found to be approximately 6.65 cc.

INTRODUCTION

A PRECISE method for measuring the refractive index of a gas by displacement interferometry has been described by the writer in earlier papers.[1, 2] The present paper deals first with an analysis of data previously reported for purified nitrogen over a range of pressures from zero up to fourteen atmospheres.[2] The reduced data give the variation of refractive index at infinite wave-length with density, so that it is now possible to report with some degree of precision the behavior of the Lorentz-Lorenz function up to a density of 0.01656 gram per cc and to evaluate the molar refraction at zero frequency, or the molar polarization for this gas. The present paper also deals with a similar analysis for pure argon over a pressure range from zero to eighteen atmospheres, and presents some preliminary results for carbon dioxide observed over approximately the same pressure range.

This work was interrupted by the transfer of the apparatus to a new location,[3] which necessitated its complete reassembly with numerous alterations. The publication of earlier data was postponed until they could be confirmed in the new location. It is now gratifying to report that recent observations taken with the reassembled equipment are in complete agreement with the earlier data, and hence lend added significance to them. The complete analysis of the new CO_2 data, however, in which the density range is extended appreciably, will be presented later.

[1] C. E. Bennett, Phys. Rev. **37**, 263 (1931).
[2] C. E. Bennett, Phys. Rev. **45**, 200 (1934).
[3] Former work done at the Massachusetts Institute of Technology.

THEORY

If the refractive index of a gas is represented by a Cauchy expansion

$$\mu=A+B/\lambda^2+C/\lambda^4+\cdots, \qquad (1)$$

where A presumably represents the infinite wave-length value of the refractive index, the fundamental equation of the displacement interferometer is

$$\Delta x/e=(A-1)+3B/\lambda^2+5C/\lambda^4+\cdots, \qquad (2)$$

where Δx is the observable displacement of the fringe system, e is the length of the gas tube, and the other symbols have the same significance as in the Cauchy equation. It was shown in the earlier work that $A-1$ is linear with pressure for pure nitrogen and that only two constants A and B are necessary to describe the data up to the limiting pressures used, namely, 14.145 atmospheres. It was also shown that these two constants, reduced to NTP values and called A_0 and B_0, respectively, are as follows: for nitrogen $A_0-1=0.0002932$ to better than one-tenth of one percent, and $B_0=1.637\times10^{-14}$.

Since, to a first approximation, pressure is proportional to density and $A-1$ is proportional to $(A^2-1)/(A^2+2)$, it was concluded that the above results constitute a rough check on the constancy of the Lorentz-Lorenz relation $(A^2-1)/(A^2+2)(1/\rho)$ in this pressure range, where ρ is the density. Also, since the refractive index measurements here reported are very accurately determined, the question of converting pressures to densities by an accurate equation of state is suggested to test the validity of this relation more precisely.

The density values reported in this paper are obtained by the use of the Keyes equation of state,[4] the constants for which are now available for several gases. This equation is usually expressed in terms of the pressure as follows:

$$p=\frac{RT}{v-\beta e^{-\alpha/v}}-\frac{A}{(v+l)^2}, \tag{3}$$

but it can be rearranged to express the specific volume (the reciprocal of density), in terms of pressure and temperature, thus

$$v=\frac{RT}{p}+\left(\beta-\frac{A}{RT}\right)-\left(\alpha\beta+\frac{2Al}{RT}\right)\frac{P}{RT}. \tag{4}$$

TABLE I. *Refractive index at zero frequency and the Lorentz-Lorenz relation as functions of density for pure nitrogen.*

ρ(g/cc)	p(cm Hg)	t°C	$A-1$	$\frac{1}{\rho}\frac{A^2-1}{A^2+2}$
0.0043061	309.75	50.0	0.0010127	0.15676
0.0045933	309.80	30.0	0.0010781	0.15645
0.0049116	331.22	30.0	0.0011541	0.15662
0.0052798	356.04	30.0	0.0012384	0.15633
0.0052904	321.09	00.0	0.0012333	0.15538
0.0072160	437.68	00.0	0.0016812	0.15528
0.0073795	497.49	30.0	0.0017282	0.15608
0.0081050	582.91	50.0	0.0019032	0.15650
0.0084055	566.56	30.0	0.0019664	0.15591
0.0084062	566.61	30.0	0.0019692	0.15612
0.0090645	549.42	00.0	0.0021146	0.15546
0.0092928	626.23	30.0	0.0021770	0.15612
0.010942	662.69	00.0	0.0025535	0.15551
0.011885	800.59	30.0	0.0027770	0.15570
0.011931	803.64	30.0	0.0027915	0.15591
0.013080	791.48	00.0	0.0030521	0.15548
0.014219	1022.20	50.0	0.0033389	0.15622
0.015977	1075.36	30.0	0.0037327	0.15565
0.016559	1000.57	00.0	0.0038584	0.15524
			MEAN	0.15596±0.00008
MOLAR REFRACTION $R_0=4.369\pm0.003$				

[4] F. G. Keyes, Proc. Nat. Acad. Sci. 3, 323 (1917).

The values of $A-1$ at each density are readily calculated either by use of the precise value of B_0 properly adjusted for density and treated as a correction factor to $\Delta x/e$ by Eq. (2) rewritten thus

$$A-1=\Delta x/e-3B/\lambda^2, \tag{5}$$

or by a direct least-squares analysis of the individual values of $\Delta x/e$ at each of several wave-lengths. In the latter method $(A-1)$ and B are determined simultaneously for each density observation. In the present work data for $\Delta x/e$ were available for each of the following wave-lengths: 5780A, 5461A, and 4359A, and calculations were made by both methods.

RESULTS

The results for nitrogen are listed in Table I, which shows the constancy of the Lorentz-Lorenz function up to a density of 0.01656 gram per cc. Attention is called to the fact that up to this density, at least, there is no observable variation of this function. The average value of the molar refraction at zero frequency is found to be 4.369±0.003 cc.

Table II contains hitherto unpublished data for pure argon. The refractive index and dispersion values are given for two different temperatures and six different pressures, reduced to density values by a Keyes equation of state as indicated above for nitrogen. The purity of the argon used was better than 99.8 percent as certified by the Air Reduction Company. It was also passed through the same purifying and drying system previously used for nitrogen.

The linearity of $(A-1)$ and B with density are clearly shown, as is also the constancy of the Lorentz-Lorenz function up to 0.033418 gram/cc. The values of A_0-1 and B_0 are found to be 0.0002771±0.0000008, and 1.477×10^{-14}, respectively. The last column gives the values of molar refraction at zero frequency, or molar polarization and shows it to be independent of density with an average value of 4.138±0.012 cc.

PRELIMINARY WORK ON CARBON DIOXIDE

A limited amount of data on pure CO_2 at 50°C is presented in Table III. As in the case of argon, the values of $(A-1)$ and B were obtained by a least-squares analysis of the observations of $\Delta x/e$

TABLE II. *Dispersion in pure argon as a function of density.*

No.	p cm Hg	t °C	ρ grams/cm³	$\Delta x/e$ 5780A	5461A	4359A
1	305.63	00.00	0.0071834	0.0011684	0.0011750	0.0012057
2	573.20	30.00	0.012143	0.0019766	0.0019880	0.0020507
3	567.26	00.00	0.013372	0.0021815	0.0021932	0.0022529
4	1071.72	30.00	0.02275	0.0037168	0.0037359	0.0038450
5	1093.21	00.00	0.025916	0.0042235	0.0042449	0.0043693
6	1405.05	00.00	0.033418	0.0054422	0.0054699	0.0056398

No.	$A-1$	$B\times10^{14}$	$\frac{A-1}{\rho}$	$\frac{B}{\rho}\times10^{14}$	$\frac{A^2-1}{A^2+2}\frac{1}{\rho}$	R_∞
1	0.0011199	5.438	0.15590	756.43	0.10391	4.1506
2	0.0018786	10.903	0.15470	897.84	0.10310	4.1182
3	0.0020877	10.465	0.15612	782.57	0.10405	4.1562
4	0.0035465	18.899	0.15572	829.83	0.10375	4.1442
5	0.0040295	21.513	0.15548	830.10	0.10359	4.1374
6	0.0051780	29.2319	0.15495	874.74	0.10321	4.1226
	MEAN		0.15548	828.58	0.10381	4.138±.012
	$A_0-1=0.0002771\pm0.0000008$				$B_0=1.4777\times10^{-14}$	

for each of three wave-lengths. In the case of CO_2 the deviations from the ideal gas law make it absolutely necessary for all pressures to be converted to densities before linearity considerations are even attempted. Here again, the Keyes equation of state was used. The observations were taken with the original apparatus for which the tube length e was 100.30 cm and the correction factor for the half-millimeter micrometer screw was 1.0104. The temperature was maintained constant to 0.01°C and pressure measurements were made with a Keyes type dead-weight gauge to approximately one millimeter of mercury over the entire range. The zero pressure reading was determined with a McLeod gauge to better than 10^{-2} mm Hg.

It is to be noted that although B is very nearly linear with density, $A-1$ deviates slightly. If one disregards for the moment this slight negative deviation, and considers the average values of $A-1$, and B, the following values of A_0-1, and B_0 are obtained by the use of standard density $\rho_0=0.0019769$: $A_0-1=0.0004419\pm0.0000036$, and $B_0=2.791\times10^{-14}$.

Incidentally, values of $\mu-1$ were also determined for several wave-lengths by Eq. (1), and the results were found to be in good agreement with those generally accepted. They are not listed here, however, since they are readily accessible in the literature.

Table III also shows the variation of the Lorentz-Lorenz function with density and the molar refraction at infinite wave-length for carbon dioxide. There appears to be a definite increase in molar refraction with density for this gas whereas this quantity seemed independent of density for nitrogen and argon. The molar refraction at zero frequency is found by extrapolation to be approximately 6.65 at zero density.

CONCLUSIONS

In view of these results it is concluded that the Lorentz-Lorenz function, and hence the molar refraction at zero frequency, are independent of density for pure nitrogen and argon over this density range, although Keyes and Oncley[5] find a slight increase in the molar polarization for nitrogen based upon dielectric constant measurements. The value of the molar refraction at zero frequency here obtained for nitrogen, however, is in good agreement with their value of molar polarization (4.37 cc), thus confirming the validity of the Maxwell law over this density range.

The results for argon represent a contribution to the rather limited amount of information available concerning the Lorentz-Lorenz function at high densities for the rare gases which are structurally quite simple. That this function

[5] F. G. Keyes and J. L. Oncley, Chem. Rev. **19**, [3] 195 (1936).

TABLE III. *Dispersion in CO_2 as a function of density (data at 50°C)*

No.	ρ cm Hg	Micrometer Reading 5780A	5461A	4359A	$\Delta x/e$ 5780A	5461A	4359A
0	0.0	00.5105	00.5790	00.9690	—	—	—
1	354.96	04.2500	04.3390	04.8500	0.0018835	0.0018939	0.0019548
2	426.61	05.0090	05.1050	05.6495	0.0022658	0.0022797	0.0023575
3	514.08	05.9565	06.0585	06.6285	0.0027431	0.0027600	0.0028506
4	612.54	07.0260	07.1345	07.7425	0.0032818	0.0033019	0.0034117
5	724.10	08.2410	08.3575	09.0180	0.0038938	0.0039180	0.0040542
6	846.31	09.5950	09.7260	10.4130	0.0045758	0.0046072	0.0047568
7	982.21	11.1395	11.2700	12.0415	0.0053537	0.0053849	0.0055771
8	1210.00	13.7780	13.9305	14.8160	0.0066827	0.0067250	0.0069746
9	1575.90	18.1455	18.3165	—	0.0088823	0.0089342	—

No.	ρ g/cc	$A-1$	$B\times10^{14}$	$\frac{A-1}{\rho}$	$\frac{B}{\rho}\times10^{14}$	$\left(\frac{A^2-1}{A^2+2}\right)\frac{1}{\rho}$	R_0
0	0.000000	—	—	—	—	—	—
1	0.0079023	0.0017886	10.529	0.22634	1332.4	0.15084	6.638
2	0.0095386	0.0021442	13.504	0.22479	1415.7	0.14981	6.593
3	0.011557	0.0026011	15.806	0.22507	1367.7	0.14998	6.601
4	0.013857	0.0031100	19.105	0.22443	1378.7	0.14955	6.582
5	0.016503	0.0036813	23.635	0.22307	1432.2	0.14862	6.541
6	0.019452	0.0043398	26.435	0.22310	1359.0	0.14863	6.541
7	0.022798	0.0050419	34.177	0.22115	1499.1	0.14731	6.483
8	0.028580	0.0062938	43.100	0.22021	1508.0	0.14665	6.454
9	0.038381	—	—	—	—	—	—

$(A_0-1)=0.0004419\pm0.0000036$ $B_0=2.791\times10^{14}$

would be constant for a monatomic gas is probably to be expected.

The negative variation of the Lorentz-Lorenz function with density for carbon dioxide, on the other hand, is also contrary to the findings of Keyes and Oncley who find a positive variation of the molar polarization. This point, however, is to be investigated further. Phillips[6] has reported such a negative variation although not so marked, but it is doubtful if the Phillips data are as accurate as that reported here over this density range. It may be that molar refraction at zero frequency is not the same as the molar polarization for carbon dioxide although Keyes and Oncley[5] show that the Phillips data, corrected for the effects of infra-red absorption bands, as suggested by Fuch,[7] yield a value for molar refraction nearly in agreement with the molar polarization. The agreement would be even better, however, on the basis of the results reported here.

ACKNOWLEDGMENTS

The writer takes this opportunity to thank the Rumford Fund of the American Academy of Arts and Sciences and the Coe Research Fund of the University of Maine for financial assistance in the continuation of this research. He also expresses his appreciation to Dr. F. G. Keyes of the Massachusetts Institute of Technology for supplying the constants used in the equation of state and for his sustained interest in the progress of this work.

[6] P. Phillips, Proc. Roy. Soc. London **97A**, 225 (1920).

[7] O. Z. Fuch, Zeits. f. Physik **46**, 519 (1928).

The Thermodynamics of Irreversible Processes

I. The Simple Fluid

CARL ECKART
Ryerson Laboratory, The University of Chicago, Chicago, Illinois
(Received April 19, 1940)

The rate of increase of the entropy of a simple viscous fluid, capable of conducting heat, is investigated in greater detail than has hitherto been customary. It is shown that, if Kelvin's hypothesis concerning the absolute temperature be adopted, and the usual law of viscosity be assumed, the requirements of the second law are satisfied.

SINCE the publication of Gibbs' "Equilibrium of heterogeneous substances,"[1] it has been obvious that the greater part of the existing thermodynamic theory would more appropriately be called thermostatics, the term thermodynamics being reserved for the rather unorganized lot of equations that govern irreversible changes in which heat plays a part. Examples of such equations are Fourier's law of heat conduction, Ohm's law, Fick's law of diffusion, etc., etc. Although this usage is dictated by the close analogy to mechanics, there has been no tendency to adopt it. This reluctance has been partly due to the chaotic state of thermodynamics proper, and partly to the belief that the laws mentioned above are much less fundamental than Newton's laws of motion or than the energy and entropy laws, and require derivation from kinetic theory. The purpose of the present investigation has been to find the general equation of which the foregoing are special cases. The problem of providing a kinetic theory derivation has not been considered. The major part of the discussion will be presented in such a manner as to bring out the connection with Gibbs' work, but by way of introduction, the case of a simple viscous fluid, conducting heat, will be discussed from a pre-Gibbsian standpoint.

Let m be the mass density of the fluid, $\mathbf{V}$ its velocity, so that the conservation of mass leads to the equation of continuity

$$\partial m/\partial t+\nabla\cdot(m\mathbf{V})=0. \tag{1}$$

Defining the specific volume $v=1/m$ and the operator

$$D/Dt=\partial/\partial t+\mathbf{V}\cdot\nabla$$

we may also write

$$mDv/Dt=\nabla\cdot\mathbf{V}. \tag{2}$$

Let S be any closed surface moving with the fluid, so that an element of its area, $d\boldsymbol{\sigma}$, sweeps out the volume $\mathbf{V}\cdot d\boldsymbol{\sigma}dt$ in time dt. If f is any function of position and time

$$\begin{aligned}(d/dt)\int\int\int_S mf\,d\tau&=\int\int\int_S[\partial(mf)/\partial t]d\tau+\int\int_S mf\mathbf{V}\cdot d\boldsymbol{\sigma}\\&=\int\int\int_S\{\partial(mf)/\partial t+\nabla\cdot(mf\mathbf{V})\}d\tau\\&=\int\int\int_S m(Df/Dt)d\tau.\end{aligned} \tag{3}$$

In the absence of external volume forces, the motion of the fluid will be governed by the hydrodynamic equation

$$m D\mathbf{V}/Dt=-\nabla p+\nabla\cdot\mathfrak{p}, \tag{4}$$

where p is the hydrostatic pressure, and $\mathfrak{p}$ is the tensor of the viscous stresses. The precise expression for the latter will not be needed until later.

The kinetic energy of the fluid enclosed by S is

$$K=\int\int\int_S \tfrac{1}{2}mV^2d\tau$$

and by Eq. (3)

$$\begin{aligned}dK/dt&=\int\int\int_S m\mathbf{V}\cdot(D\mathbf{V}/Dt)d\tau\\&=\int\int\int_S\mathbf{V}\cdot(-\nabla p+\nabla\cdot\mathfrak{p})d\tau\end{aligned}$$

[1] J. W. Gibbs, *Scientific Papers* (Longmans, 1906), Vol. I., p. 55.

or, on using the divergence theorem

$$dK/dt=-\int\int_S(p\mathbf{V}-\mathfrak{p}\cdot\mathbf{V})\cdot d\sigma$$
$$+\int\int\int_S\{p\nabla\cdot\mathbf{V}-(\mathfrak{p}\cdot\nabla)\cdot\mathbf{V}\}d\tau. \quad (5)$$

The surface integral is the rate at which the fluid inside S does work on the fluid outside S.

The energy law as applied to this simple fluid, states that there is a function $w(p, v)$ (the internal energy per gram) and a vector $\mathbf{q}$ (the heat flow) such that

$$(d/dt)\int\int\int_S\{\tfrac{1}{2}mV^2+mw\}d\tau$$
$$=-\int\int_S\mathbf{q}\cdot d\sigma-\int\int_S(p\mathbf{V}-\mathfrak{p}\cdot\mathbf{V})\cdot d\sigma. \quad (6)$$

The first integral on the right is the rate at which heat enters S and the other has already been identified. Subtracting Eq. (5) from Eq. (6) gives

$$\int\int\int_S\{m(Dw/Dt)+p\nabla\cdot\mathbf{V}-(\mathfrak{p}\cdot\nabla)\cdot\mathbf{V}$$
$$+\nabla\cdot\mathbf{q}\}d\tau=0, \quad (7)$$

and since this must be true for all closed surfaces, it follows that the integrand itself must vanish.

Since w is a function of p and v only, and because of Eq. (2), the first two terms may be transformed:

$$m(Dw/Dt)+p\nabla\cdot\mathbf{V}$$
$$=m\{[(\partial w/\partial v)+p](Dv/Dt)+(\partial w/\partial p)(Dp/Dt)\}. \quad (8)$$

Now, there are always two functions θ and η such that

$$(\partial w/\partial v)+p=\theta(\partial\eta/\partial v),\quad (\partial w/\partial p)=\theta(\partial\eta/\partial p), \quad (9)$$

so that finally

$$m(Dw/Dt)+p\nabla\cdot V=m\theta(D\eta/Dt),$$

whence

$$m\theta(D\eta/Dt)+\nabla\cdot\mathbf{q}=(\mathfrak{p}\cdot\nabla)\cdot\mathbf{V}. \quad (10)$$

Before making use of this equation, it is worth while to consider this definition of θ and η, despite the fact that it is discussed in all standard texts on thermostatics. Differentiating the first of Eq. (9) with respect to p and the second with respect to v, and subtracting gives:

$$(\partial\theta/\partial p)(\partial\eta/\partial v)-(\partial\theta/\partial v)(\partial\eta/\partial p)=1.$$

Elimination of η by means of Eq. (9) results in

$$(\partial\log\theta/\partial p)[(\partial w/\partial v)+p]-(\partial\log\theta/\partial v)(\partial w/\partial p)=1, \quad (11)$$

which can be solved for $\log\theta$, since w is supposed known. If $\theta=\theta_0(p, v)$ is one solution of Eq. (11) and $\phi(p, v)$ is any solution of

$$(\partial\phi/\partial p)[(\partial w/\partial v)+p]-(\partial\phi/\partial v)(\partial w/\partial p)=0, \quad (12)$$

then the most general solution of Eq. (11) is

$$\theta=\theta_0 f(\phi), \quad (13)$$

where f is arbitrary. To complete the definition of θ, this function must be determined in some way.

Thereafter, the function η is determined except for an additive constant. From Eq. (9)

$$\eta(p, v)=\eta(p_0, v_0)+\int_{p_0, v_0}^{p, v}(1/\theta)\{[(\partial w/\partial v)+p]dv+(\partial w/\partial p)dp\}$$

and Eq. (11) is the condition that the integral be independent of the path.

The definition of θ is completed on the basis of what may be called the Kelvin hypothesis:

The arbitrary function f may be chosen so that the heat flow $\mathbf{q}$ is related to θ by Fourier's equation

$$\mathbf{q}=-k\nabla\theta, \quad (14)$$

where k is a function of p and v that does not change sign.

When f is so chosen, θ is unique except for sign and unit. For, let θ_0 also satisfy the equation

$$\mathbf{q}=-k_0\nabla\theta_0$$

then it follows that

$$\theta=F(\theta_0)$$

or

$$f(\phi)=F(\theta_0)/\theta_0.$$

But, because of Eqs. (11) and (12), ϕ cannot be a proper function of θ_0, so that both sides of the equality must be constants; hence

$$\theta=a\theta_0.$$

The constant a can always be chosen so that k is positive. When thus defined, θ is called the absolute temperature and η the entropy (per gram) of the substance.

Returning to Eq. (10), we may write it

$$m(D\eta/Dt)+\nabla\cdot(\mathbf{q}/\theta) = -[\mathbf{q}\cdot\nabla\theta]/\theta^2+[(\mathfrak{p}\cdot\nabla)\cdot\mathbf{V}]/\theta$$

or, using Eq. (3) and the divergence theorem

$$(d/dt)\int\int\int_S m\eta d\tau+\int\int_S(1/\theta)\mathbf{q}\cdot d\sigma = \int\int\int_S\{[k(\nabla\theta)^2]/\theta^2+[(\mathfrak{p}\cdot\nabla)\cdot\mathbf{V}]/\theta\}d\tau. \quad (15)$$

The first term on the left is the rate of increase of the entropy of the matter inside S; the surface integral is the familiar ratio of heat loss to temperature. Thus, if $\nabla\mathbf{V}=0$ and $\nabla\theta=0$, this equation expresses the ordinary relation between entropy, temperature and heat in reversible processes.

Furthermore, if $\mathfrak{p}=0$ (nonviscous fluid), the right side is never negative—as is asserted by the second law of thermodynamics. It remains to consider the case of a viscous fluid; the commonly accepted expressions for the components of $\mathfrak{p}$ are[2]

$$\mathfrak{p}_{xx}=(2\lambda/3)[2(\partial V_x/\partial x)-(\partial V_y/\partial y)-(\partial V_z/\partial z)],$$
$$\mathfrak{p}_{xy}=\mathfrak{p}_{yx}=\lambda[(\partial V_x/\partial y)+(\partial V_y/\partial x)], \text{ etc.,}$$

where $\lambda(\geqslant 0)$ is the coefficient of viscosity. Hence

$$(\mathfrak{p}\cdot\nabla)\cdot\mathbf{V}=(2\lambda/3)\{[(\partial V_x/\partial x)-(\partial V_y/\partial y)]^2+\cdots\} +\lambda\{[(\partial V_x/\partial y)+(\partial V_y/\partial x)]^2+\cdots\}\geqslant 0.$$

If, now $\theta>0$, it follows that the right side of Eq. (15) is never negative even for a viscous fluid. If this be accepted as an empirical fact, or included in Kelvin's hypothesis, the latter and Eq. (15) have the inequality

$$(d/dt)\int\int\int_S m\eta d\tau+\int\int_S(1/\theta)\mathbf{q}\cdot d\sigma\geqslant 0 \quad (16)$$

as consequence. As has been remarked, this inequality is a partial expression of the second law of thermodynamics.

[2] H. Lamb, *Hydrodynamics* (Cambridge, 1924), fifth edition, p. 544.

AUGUST 1, 1940 PHYSICAL REVIEW VOLUME 58

The Thermodynamics of Irreversible Processes

II. Fluid Mixtures

CARL ECKART,
Ryerson Laboratory, The University of Chicago, Chicago, Illinois

(Received April 19, 1940)

The possibility of constructing a systematic theory of irreversible processes is surveyed in general terms, by utilizing some of the results established in later parts of the paper. Three assumptions underlying Gibbs' application of the second law to equilibrium problems are formulated in explicit but general mathematical form. It is shown that they restrict the equations governing irreversible changes. The theory of a general fluid mixture is developed in some detail, and is then applied to mixtures of ideal gases. It is shown that the usual equations for the velocity of chemical reactions are consistent with the second law provided that the departure from equilibrium is not too great. Mathematical complexities make it difficult to decide whether this is the case for larger deviations also. A somewhat general theory of diffusion and heat flow is considered and the requirements of the second law are formulated as the positive definiteness of a certain matrix whose elements depend on the diffusion coefficients, thermal conductivity, etc.

SURVEY

IN the preceding paper, the rate of increase of the entropy of a simple fluid was calculated and found to be in accord with the second law of thermodynamics. Before proceeding to more complicated cases, it is well to consider what may be accomplished.

In the case of the simple fluid, it was possible

to establish the existence of entropy and temperature functions. This depended on mathematical properties that are peculiar to Pfaffian forms in two variables (p, v), and it is not to be expected that the discussion can be extended to the case of more variables.[1] It will therefore be advisable to follow Gibbs and suppose that the concepts of temperature and entropy are not in need of definition or existence proof.

It was also possible to deduce the usual incomplete form of the second law from Kelvin's hypothesis, the positiveness of the absolute temperature, and the usual expression for the viscous stresses. This may seem of doubtful interest, since these hypotheses are all less general than the second law itself. Thus the object of the considerations will not be the derivation of the entropy law from other laws.

It will rather be to derive equations of the form[2]

$$(d/dt)\int\int\int_S m\eta d\tau+\int\int_S(1/\theta)\mathbf{q}\cdot d\boldsymbol{\sigma} =\int\int\int_S G d\tau, \quad (1)$$

which, when combined with the second law, yields the inequality

$$G\geqslant 0. \quad (2)$$

At this stage of the considerations, it will be shown that G is always the sum of a number of terms, each of which is the product of two factors:

$$G=\Sigma_a X_a Y_a. \quad (3)$$

This decomposition of G, and more particularly, the classification of the factors into X's and Y's, is to a great extent arbitrary. However, it will then be shown that it can be done so that

A. the definition of thermostatic equilibrium is

$$X_a=0$$

together with the vector equation

$$\partial\mathbf{V}/\partial t=0.$$

For example, the X's are the components of the heat flow $\mathbf{q}$, of the velocity gradients, of the diffusion velocity, the rates of production of chemical compounds, etc., etc.

The Y's are determined by this choice of the X's, and it will then be shown that

B. the Gibbsian criteria of thermostatic equilibrium are equivalent to the equations

$$Y_a=0$$

together with the vector equation

$$\nabla p=0.$$

The Y's corresponding to the X's enumerated above are proportional to the components of the temperature gradient, of a stress tensor, of the gradients of chemical potential, and the differences of chemical potential, in the same order as above.

It is desirable to have an inclusive terminology for the X's and Y's; because of the diverse natures of the quantities thus combined into classes, it is difficult to find a terminology that is free from serious objections. The most satisfactory that has occurred to the author is *D-factor* for the X's, (D for *definition*) and *C-factor* for the Y's (C for *criterion*). The components of the acceleration and pressure gradient should be considered D- and C-factors, respectively.

It remains to give an explanation of these observations. This is to be found in tacit assumptions that enter into all discussions of thermodynamics and thermostatics, but are rarely or never formulated clearly:

a. The irreversible changes of thermodynamic state are governed by equations expressing the D-factors as functions of the C-factors and certain other variables (*say* ξ):

$$X_a=F_a(Y,\xi). \quad (4)$$

These may be called the thermodynamic equations of motion; it should be noted that the C- and D-factors have been defined without reference to the equations of motion. The definition

[1] In this connection, the work of C. Carathéodory should be mentioned: Math. Ann. **67**, 355 (1909), Berl. Ber. p. 39 (1925); also T. Ehrenfest Afanassjewa, Zeits. f. Physik **33**, 933 (1925), and S. Chandrasekhar, *Introduction to the Study of Stellar Structure* (Chicago, 1939), Chap. I.

There is reason to believe that Carathéodory's theory affords a better basis for a theory of irreversible processes than does that of Gibbs. The author has chosen the latter because of its greater familiarity.

[2] The notation is the same as that of the previous paper; m, η, θ, q are the mass density, entropy per gram, temperature and heat flow, respectively. S is any closed surface moving with the matter.

of thermostatic equilibrium then leads immediately to the equations

$$F_a(Y, \xi)=0, \tag{5}$$

but it must be assumed that

b. The Eq. (5) are equivalent to the equations under B, i.e., to the vanishing of the C-factors.

c. The inequality

$$\Sigma_a X_a Y_a \geqslant 0 \tag{6}$$

is a consequence of the thermodynamic equations of motion.

Unless *a*, *b*, and *c* are true, it is not true that "For the equilibrium of any isolated system it is necessary and sufficient that in all possible variations of the state of the system which do not alter its energy, the variation of its entropy shall either vanish or be negative"[3] which is the principle on which Gibbs based his theory of thermostatics. In order that this principle follow from *a*, *b*, *c*, it is further necessary that *B* be true.

In the next section, the results that have been anticipated in this survey will be established for the case of a fluid mixture.

Fluid Mixtures

For the sake of formal simplicity, it is essential to consider the possibility that the mixture may contain all of its chemical elements in the free monatomic form; let c_α, $\alpha=1, 2, \cdots n$ be the concentrations of the free elements in moles/gram of mixture. Let the other possible components of the mixture be molecular compounds, the ith containing $\nu_{i\alpha}$ atoms of element α in each of its molecules. For simplicity, the numbering may be such that i runs from $n+1$ to N, and let c_i be the concentration of compound i. The word *substance* will be used to designate either free elements or compounds.

Let $\mathbf{V}_k$ be the velocity of the substance k and m the density of the mixture in g/cm³; then

$$\partial(mc_k)/\partial t+\nabla\cdot(mc_k\mathbf{V}_k)=m\Gamma_k \tag{7}$$

defines Γ_k, the rate of production of substance k in moles/g/sec. Since the atoms of the elements are not created or destroyed by the chemical reactions, the Γ_k are not independent, but related by

$$\Gamma_\alpha+\Sigma_{i=n+1}^{N}\nu_{i\alpha}\Gamma_i=0, \quad \alpha=1\cdots n. \tag{8}$$

If M_k is the molecular (atomic) weight of substance k, the concentrations are related by

$$\Sigma_{k=1}^{N}M_kc_k=1, \tag{9}$$

and the M_k by

$$M_i=\Sigma_{\alpha=1}^{n}\nu_{i\alpha}M_\alpha, \quad i=n+1, \cdots N. \tag{10}$$

Equations (8) and (10) combine to give the equation of conservation of mass

$$\Sigma_{k=1}^{N}M_k\Gamma_k=0. \tag{11}$$

The momentum density of the mixture is $m\mathbf{V}$, where

$$\mathbf{V}=\Sigma_{k=1}^{N}M_kc_k\mathbf{V}_k, \tag{12}$$

and the Eqs. (7), (9), (11), (12) combine to give the equation of continuity:

$$\partial m/\partial t+\nabla\cdot(m\mathbf{V})=0$$

or

$$mDv/Dt=\nabla\cdot\mathbf{V}. \tag{13}$$

The diffusion velocities of the various substances are

$$\mathbf{U}_k=\mathbf{V}_k-\mathbf{V}, \tag{14}$$

and Eqs. (7), (13), (14) combine to give

$$mDc_k/Dt=m\Gamma_k-\nabla\cdot(mc_k\mathbf{U}_k). \tag{15}$$

The hydrodynamic equation will be assumed in the form

$$m D\mathbf{V}/Dt=\nabla\cdot\mathfrak{p}, \tag{16}$$

the stress tensor $\mathfrak{p}$ now including the hydrostatic pressure as well as the viscous stresses. There is now the possibility that $\mathfrak{p}$ may also depend on the $\mathbf{U}_k$, but this complication may be ignored. In any case, the kinetic energy equation in the form

$$(d/dt)\int\int\int_S \tfrac{1}{2}mV^2d\tau=\int\int\int_S \mathbf{V}\cdot(\nabla\cdot\mathfrak{p})d\tau \tag{17}$$

will still be valid. Following Gibbs, it will be assumed that the internal energy (per gram of mixture), ϵ, is a function only of v, of the c_k, and of the entropy η. The possibility that ϵ may depend on the $\mathbf{U}_k$ will be ignored, but this constitutes an approximation.

Because of the arbitrary zero of energy, and of Eq. (9), all equations must be invariant when

[3] J. W. Gibbs, *Scientific Papers* (Longmans Green & Co., New York), Vol. I, p. 56.

ϵ is replaced by $\epsilon+f(\Sigma_k M_k c_k)$, where f is arbitrary. This will be called an ϵ-substitution.[4]

An application of the energy law to the volume whose boundary S moves with the mass of the fluid yields

$$(d/dt)\int\int\int_S \{\tfrac{1}{2}mV^2+m\epsilon\}d\tau = -\int\int_S \mathbf{q}\cdot d\boldsymbol{\sigma}+\int\int_S (\mathfrak{p}\cdot\mathbf{V})\cdot d\boldsymbol{\sigma} - \Sigma_{k=1}^{N}\int\int_S (\partial\epsilon/\partial c_k)mc_k\mathbf{U}_k\cdot d\boldsymbol{\sigma}. \quad (18)$$

The first integral on the right is the rate at which heat enters the volume; the second is the rate at which the fluid outside S does work on the fluid inside S; the remainder is the rate at which energy enters the volume due to the diffusion processes. It is readily verified that this equation is invariant under an ϵ-substitution.

Subtracting Eq. (17) from (18), transforming the surface integrals into volume integrals, and recalling that S is arbitrary, one obtains:

$$mD\epsilon/Dt-(\mathfrak{p}\cdot\nabla)\cdot\mathbf{V}+\nabla\cdot\mathbf{q} +\Sigma_{k=1}^{N}\nabla\cdot[m(\partial\epsilon/\partial c_k)c_k\mathbf{U}_k]=0. \quad (19)$$

Following Gibbs, the temperature is defined by

$$\theta=\partial\epsilon/\partial\eta, \quad (20)$$

the chemical potentials[5] by

$$\mu_k=\partial\epsilon/\partial c_k, \quad (21)$$

and the hydrostatic pressure by

$$p=-\partial\epsilon/\partial v. \quad (22)$$

(Under an ϵ-substitution, μ_k is replaced by $\mu_k+M_kf'(1)$, so that $\nabla\mu_k$ is invariant.) Then

$$D\epsilon/Dt=\theta D\eta/Dt-pDv/Dt+\Sigma_{k=1}^{N}\mu_k Dc_k/Dt,$$

which combines with Eqs. (13), (15), and (19) into

$$m\theta D\eta/Dt-p\nabla\cdot\mathbf{V}-(\mathfrak{p}\cdot\nabla)\cdot\mathbf{V}+\nabla\cdot\mathbf{q} +\Sigma_{k=1}^{N}m\{\mu_k\Gamma_k+c_k\mathbf{U}_k\cdot\nabla\mu_k\}=0. \quad (23)$$

From Eq. (8), it follows that

$$\Sigma_{k=1}^{N}\mu_k\Gamma_k=\Sigma_{i=n+1}^{N}\Delta_i\Gamma_i, \quad (24)$$

where

$$\Delta_i=\mu_i-\Sigma_{a=1}^{n}\nu_{ia}\mu_a \quad (25)$$

is the difference in chemical potential between the compound i and its equivalent in free elements. Because of Eq. (10) the Δ_i and therefore also the Eq. (23) are invariant under an ϵ-substitution.

Dividing Eq. (23) through by θ, integrating the result over the volume bounded by S, and comparing with Eq. (1), show clearly that

$$G=\mathbf{q}\cdot\nabla(1/\theta)+(1/\theta)\{p\nabla\cdot\mathbf{V}+(\mathfrak{p}\cdot\nabla)\cdot\mathbf{V} -\Sigma_{i=n+1}^{N}m\Delta_i\Gamma_i-\Sigma_{k=1}^{N}mc_k\mathbf{U}_k\cdot\nabla\mu_k\}. \quad (26)$$

The derivation of Eq. (26) completes the first stage of the program outlined in the survey (cf. Eq. (3)). It remains to verify the propositions A and B.

It will be obvious that when the mixture reaches thermodynamic equilibrium, the following quantities will vanish: (1) the heat flow, $\mathbf{q}$; (2) the velocity gradient, $\nabla\mathbf{V}$ (and therefore also $\nabla\cdot\mathbf{V}$); (3) the rates of production of the various substances, $m\Gamma_i$; (4) the diffusion currents, $mc_k\mathbf{U}_k$; (5) the acceleration, $\partial\mathbf{V}/\partial t$. The first four of these quantities appear as factors in the various terms of G, thus verifying A. The corresponding C-factors are

(1)	$\nabla(1/\theta)$;	(3)	$-(1/\theta)\Delta_i$;
(2)[6]	$(1/\theta)(p\mathfrak{i}+\mathfrak{p})$;	(4)	$-(1/\theta)\nabla\mu_k$;

while the Gibbs criteria for thermostatic equilibrium are

(1)	$\nabla\theta=0$;	(2)	$\mathfrak{p}=-p\mathfrak{i}$;	(3)	$\Delta_i=0$;
		(4)	$\nabla\mu_k=0$;	(5)	$\nabla p=0$;

thus verifying B.

However several remarks are called for in this connection: the second criterion is not found explicitly in Gibbs' paper, but is implicitly as-

[4] It will be noted that the theory of ϵ-substitutions is not used to prove any equation, but only as a check and guide. Because of the equivalence of mass and energy, the status of the ϵ-substitutions in a fundamental theory is not clear, and it has seemed preferable to restrict the use of these methods. Other types of invariance are also associated with Eq. (9) and can presumably be used in a similar manner.

[5] Gibbs calls the μ_i simply "the potential of the substance i." Other writers call them "partial molal thermodynamic potentials."

[6] Here $\mathfrak{i}$ is the unit tensor.

sumed at an early stage of the calculations. The criterion (5) follows from criterion (2), the hydrodynamic equation (Eq. (16)), and $\partial V/\partial t=0$. The exceptional character of the fifth criterion is thus seen to be related to the exceptional position accorded the hydrodynamic equation as compared to the other equations of motion.

Elimination of the Entropy from the Equations

The equations just derived involve functions of v, the c_i, and the entropy, η. This proves to be inconvenient, for it is an empirical fact that these functions are very complicated. The equations are very much simplified by eliminating the entropy and replacing it by the temperature, using Eq. (20) to accomplish this. This is an algebraic process, but can be very laborious, so that it deserves some consideration.

It appears that the process can be much simplified by introducing the function

$$\psi(v, c_i, \theta)=\epsilon(v, c_i, \eta)-\theta\eta, \tag{27}$$

the entropy being eliminated from the right side. The function ψ is one of those introduced by Massieu under the name *characteristic function*, and is usually called the *free energy*, or *work function* (per g of the mixture). Once ψ has been determined, the quantities p, μ_i and η can be expressed as functions of v, c_i and θ by means of the equations

$$p=-\partial\psi/\partial v, \tag{28}$$

$$\mu_i=\partial\psi/\partial c_i, \tag{29}$$

$$\eta=-\partial\psi/\partial\theta, \tag{30}$$

which follow from Eqs. (20), (21), (22) and (27).

General Consequences of a, b, c

The assumptions a, b, c have important consequences for the theory of irreversible processes, inasmuch as b, and c impose marked restrictions on the equations of motion. From b it follows that

$$(\partial F_a/\partial\xi)_0=0, \tag{31}$$

the subscript zero indicating that the $Y_a=0$ while the ξ's have general values.[7] Equation (6) imposes further restrictions on the F_a; it can be given another form if the F_a are linear functions of the Y_a, which is probably the case whenever the departure from equilibrium is not very great. In this case, Eq. (4) becomes

$$X_a=\Sigma_b A_{ab}Y_b, \tag{32}$$

where

$$A_{ab}=(\partial F_a/\partial Y_b)_0, \tag{33}$$

is in general a function of the ξ's. Equation (6) is then

$$\Sigma_a\Sigma_b A_{ab}Y_aY_b\geqslant 0, \tag{34}$$

which must be true for all values of the Y_a and the ξ's. Therefore the matrix

$$B_{ab}=\tfrac{1}{2}(A_{ab}+A_{ba}) \tag{35}$$

must be positive definite. This implies such inequalities as

$$B_{aa}\geqslant 0, \tag{36}$$

$$B_{aa}B_{bb}-(B_{ab})^2\geqslant 0. \tag{37}$$

Mixtures of Ideal Gases

In order to work out special cases of the general principles, it is convenient to consider a mixture of ideal gases, for which the work function is

$$\psi(v, c_i, \theta)$$

$$=\Sigma_{i=1}^{N}c_i\{u_i(\theta)+R\theta[\log(c_i/v)-1]\}, \tag{38}$$

the u_i being functions characteristic of the substances and R the gas constant per mole.[8] Equation (29) then yields

$$\mu_i=u_i(\theta)+R\theta\log(c_i/v), \tag{39}$$

and Dalton's law of partial pressures, etc., can also be derived.

This ideal mixture may be the scene of chemical reactions, proceeding at rates given by the usual formulae. It is to be considered, whether these formulae are consistent with a, b, c. Before doing so, however, it will be shown that Eq. (39) leads to the usual form of the law of mass action.

Let M_k stand for the chemical symbol of substance k, as well as for its molecular weight. Then the general form of a reaction may be

[7] If the quantities dX_a/dt are among the ξ's, this generality must be restricted, since these derivatives vanish at equilibrium.

[8] See, e.g., K. F. Herzfeld, *Handbuch der Physik*, Vol. 9, p. 101, Eq. (1).

written (the ν's are integers)

$$\Sigma_{k=1}^{N}\nu_k'M_k \rightleftarrows \Sigma_{k=1}^{N}\nu_k''M_k. \tag{40}$$

Since the reaction balances,

$$\Sigma_{k=1}^{N}\nu_k'\nu_{k\alpha}=\Sigma_{k=1}^{N}\nu_k''\nu_{k\alpha}=n_\alpha, \quad \alpha=1\cdots n, \tag{41}$$

$\nu_{k\alpha}$ being the number of atoms of element α in one molecule of substance k. (If $\alpha\leqslant n$, $\nu_{k\alpha}=\delta_{k\alpha}$.) The criteria for chemical equilibrium ($\Delta_i=0$) yield

$$\Sigma_{i=n+1}^{N}(\nu_i''-\nu_i')\Delta_i=0,$$

which may also be written

$$\Sigma_{i=1}^{N}(\nu_i''-\nu_i')\mu_i=0 \tag{42}$$

because of Eq. (41). Substituting from Eq. (39) gives

$$\Sigma_{i=1}^{N}(\nu_i''-\nu_i')[u_i/R\theta+\log(c_i/v)]=0, \tag{43}$$

which is essentially the Arrhenius form of the law of mass action.

The commonly accepted (and empirically verified) formulae for the rate of a chemical reaction in the gaseous phase were first deduced by Guldberg and Waage from rather vague kinetic theory considerations. These have since been made somewhat more specific and brought into agreement with Eq. (42).[9] According to these formulae, the net rate at which the reaction proceeds to the right is the difference $\rho'-\rho''$, where

$$\begin{aligned}\rho'&=\phi\exp(\Sigma_{i=1}^{N}\nu_i'\mu_i/R\theta),\\ \rho''&=\phi\exp(\Sigma_{i=1}^{N}\nu_i''\mu_i/R\theta),\end{aligned} \tag{44}$$

ϕ being a positive quantity. It is clear that Eq. (42) follows from this and

$$\rho'-\rho''=0, \tag{45}$$

but that Eq. (45) does not follow from the definition of thermostatic equilibrium. It is usually deduced from the principle of detailed balancing, but also follows from the Gibbsian criteria of equilibria.

If there are many possible reactions, these must be distinguished by an index (ϕ_s, ρ_s', $n_{\alpha s}$, etc.). The rate of production of substance i is then

$$\Gamma_i=\Sigma_s(\nu_{is}''-\nu_{is}')(\rho_s'-\rho_s''), \tag{46}$$

and the definition of equilibrium is $\Gamma_i=0$. Eq. (45) cannot follow directly from this and Eq. (46) unless there are at least as many substances as possible reactions. It may, however, follow indirectly because of other considerations leading to the Gibbsian criteria of equilibrium.

From Eq. (25),

$$\begin{aligned}\rho_s'&=a_s\exp(\Sigma_{k=n+1}^{N}\nu_{ks}'\Delta_k/R\theta),\\ \rho_s''&=a_s\exp(\Sigma_{k=n+1}^{N}\nu_{ks}''\Delta_k/R\theta),\end{aligned} \tag{47}$$

where

$$a_s=\phi_s\exp(\Sigma_{\alpha=1}^{n}n_{\alpha s}\mu_\alpha/R\theta)\gtrless 0.$$

Since ρ and Δ are invariant under an ϵ-substitution, a must also be; there is thus a presumption that the interpretation of a will be simpler than that of ϕ. Equation (46) then becomes

$$\begin{aligned}\Gamma_i=\Sigma_s(\nu_{is}''-\nu_{is}')a_s\{&\exp(\Sigma_{k=n+1}^{N}\nu_{ks}'\cdot\Delta_k/R\theta)\\ &-\exp(\Sigma_{k=n+1}^{N}\nu_{ks}''\Delta_k/R\theta)\}.\end{aligned} \tag{48}$$

For sufficiently small values of Δ_i,

$$\Gamma_i=-\Sigma_{s,k}(\nu_{is}''-\nu_{is}')a_s(\nu_{ks}''-\nu_{ks}')\Delta_k/R\theta,$$

so that

$$\begin{aligned}&\Sigma_{i=n+1}^{N}\Gamma_i(-\Delta_i/\theta)\\ &\quad=(1/R)\Sigma_{s,k}a_s\{\Sigma_k(\nu_{ks}''-\nu_{ks}')(\Delta_k/\theta)\}^2.\end{aligned}$$

These last two equations are in complete accord with the general considerations leading to Eq. (34). The more general Eq. (48) is in accord with Eq. (31), and the Gibbsian criteria $\Delta_i=0$ are a sufficient condition for $\Gamma_i=0$. It is not easy to see whether they are also the necessary condition, as Gibbs asserts, nor whether

$$\Sigma_i\Gamma_i(-\Delta_i/\theta)\gtrless 0$$

for all values of Δ_i, as is required by the present assumption c.

Turning now to the conduction of heat and the diffusion of matter in the mixture, it may be supposed that the equations governing these processes are

$$\begin{aligned}\mathbf{q}&=\kappa_{00}\nabla(1/\theta)-\Sigma_{i=1}^{N}(\kappa_{0i}/\theta)\nabla\mu_i,\\ mc_j\mathbf{U}_j&=\kappa_{j0}\nabla(1/\theta)-\Sigma_{i=1}^{N}(\kappa_{ji}/\theta)\nabla\mu_i.\end{aligned} \tag{49}$$

In order that these equations be consistent with the general principles, it is necessary and sufficient that the matrix $\frac{1}{2}(\kappa_{ij}+\kappa_{ji})$ be positive

[9] R. H. Fowler, *Statistical Mechanics* (Cambridge University Press, 1936) second edition, p. 700.

definite. Insofar as the mixture is an idealized one, there is no need to justify the assumption of Eq. (49), but the question of its departure from actual mixtures does arise.

The conduction of heat is usually supposed to be given by Fourier's law that q is proportional to $\nabla\theta$; similarly, Fick's law that $\mathbf{U}_i$ is proportional to $\nabla(mc_i)$ is supposed to govern diffusion. However, more general cases have been considered, in which $\mathbf{U}_i$ is a linear function of all the concentration gradients. Such "diffusion-drag" forces have been invoked to explain certain biophysical phenomena, and it seems likely that they are important in the separation of isotopes. Except for a difference in notation, and the terms in κ_{0i}, the Eq. (49) are identical with those considered in the diffusion-drag theories.

To see this, note that because of Eq. (39) and $m=1/v$

$$\nabla\mu_i=\theta\alpha_i\nabla\theta+(R\theta/mc_i)\nabla(mc_i), \tag{50}$$

where

$$\theta\alpha_i=du_i/d\theta+R\log(mc_i),$$

so that Eq. (49) becomes

$$\begin{aligned}-\mathbf{q}&=k_{00}\nabla\theta+\Sigma_{i=1}^{N}k_{0i}\nabla(mc_i),\\ -mc_j\mathbf{U}_j&=k_{j0}\nabla\theta+\Sigma_{i=1}^{N}k_{ji}\nabla(mc_i),\end{aligned} \tag{51}$$

with

$$\begin{aligned}k_{j0}&=\kappa_{j0}/\theta^2+\Sigma_{i=1}^{N}\kappa_{ji}\alpha_i,\\ k_{ji}&=R\kappa_{ji}/mc_i.\end{aligned} \tag{52}$$

The coefficient k_{00} is the thermal conductivity, the k_{ii} $(i=1\cdots N)$ are the diffusion coefficients, while the k_{ij} $(i\neq j=1\cdots N)$ are the drag coefficients. If the coefficients $k_{j0}\neq 0$, this amounts to assuming that a temperature gradient tends to produce a diffusion of matter; similarly, if $k_{0i}\neq 0$ the concentration gradients tend to produce a flow of heat. Both of these phenomena occur; they are closely related to the various thermoelectric effects.

Since the matrix κ_{ij} is positive definite, the thermal conductivity and diffusion coefficients must be positive quantities, and

$$4c_ic_jk_{ii}k_{jj}\geqslant(k_{ij}c_j+k_{ji}c_i)^2,$$

etc. However, these particular inequalities are based on Eq. (40); they may have different forms for liquid mixtures. The general conclusion that the numerical values of the drag coefficients are restricted by the numerical values of the diffusion coefficients is valid in all cases.

Finally, it would be possible to consider generalizations of the usual formulae for the viscous stresses, but this seems of slight interest here.

Summary

The restrictions imposed by the second law of thermodynamics on the equations governing irreversible changes have been investigated, first somewhat generally, and then for the particular case of a mixture of ideal gases. It was found that they are automatically fulfilled by the usual law of mass action for chemical reaction velocities. In the case of general diffusion processes, the diffusion coefficients must be positive, and certain other inequalities must be satisfied. The general methods used can be applied to other irreversible processes, and will always yield such inequalities. The experience of the author suggests that many of these inequalities have already found their place in physical theories, having been introduced on the basis of "physical intuition," but that the latter cannot deal with the more elaborate cases.

Note added April 26, 1940. Since writing the above, my attention has been called to the work of E. Lohr on similar problems.* A first reading of his extensive papers shows that some of his conclusions practically coincide with mine, though there seem to be appreciable differences in our points of view. The entropy law has also been formulated as a differential equation by R. C. Tolman,†, independently of the work of Lohr.

* E. Lohr, Wiener Denkschriften, **93**, 339–421 (1917); **99**, 11–37, 59–91 (1924). Vektor- und Dyadenrechnung, p. 312 (Berlin, 1939).

† Literature references in R. C. Tolman and H. P. Robertson, Phys. Rev. **43**, 564 (1933).

LETTERS TO THE EDITOR

Prompt publication of brief reports of important discoveries in physics may be secured by addressing them to this department. Closing dates for this department are, for the first issue of the month, the eighteenth of the preceding month, for the second issue, the third of the month. Because of the late closing dates for the section no proof can be shown to authors. The Board of Editors does not hold itself responsible for the opinions expressed by the correspondents.

Communications should not in general exceed 600 words in length.

Induced Radioactivity of Rhenium and Tungsten

Rhenium, with two stable isotopes, mass numbers 185 and 187,[1] has been made radioactive and one new activity, with a half-life of 52 ± 2 days, found in addition to the 18-hour[2] and the 90-hour[3] periods reported previously. The probable assignment of these activities to their isotopes is shown in the diagram below.

184	185	186	187	188
52days	stable	90hr.	stable	20hr.

Experimental results supporting these conclusions follow. Slow neutron and deuteron bombardments, followed by chemical separations, produce two activities in rhenium, whose half-lives are 18 hours and 90 hours. Fast neutrons yield three activities, chemically identified as rhenium, with half-lives of 18 hours, 90 hours, and 50 ± 5 days. From the relative intensities of the 18-hour and 90-hour periods produced by slow and fast neutrons, Yamasaki and Sinma's[4] assignment of the 18-hour period to Re^{188} and the 90-hour period to Re^{186}, has been confirmed.

The rhenium separation from the bombardment of tungsten with deuterons has given three activities with half-lives of 20 min., 90 hours, and 52 days. Production of the 90-hour activity in this way, no 18-hour activity being present, is an additional confirmation of the assignment of the former to Re^{186}, and indicates a $d,2n$ reaction from W^{186}. Deuteron capture would probably give both the 18-hour and 90-hour activities from the equally abundant W^{184} and W^{186} isotopes, or if the placement were reversed and the $d,2n$ reaction alone occurred, only the 18-hour activity would be produced.

The 52-day activity, which was identified as a rhenium isotope through a series of chemical reactions, has been assigned to mass number 184 for the following reasons. It is produced from rhenium by fast neutrons ($n,2n$ reaction from Re^{185}), and appears in rhenium, chemically separated from tungsten bombarded with deuterons (probably a d,n reaction from W^{183}, although a $d,2n$ reaction from W^{184} is an additional possibility). It is a negatron emitter, having a gamma-ray of 0.85 ± 0.1 Mev associated with it.

The 20-min. activity, a positron emitter, follows the chemistry of rhenium but is probably due to Mn^{52} formed from iron, an impurity in the tungsten foil, since the intensity differed in different tungsten samples.

Investigations, during the past year, upon the radioactivity produced in tungsten, by deuterons, fast and slow neutrons, have given two activities, 24.1 ± 0.1 hours and 74.5 ± 1.5 days. The 24-hour period is identical with that found by Fermi,[2] while the 74.5-day period corresponds to that of 77 ± 3 days, just reported by Minakawa.[5]

Both activities are negatron emitters, the upper limit of the β-ray energy for the 24-hour period being 1.40–1.44 Mev by absorption in Al, and 1.40 ± 0.05 Mev from preliminary cloud-chamber measurements. A γ-ray of 0.87 ±0.03 Mev, as measured by absorption in Pb, is associated with the 24-hour activity. The upper limit of the β-ray energy of the 74.5-day period is 0.55–0.65 Mev, from absorption measurements in Al, and 0.64–0.72 Mev from preliminary cloud-chamber measurements.

The results of extensive investigations of the relative intensities of the two periods, produced by fast and slow neutrons, does not give as clear a picture as would be expected from the assignment, made by Minakawa,[5] of the 24-hour to W^{187} and the 74.5-day to W^{185}. However, from the deuteron bombardment of rhenium, a weak activity of 70 ± 6 days is found in the tungsten separation, no 24-hour activity being present. Such an activity could be produced by a Re^{187} $(d,\alpha)W^{185}$ reaction. This additional evidence supports the conclusions of Minakawa, thus the following scheme is most probable.

180		182	183
0.2%		22.6%	17.3%
184	**185**	**186**	**187**
30.1%	74.5days	29.8%	24hr.

In conclusion, we wish to thank Professor J. M. Cork for his active cooperation during all phases of the work and we are very grateful to others of the Physics and Chemistry Departments who gave assistance, especially to Dr. J. L. Lawson.

KASIMIR FAJANS
WILLIAM H. SULLIVAN

Chemistry Department,
University of Michigan,
Ann Arbor, Michigan,
July 2, 1940.

[1] F. W. Aston, Proc. Roy. Soc. **A132**, 487 (1931).
[2] E. Amaldi, E. Fermi, *et al.*, Proc. Roy. Soc. **A149**, 522 (1935).
[3] I. V. Kurtchatow, *et al.*, Physik. Zeits. Sowjetunion **8**, 589 (1935).
[4] H. Yamasaki and K. Sinma, Sci. Pap. Inst. Phys. Research (Tokyo), **37**, 10 (1940).
[5] O. Minakawa, Phys. Rev. **57**, 1189 (1940).

On the Efficiency of γ-Ray Counters

The efficiency curve for γ-ray counters (efficiency defined as the ratio of the number of incident quanta to the number of registered quanta) is a valuable key for the interpretation of every counting experiment involving γ-rays, but a careful determination of such curves meets with some difficulty. It implies an accurate knowledge of the number of quanta emitted in some transformations, but only a few (if any) energy-level schemes involving γ-rays are quite definite at present. The coincidence method is one of the best ways of testing such schemes, but it, in turn, makes use of efficiency curves. Because of the low efficiency of γ-ray counters, whereby counting experiments often become laborious, it is also of interest to see whether different materials show different efficiencies.

Counters of brass, aluminum and lead, all of the same geometric size (effective length 6 cm, inner diameter 1.4 cm, wall thickness 0.2 cm), have been compared (Fig. 1).

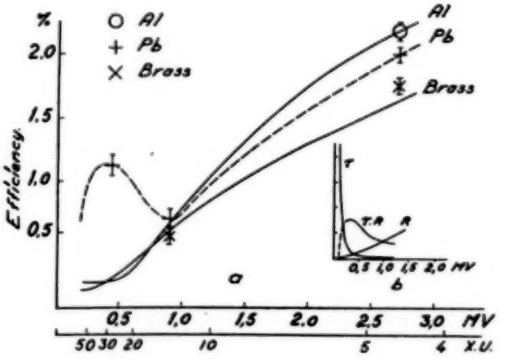

FIG. 1. Comparison of efficiency of counters of different materials.

The curve for brass was published by Droste,[1] who measured the end points and estimated the form semi-empirically; it was recently verified also by Dunworth.[2] Yukawa and Sakata[3] have calculated the *shape* of the Al curve. The point reported here for 2.7 Mev will thus fix this curve. The measurements at 2.7 Mev were made by a radio-thorium source of known strength (ThC″ γ-rays, filter 2.5 cm Pb). Points on the Pb and Al curves at about 0.9 Mev were determined by β−γ-coincidence measurements of $^{*}Mn^{56}$ with the source surrounded by a 0.24 g/cm² brass filter to eliminate the low energy β-group. According to Curran, Dee and Strothers[4] the high energy β-group should be coupled chiefly to a 0.9-Mev line. At still lower energy $^{*}Au^{198}$, having γ-components of 0.28 Mev and 0.44 Mev,[5] was used. The β−γ-coincidence rate corresponds to an efficiency of about 1.1 percent for the 0.44-Mev line, if the β-spectrum is simple, which is plausible. In any case the efficiency of the lead counter for the 0.44-Mev line was about 5.6 times greater than the efficiency of the brass counter (after correcting for absorption). This fact, which must be related to the large photo-effect in lead at these energies (see Fig. 1*b* where τ is the photoelectric absorption coefficient, *R* the range of photo-electrons), makes the lead counter very effective in the region of 0.5 Mev, where the other counters have low

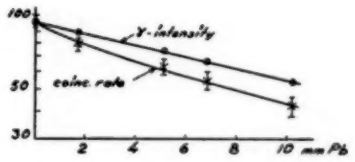

FIG. 2. Comparison of absorption of γ-rays and coincidence rate.

efficiency. Therefore, a brass counter with thin lead foils on the inside probably should be most useful. For RaC γ-rays, filtered through 2.5 cm Pb, (~2 Mev) the relative efficiencies were: Pb = 100, brass = 84±4, Al = 109±4, and for unfiltered Ra γ-rays correspondingly: Pb = 100, brass = 67±3, Al = 75±3.

It may be pointed out, that a γ-component in favorable cases (highly different absorption coefficients of the components) can be correlated to other particles without use of an efficiency curve by measuring the decrease of the coincidence rate when absorbers are inserted in front of the γ-ray counter. It seemed worth while to try this method in the important case of $^{*}Mn^{56}$ above. In Fig. 2 the upper curve is a simple absorption curve (Pb-counter), whereby the bad geometry may be taken into account. The coincident rate curve below it (β-filter 0.24 g/cm² brass) gives some support to the assumption of Curran, Dee and Strothers, that the most energetic β-particles are coupled to the soft γ-component, but the curve is not quite conclusive, since a still softer γ-component of low intensity (possibly "Bremsstrahlung") seems to be present.

Because of the higher effectivity of obliquely incident rays the coincidence measurements have been reduced to a "large distance" between source and counter by a distance function:

$$\Psi\frac{R}{\pi b}F(x,k) \qquad (1)$$

and not by the relative space angle, approximately given as:

$$\Phi=\frac{l}{\pi}\arctan\frac{R\cdot l}{[bc(l^2+4bc)]^{\frac{1}{2}}} \qquad (2)$$

($2R$ internal diameter, a the distance from source to counter axis, F elliptic integral of first kind, l effective counter length, $x=\arctan(l/2c)$, $b=a+R$, $c=a-R$, $kb=(b^2-c^2)^{\frac{1}{2}}$.) The difference between these formulas is appreciable only for small distances such as are common in coincidence experiments. For high γ-energy and light elements the formula (2) should be best (Compton recoil forward).

A more detailed account will be published later elsewhere.

I wish to thank Professor M. Siegbahn and Professor L. Meitner for their interest in this work.

FOLKE NORLING

Forskningsinstitutet för Fysik, Vetenskapsakademien,
Stockholm 50, Sweden,
June 4th, 1940.

[1] G. v. Droste, Zeits. f. Physik **104**, 474 (1937).
[2] J. V. Dunworth, Rev. Sci. Inst. **11**, 167 (1940).
[3] H. Yukawa and S. Sakata, Sci. Pap. Inst. Phys. and Chem. Research (Japan) **31**, 187 (1937).
[4] S. C. Curran, P. I. Dee and J. E. Strothers, Proc. Roy. Soc. **174**, 553 (1940).
[5] J. R. Richardson, Phys. Rev. **55**, 609 (1939).

Pair Production of Mesotrons at 29,000 Feet

In a second airplane flight[1] made on April 30, carrying a cloud chamber in a magnetic field of 700 gauss up to 29,000 feet altitude, we found one particularly interesting photograph which shows the occurrence of a mesotron pair. A reproduction is given in Fig. 1.

The radii of curvature of the two partner tracks are 45 and 75 cm. Both particles are stopped in a copper plate of 0.32 cm which was placed in the middle of the chamber. They enter this plate at an angle of 45°, which gives a maximum path length inside the copper of 0.45 cm. If the particles were electrons and were stopped in this amount of copper their maximum energy is 6 Mev. This corresponds to a radius of curvature in the magnetic field smaller than 28 cm. The measured radii are larger by an amount far beyond the errors of measurement. Thus the tracks cannot be produced by electrons. For mesotrons of a mass 200, similar considerations give 25 Mev as the maximum kinetic energy of the particles and a radius of curvature smaller than 350 cm. This curvature limit covers well the measured values. The same holds true, of course, if one considers the particles to be protons.

One can further estimate the masses from the ionization produced in the gas of the chamber. Fortunately the picture shows two slower particles and a fast one. Their ionization is markedly smaller and corresponds to the kind of tracks we get from β-particles and penetrating cosmic rays in the laboratory. There is no doubt that the particles of small radii of curvature are electrons. The ionization of the two particles in the pair is distinctly higher although the radii of curvature are greater. This proves again that the pair must consist of heavier particles.

For the observed curvature of the pair, mesotrons should ionize from 6 to 15 times as strongly as electrons, and protons 10 times as strongly as mesotrons. Such an enormous ionization excludes positively the possibility of assuming that the pair is protons. The theoretical ionization of mesotrons, on the contrary, lies well within the limits one estimates from the pictures.

We therefore must conclude that this pair consists of a slow positive and a slow negative mesotron.

The two stereoscopic pictures taken show that the slow electron emerging upward from the copper plate is possibly associated with this pair and may be a decay electron of one of the mesotrons. It is difficult to state from which mesotron this electron might come. Assuming that it moves upward from the plate its charge is negative. It has a kinetic energy of 0.2 Mev.

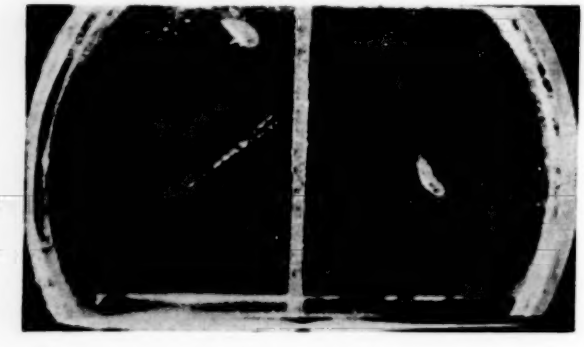

FIG. 1.

Other pictures taken on this flight likewise show mesotrons stopping in the copper plate. In several cases electrons appear which may originate from mesotron decay. A full report on this material will shortly be published.

G. HERZOG

The Texas Company,
Houston, Texas,

W. H. BOSTICK

Ryerson Physical Laboratory,
University of Chicago,
Chicago, Illinois,
July 15, 1940.

[1] G. Herzog, Phys. Rev. **57**, 337 (1940).

Transport Cross Section of Helium

Endeavors to fit the low temperature viscosity measurements of helium[1] have in the past not yielded very satisfactory results. Use of the Slater-Kirkwood field,[2] the Lennard-Jones potential,[3] the elastic sphere[4] and the modified elastic sphere models[5] have all failed in predicting correctly the quantum effect at low energies. It has been pointed out by the author that the general behavior of the transport cross section which is required for a correct temperature dependence is: the existence of minima at low energies, a broad maximum at higher energies, and at energies corresponding to room temperatures an asymptotic approach to a value approximating 4.46×10^{-16} cm^2.

The physical characteristics of the interaction underlying this behavior are that two elements of differing order of magnitude must exist: a strong repulsive potential with a rather sharply defined boundary, and a weak interaction composed of attractive and repulsive terms. It is essential for the existence of minima in the low energy range that the interaction contain attractive terms, as, although the elastic sphere and modified elastic sphere models show minima in the kinetic cross section, these disappear in the viscosity cross sections due to the presence of two compensating series.

It has seemed of interest therefore to determine as exactly as possible the form of the cross section necessary to fit the experimental data. That is, one might attempt to solve the integral equation for $\theta(\gamma)$ the cross section, using the relation given by Enskog[6]

$$\int_0^\infty \gamma^7\theta(\gamma)e^{-\gamma^2}d\gamma=\frac{15}{32\pi^{\frac{1}{2}}}\frac{(mkT)^{\frac{1}{2}}}{\eta(T)}, \tag{1}$$

where

$$\gamma=\frac{h}{2\pi}\frac{k^*}{(mkT)^{\frac{1}{2}}};\quad (k^*)^2=\frac{8\pi^2mE}{h^2}. \tag{2}$$

The exact solution of the above equation presupposes the knowledge of $\eta(T)$ for all values of T. One has, however, only its values for a limited set of values of the temperature. The solution of $\theta(\gamma)$ is then subject to a certain degree of indefiniteness. It has, therefore, seemed most advantageous to assume for θ the expansion

$$\theta(k^*)\equiv\Sigma A_j\exp\left[-j(k^*)^2\phi\right] \tag{3}$$

and so determine A_j so as to fit the experimental points. The arbitrary choice of the parameter φ (unless determined in the same manner as the A_j) introduces the indeterminacy of definition previously mentioned. Retaining the idea of a hard core, the term for $j=0$ was included in the sum although the behavior of $\eta(T)$ does not necessarily justify this step.

In carrying through the calculation it was found possible to fit the points with better than a one percent accuracy by retaining only the first six terms of the sum.

The values of $\theta(k^*)$ are given in Table I for values of $k^*\times10^{-8}\times2$.

TABLE I. *Values of $\theta(k^*)$ for various values of k^*.*

$k^*\times2\times10^{-8}$	$\theta\times10^{16}$	$k^*\times2\times10^{-8}$	$\theta\times10^{16}$	$k^*\times2\times10^{-8}$	$\theta\times10^{16}$
0.00	9.39	4.52	3.82	8.02	2.75
2.05	4.41	4.89	3.72	9.60	3.04
2.55	3.62	5.26	3.51	9.81	3.04
2.99	3.41	6.05	2.96	10.05	3.03
3.39	3.49	6.48	2.74	10.61	2.96
3.78	3.67	6.94	2.63	12.51	2.58
4.15	3.79	7.45	2.63	16.63	2.25

The results reveal the existence of two minima. In general the trend is that of the elastic sphere cross section for $S=2.11\times10^{-8}$ cm. The values of θ in the neighborhood of $k^*\to0$ permit large variations due to the form of (1) and hence for both $k\to0$ and $k\to\infty$, must be regarded as indeterminate.

E. J. HELLUND

Department of Physics,
University of Washington,
Seattle, Washington,
July 10, 1940.

[1] A. v. Itterbeek and W. H. Keesom, Physica **5**, 257 (1938); A. v. Itterbeek and O. v. Paemel, Physica **7**, 265 (1940).
[2] H. S. W. Massey and R. A. Buckingham, Proc. Roy. Soc. **A168**, 378 (1938).
[3] E. A. Uehling and E. J. Hellund, Phys. Rev. **54**, 479 (1939).
[4] H. S. W. Massey and C. B. O. Mohr, Proc. Roy. Soc. **A141**, 434 (1933); **A144**, 188 (1934).
[5] E. J. Hellund (unpublished).
[6] D. Enskog, "Kinetische Theorie der Vorgänge in Mässig Verdünnten Gasen" (Dissertation, Upsala, 1917).

Electric Breakdown of Alkali Halides

In discussions of the electric breakdown of alkali halide crystals an expression for the force between a free electron in the crystal and an ion in the lattice has proved to be of importance. Such a force is of the Coulomb type, of course, but it also contains a factor that depends on the dielectric constant and other properties of the lattice. Designating this factor by the symbol ϵ, we may express the force between a free electron of charge e and an ion of z-fold electronic charge by $\epsilon ze^2/r^2$, where r is their distance of separation. In the case of an electron that is moving sufficiently slowly, the following formula for ϵ has been given[1]

$$\epsilon=\frac{1}{e}\left\{2\pi\mu\nu a^2\left(\frac{1}{k}-\frac{1}{k'}\right)\right\}^{\frac{1}{2}},$$

in which μ is the "reduced mass" of the ions, a is the distance between neighboring ions, k' is the dielectric constant extrapolated from high (visible) frequencies, and k is the actual dielectric constant. The frequency ν which appears here is one appropriately averaged over the crystal vibrations that are excited by the passage of the electron. In making such an average, vibrations of rather long wavelength have considerable weight because of the interaction between the electron and somewhat distant ions. Since transverse vibrations are not excited by an electric field with $\nabla\times E=0$, only longitudinal ones need be considered here. According to Mott and Littleton[2] the frequencies of the longitudinal vibrations differ considerably from those of the transverse ones, the observed values of which have previously been employed in the calculation of breakdown fields. For in a longitudinal vibration in which positive and negative ions are displaced by unit length relative to each other, a surface charge density accumulates near the nodes, *viz.*, $\pm e^*/a^3$. (The formulae used in this letter include the effect of electronic polarizability in a rough approximation; they are not based on the customary assumption of a full electronic charge rigidly attached to an ion.) Here e^* is the apparent charge attached to an ion; it may differ from the electronic charge on account of the distortion of the ions. This surface charge at the nodes gives rise to an additional restoring force, which is equal to $2\pi e^{*2}/a^3k'$ for longitudinal waves and which is altogether absent for transverse ones, there being no accumulation of charge in the interior of the crystal in this case. We find, therefore, the relation

$$4\pi^2\mu\nu_L^2-4\pi^2\mu\nu_T^2=2\pi e^{*2}/a^3k'$$

for the frequency ν_L of the longitudinal vibrations in terms of the frequency ν_T of the transverse ones. (Our formulae become equal to those of Mott and Littleton for $k'=1$ and for $e^*=e$.) It can be shown that the transverse frequency satisfies also the following equation of Born and Göppert-Mayer,[3] which has only been modified by the replacement of e with e^*:

$$2\pi\mu a^3\nu_T^2=e^{*2}/(k-k').$$

From these two expressions we obtain

$$(\nu_L/\nu_T)^2=k/k'.$$

Finally, the factor ϵ becomes

$$\epsilon=\frac{1}{e}\left\{2\pi\mu\nu_L^2a^3\left(\frac{1}{k'}-\frac{1}{k}\right)\right\}^{\frac{1}{2}},$$

or

$$\epsilon=\frac{1}{e}\left\{2\pi\mu\nu_T^2a^3\left(\frac{1}{k'}-\frac{1}{k}\right)\right\}^{\frac{1}{2}}\left(\frac{k}{k'}\right)^{\frac{1}{2}}.$$

Using this value for ϵ and substituting ν_T for ν throughout

TABLE I. *Comparison of calculated and observed values of the breakdown potentials in alkali halides.*

ALKALI HALIDES	λ_T	$E_{B\text{-calc}}$	$E_{B\text{-obs}}$
LiF	18.9*μ	58.0 $(10)^5$ v/cm	31.0 $(10)^5$ v/cm
NaF	41.3*	22.	24
NaCl	61.1	7.2	15
NaBr	74.7	3.5	8.1
KCl	70.7	5.3	10.0
KBr	88.3	3.7	7.0
KI	102	2.7	5.7
RbCl	84.8	4.8	8.3
RbBr	118 *	2.8	6.3
RbI	130 *	2.3	4.9

the derivation for the formula for the breakdown field E_{Bq}, we find

$$E_{Bq}=\frac{1.82\pi^2 me\nu_T}{h}\left(\frac{1}{k'}-\frac{1}{k}\right)\left(\frac{k}{k'}\right)^{\frac{1}{2}},$$

where m is the so-called "effective mass" of the electron in the lattice.

In the second column of Table I we give the values of the wave-lengths λ_T corresponding to the frequencies ν_T, which we have used in the calculations of the breakdown fields of the alkali halides listed in the first column. In general, the values are those that have been obtained from absorption measurements in thin crystal layers; those marked with an asterisk, however, are the "reststrahl" wave-lengths multiplied by the number 1.10 (the factor 1.10 being due to the fact that the wave-length measured by the method of maximum reflecting power does not coincide with that of the lattice vibrations). In the third and fourth columns, respectively, the values of the breakdown fields calculated by means of the new formula are compared with the values originally observed. The computation has been carried out with the substitution of the mass of a free electron for the mass m in the formula.

The deviations between the calculated values and those observed cannot be ascribed merely to the coarseness of the theoretical approximations, but may be due even more to the omission of several physical factors, of which two important ones are the following: (1) The "effective mass" of the electron, which should be used in the calculation, if known, differs from the mass of a free electron; it may, indeed, be greater or less than this mass. (2) Breakdown fields calculated for absolute zero temperature, as in this case, are necessarily lower than those observed at room temperature (on account of a temperature dependence).[4] For example, in the case of KBr the calculated value of the breakdown field at 0°K is 3.7 $(10)^5$ v/cm as compared with the observed one of 7.0 $(10)^5$ v/cm at 300°K, whereas the measured value at 200°K is only 5.3 $(10)^5$ v/cm.

R. J. SEEGER
E. TELLER

George Washington University,
Washington, D. C.,
July 3, 1940.

[1] R. J. Seeger and E. Teller, Phys. Rev. **54**, 519 (1938).
[2] N. F. Mott and M. J. Littleton, Trans. Faraday Soc. **34**, 485 (1938); R. J. Seeger and E. Teller, Phys. Rev. **56**, 353 (1939).
[3] M. Born and M. Göppert-Mayer, *Handbuch der Physik* **24**, 646 (1933).
[4] R. C. Buehl and A. von Hippel, Phys. Rev. **56**, 946 (1939).